Aerosols in aerospace and stochastic modelling

Adam Durant
University of Oslo, Norway

UiO : University of Oslo

AMBIT Workshop (6-7 November) Aarhus University

SPEEDBIRD 9

SPEEDBIRD 9

"Ladies and Gentlemen, this is your Captain speaking. We have a small problem. All four engines have stopped. We are doing our damnedest to get them going again. I trust you are not in too much distress."

Captain Eric Moody, British Airways Flight 9
during 1982 Galunggung encounter

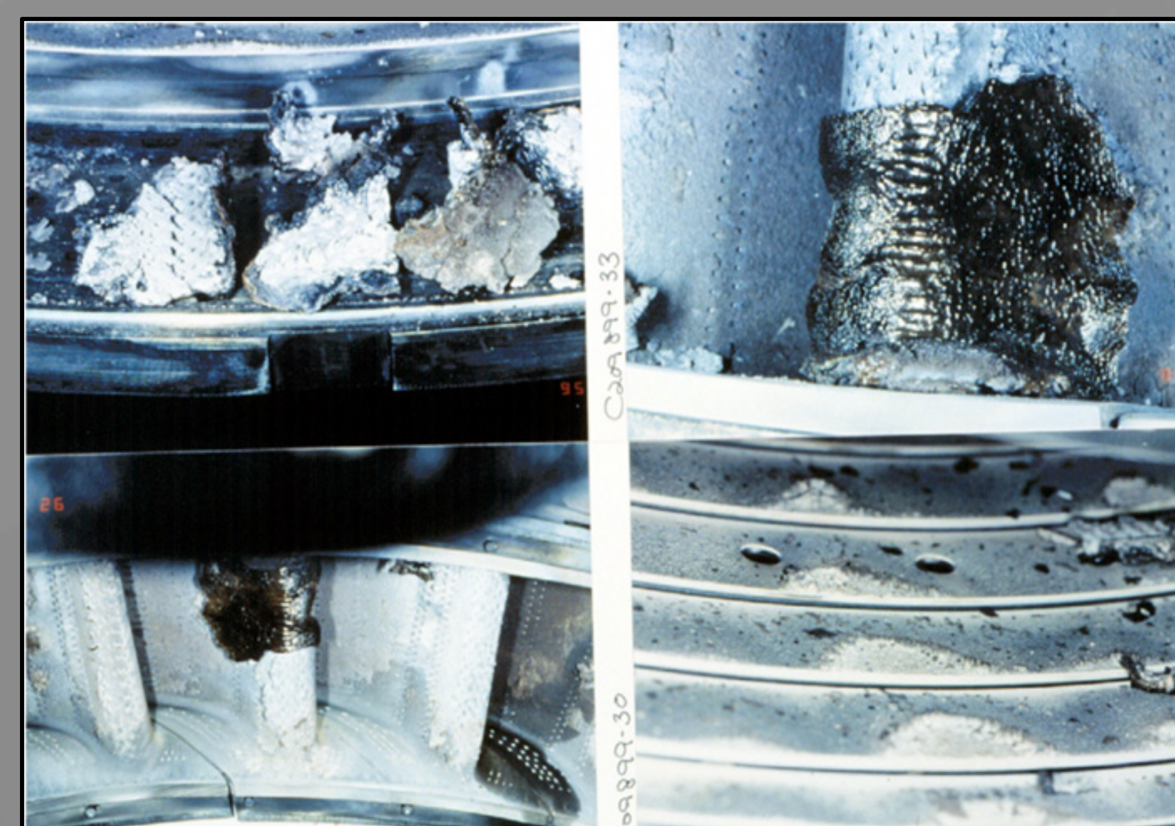

Volcanic ash ingestion – rapid effects

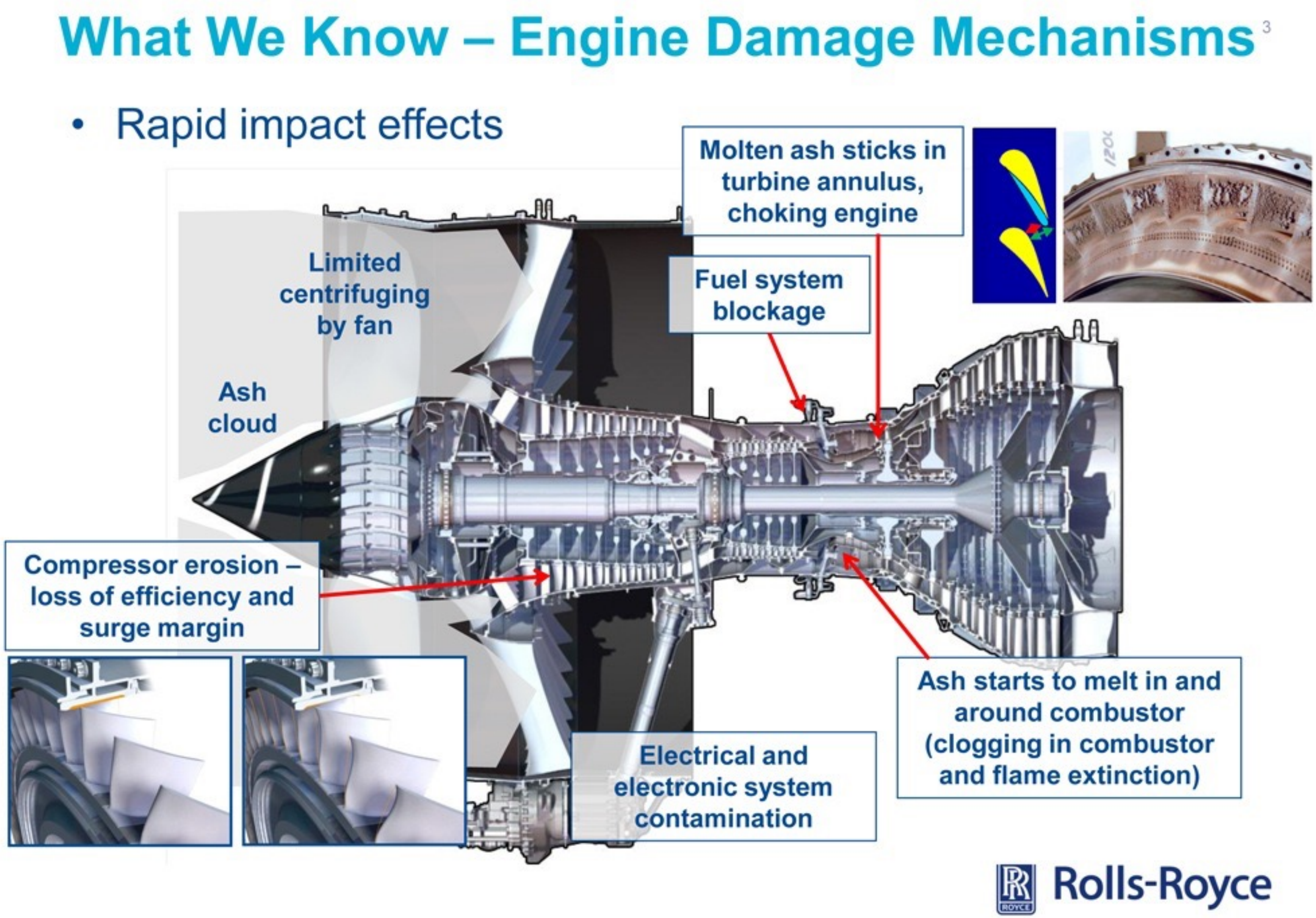

High level ice clouds are hazardous to aviation

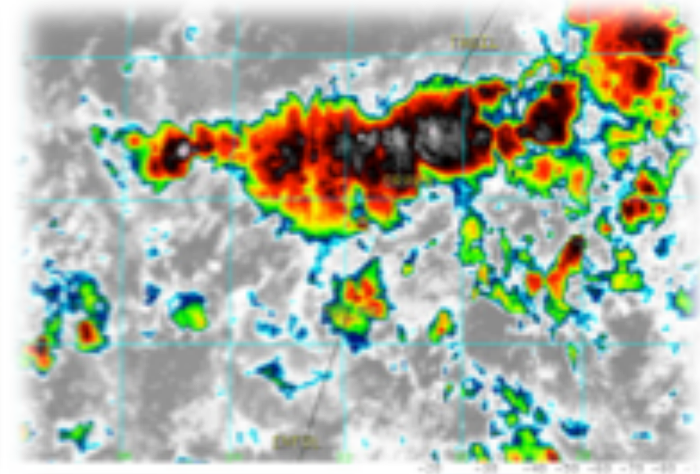

Altitude/airspeed errors from ice particle icing

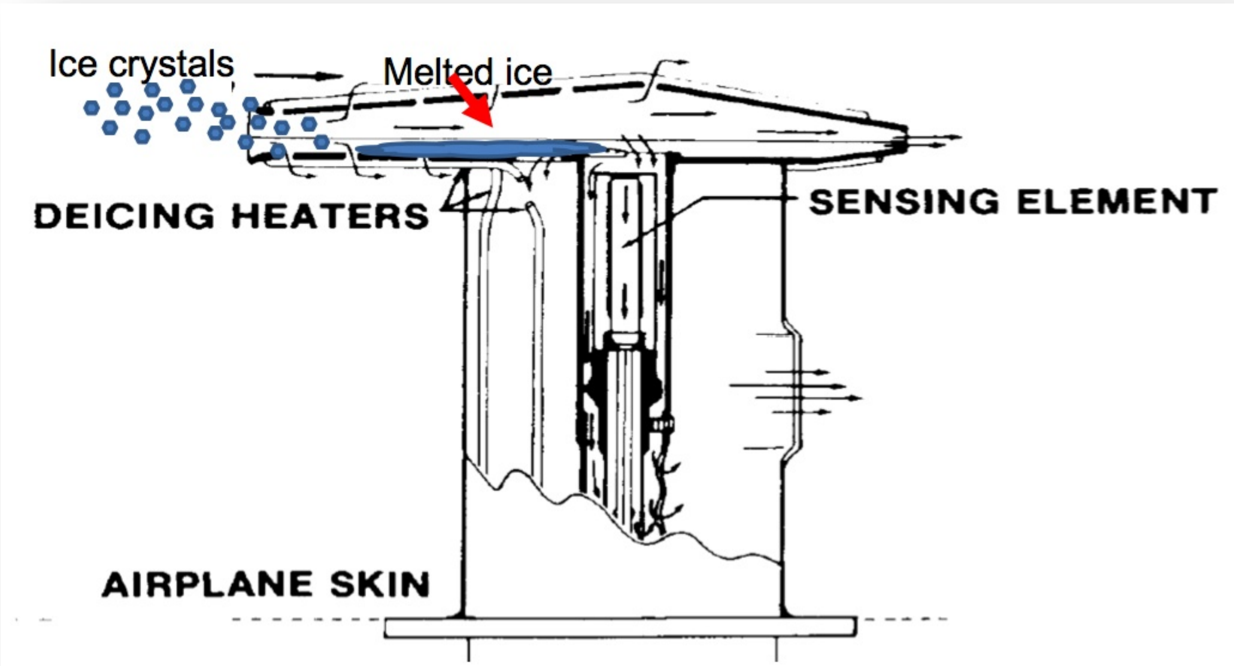

In the case of temperature probes, ice crystals may melt at the inlet and form a flow of liquid water into the sensing element. This causes a temperature increase that may be interpreted as loss of altitude or engine power.

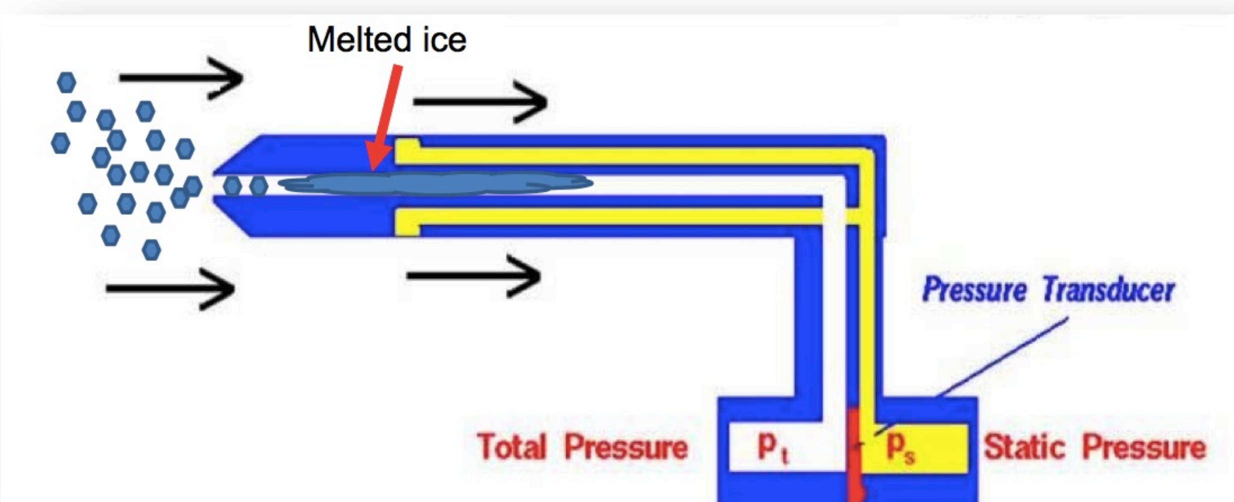

In the case of air speed measurements, ice crystals may melt at the inlet of the heated air speed sensor and accrete ice causing a decrease in total pressure that may be interpreted as loss of airspeed or engine power.

Ice particle icing aeroengine incidents on the rise (at altitudes above 22,000 ft)

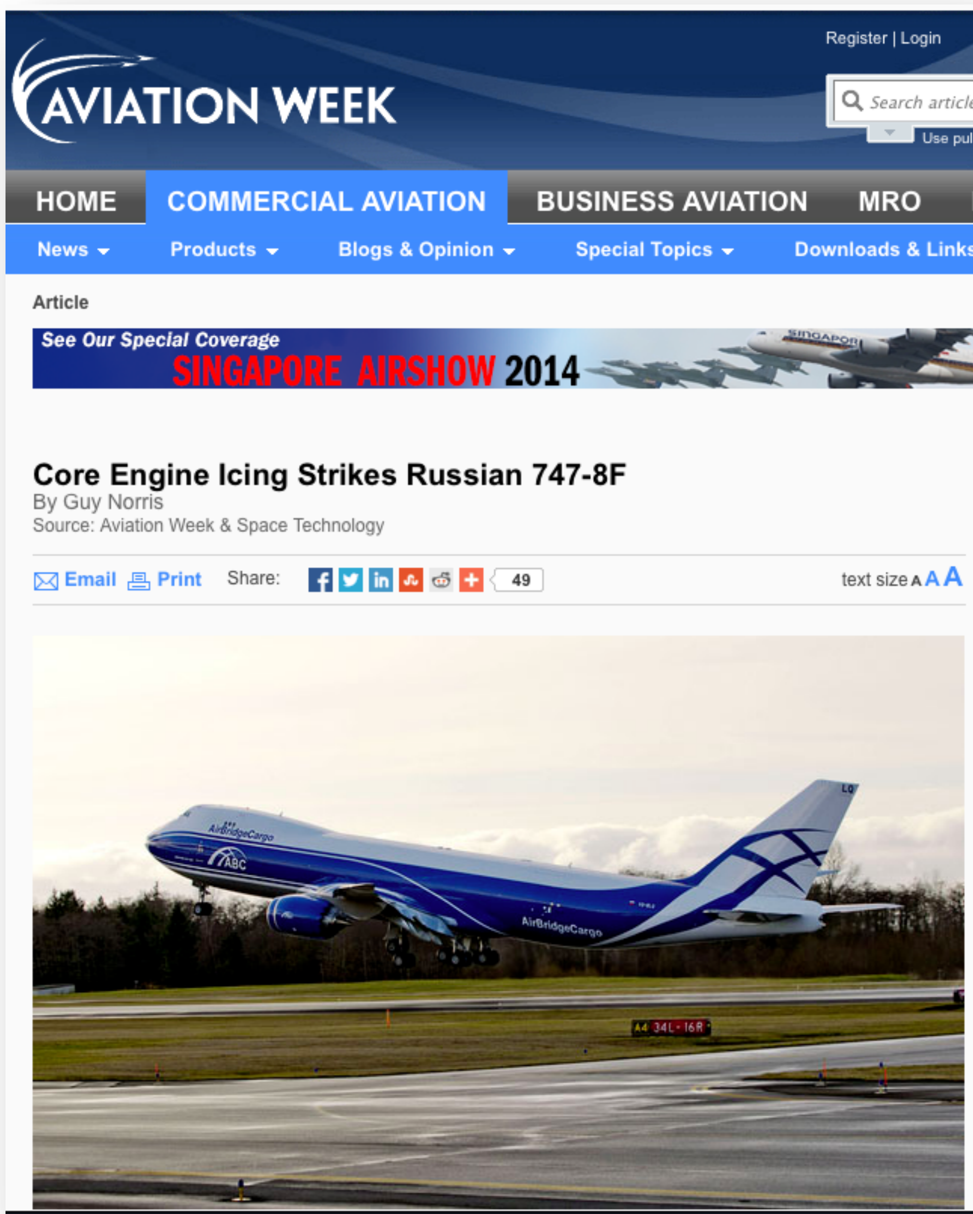
Register | Login
AVIATION WEEK
HOME | COMMERCIAL AVIATION | BUSINESS AVIATION | MRO
News | Products | Blogs & Opinion | Special Topics | Downloads & Links
Article
See Our Special Coverage SINGAPORE AIRSHOW 2014

Core Engine Icing Strikes Russian 747-8F
By Guy Norris
Source: Aviation Week & Space Technology

Email Print Share: 49 text size A A A

General Electric GenX 2B


Register | Login
AVIATION WEEK
HOME | COMMERCIAL AVIATION | BUSINESS AVIATION | MRO
News | Products | Blogs & Opinion | Special Topics | Downloads & Links
Article
See Our Special Coverage SINGAPORE AIRSHOW 2014

Growing GEnx Ice Core Problems Prompt Advisory
By Guy Norris guy.norris@aviationweek.com
Source: AWIN First

Email Print Share: 24 text size A A A

November 24, 2013
Credit: Guy Norris, Aviation Week

General Electric and Boeing are accelerating efforts to introduce new engine control software to counter core icing following further incidents of power loss in GEnx-powered 747-8s and 787s.

Although the two companies remain on track to roll out corrective software to operators in the first quarter of 2014, the increasing number of events affecting the GEnx-powered fleet has prompted Boeing to issue an advisory to

Outline

- Fine ash settling and aggregation
- Deviations from "Classical" theory
- Link to cloud microphysics

Physical characterisation of volcanic tephra deposits can be used as a "forensic" tool to understand atmospheric processing during ash cloud transport and sedimentation

Volcanic ash clouds

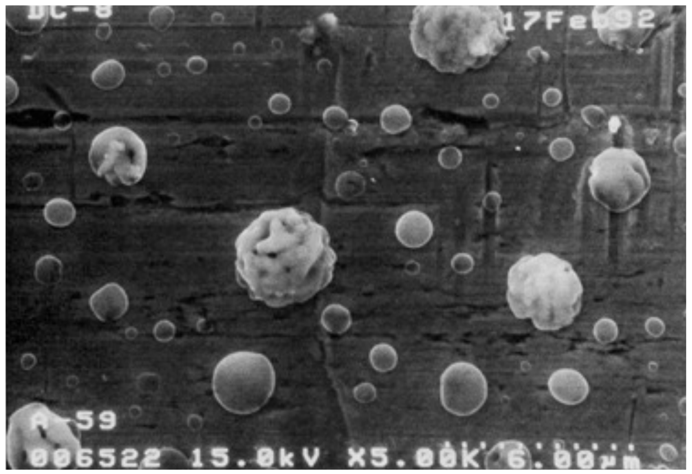

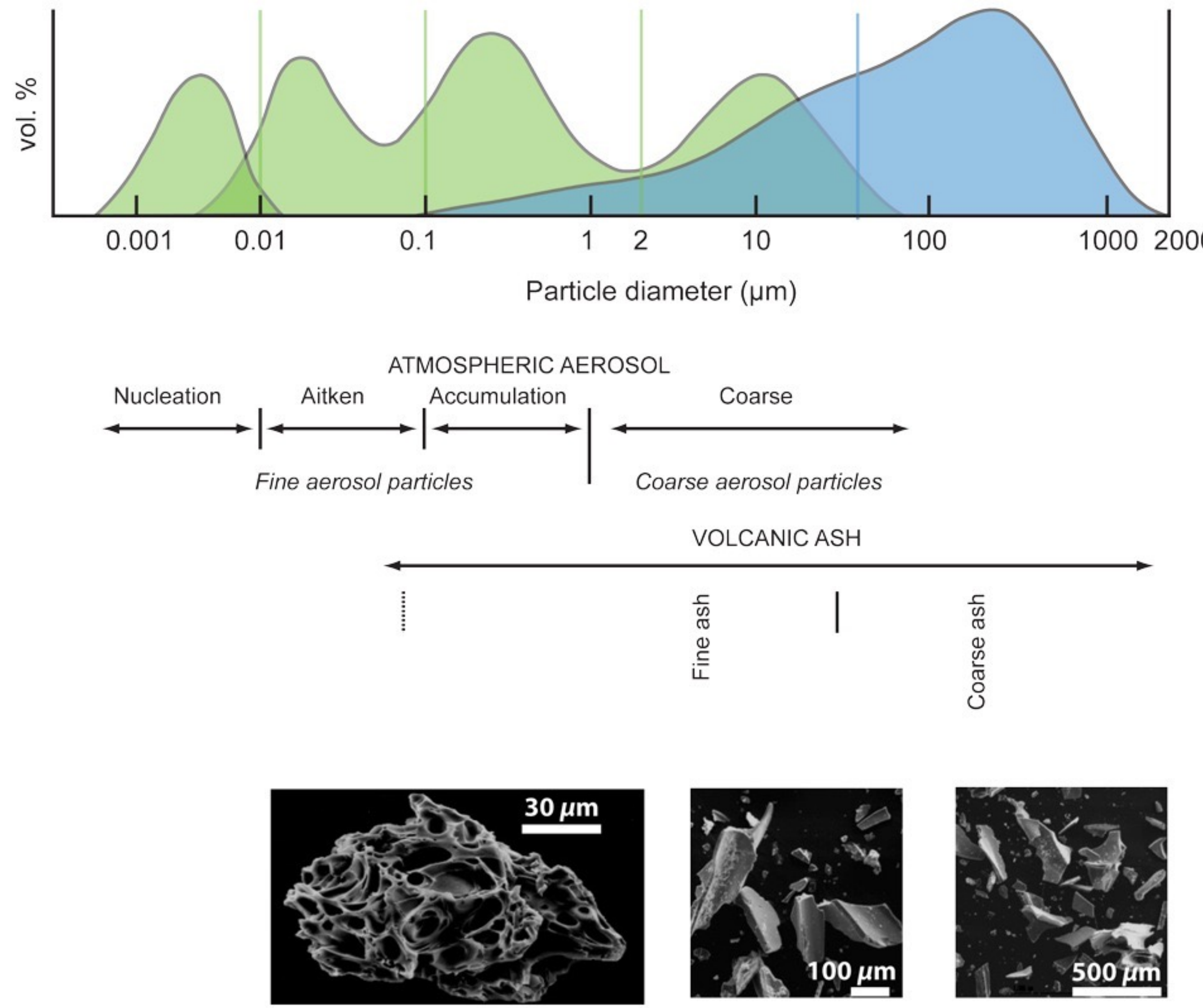

Durant, A.J., Bonadonna, C., Horwell, C.J., (2010), Atmospheric and Environmental Impacts of Volcanic Particulates. Elements 6, 235-240.

Modelling ash clouds: atmospheric source and sink

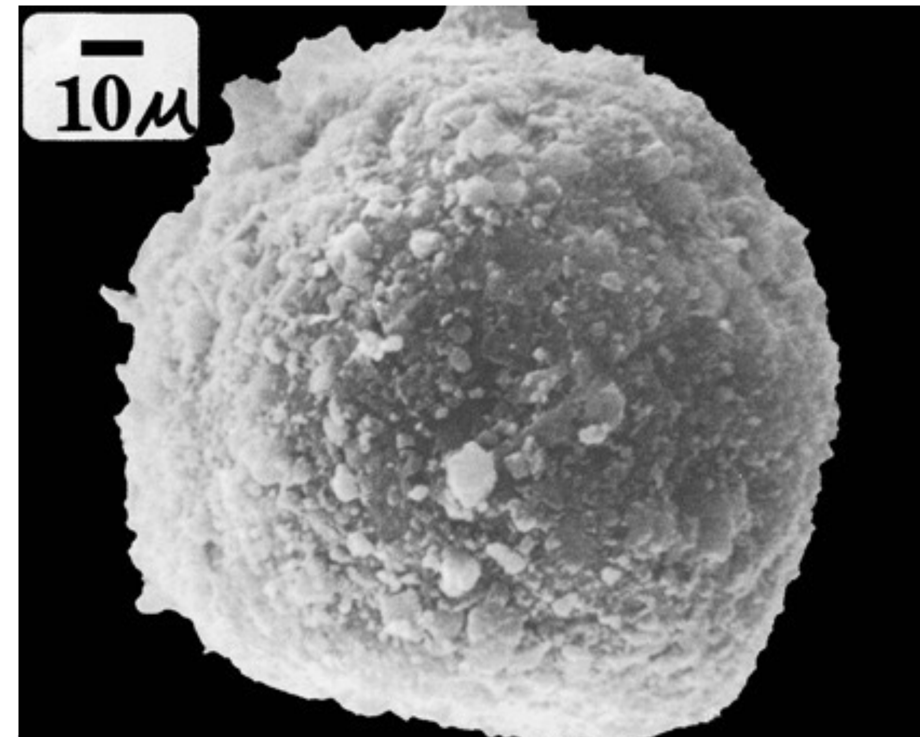

Short-fallings in ash cloud forecasting: source error

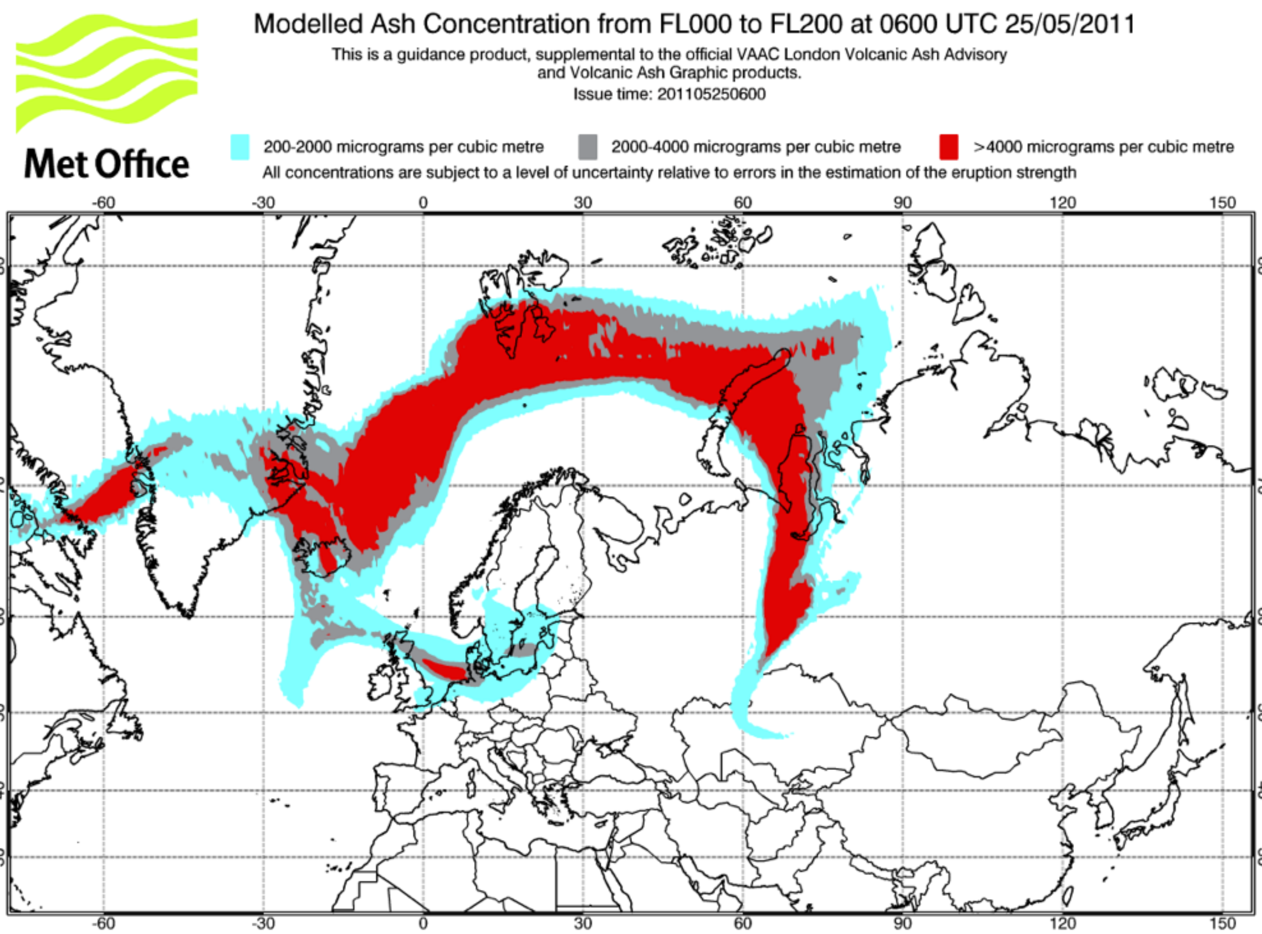

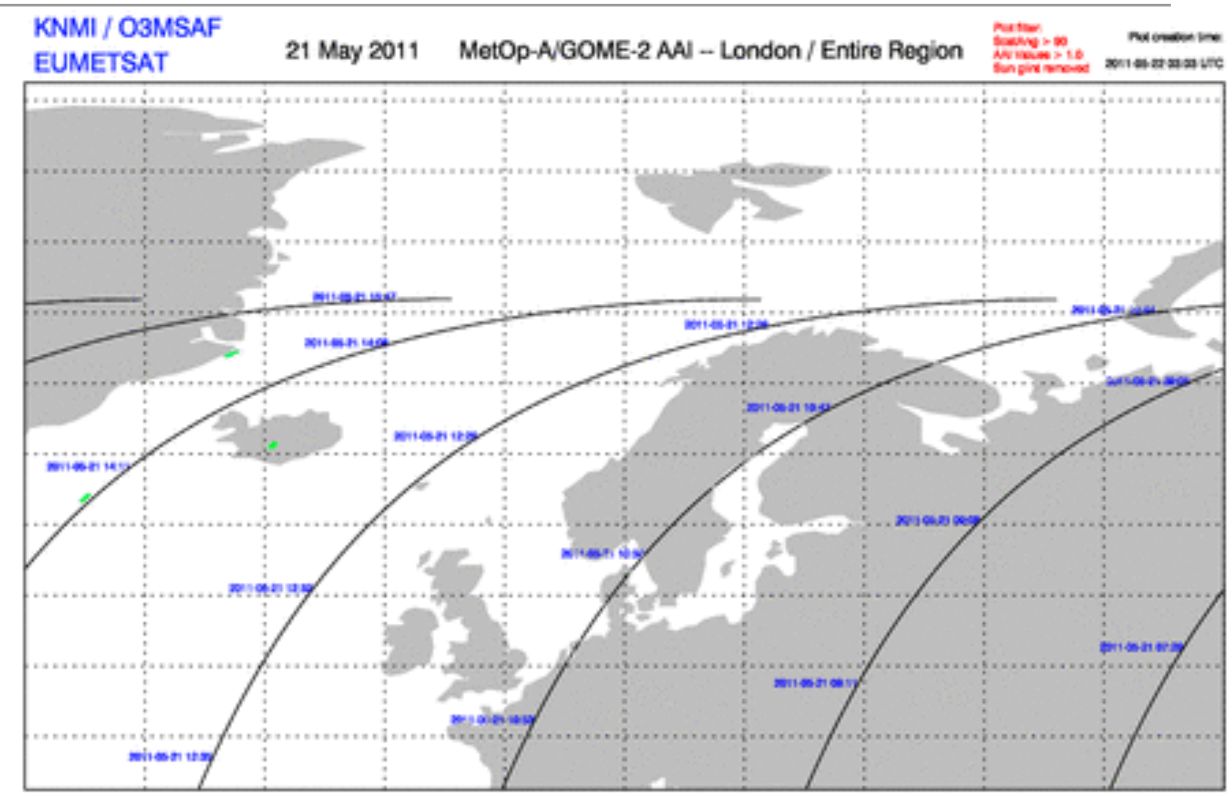

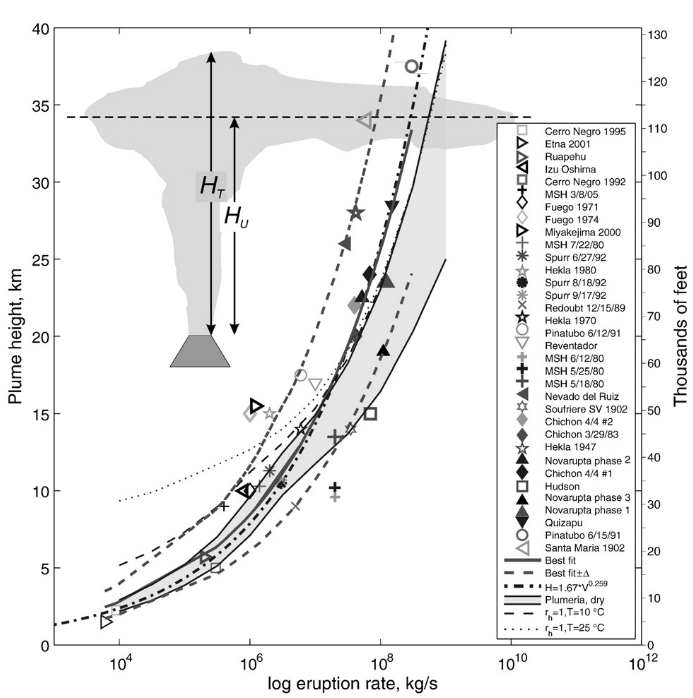

Mastin et al. (2009)

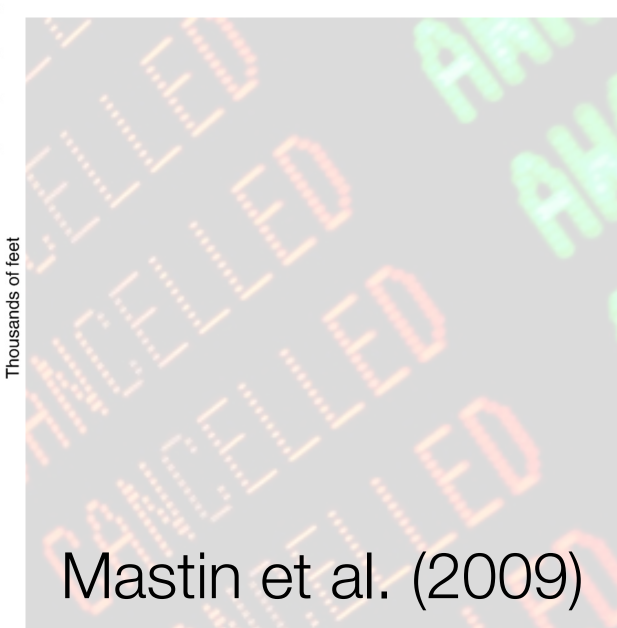

Metop-A/IASI SO2 signal, 20110521 AM

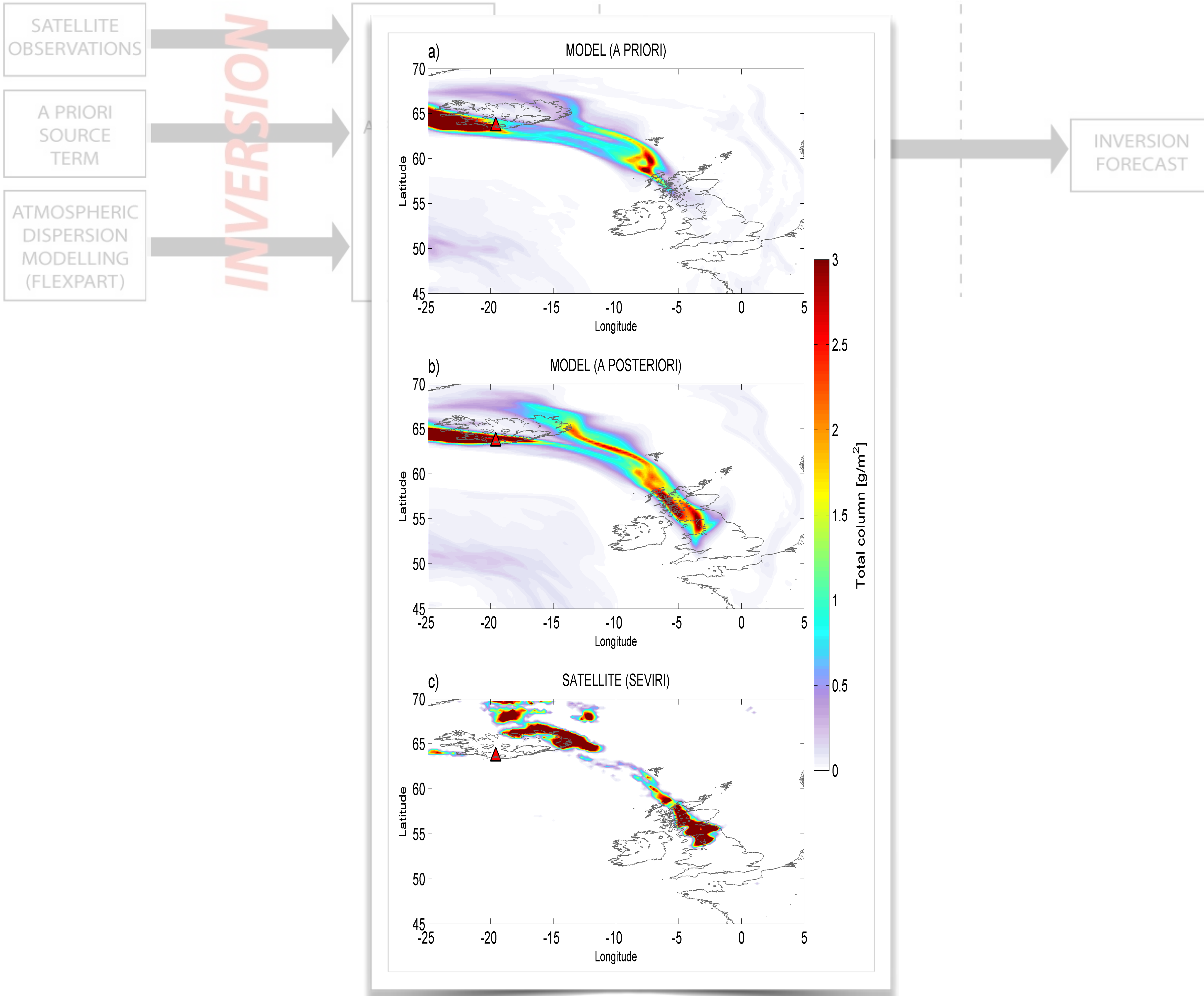

Stohl et al., ACPD, 2011; Kristiansen et al., *J. Geophys. Res.*, 2013; Moxnes et al., *J. Geophys. Res.,* 2014.

FINE ASH SETTLING AND PARTICLE AGGREGATION (COAGULATION)

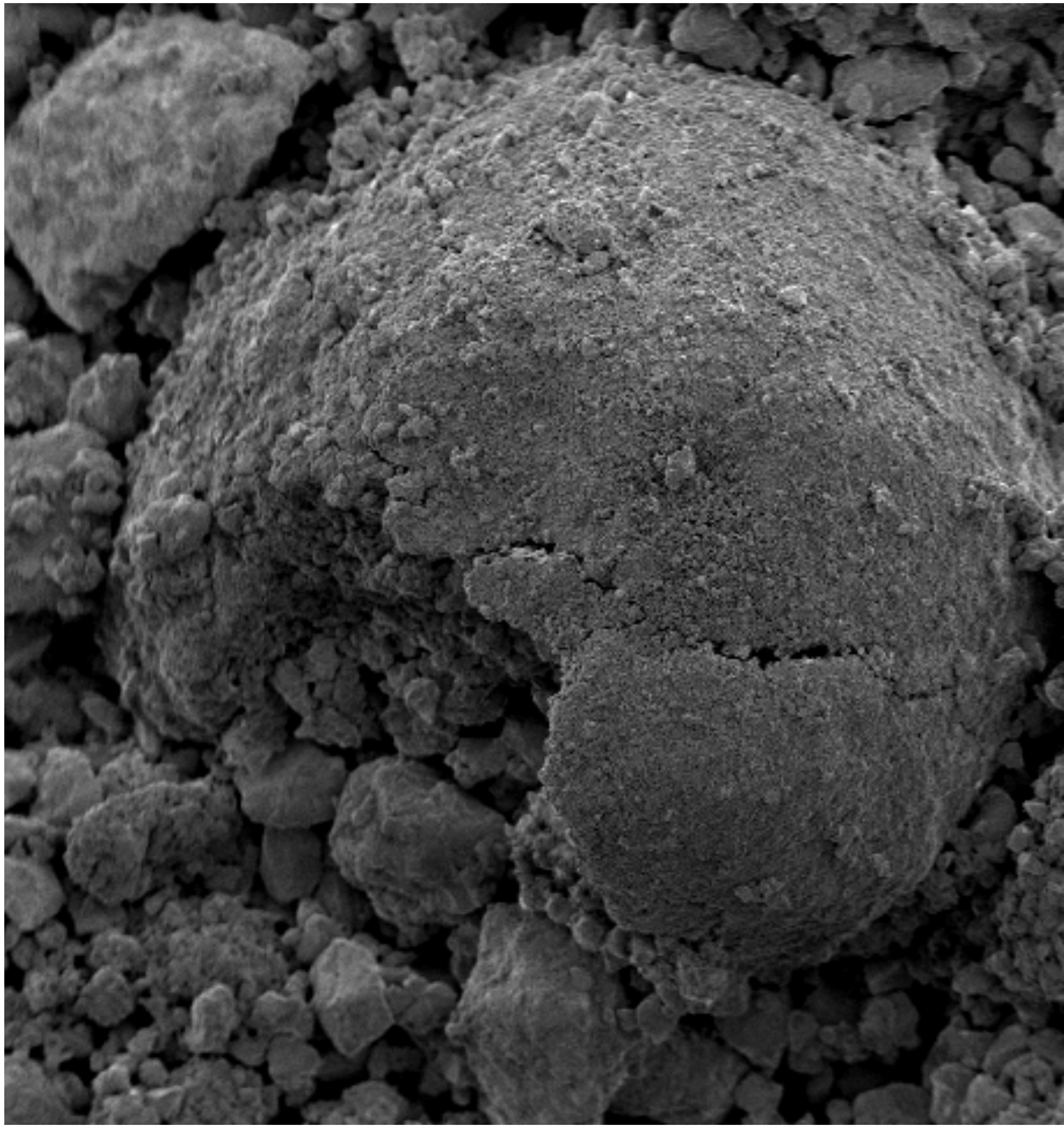

“Classical” theory: single particle terminal velocity

- **For large particles (Re_p > 500) –** inertial forces dominate:

$$V_t \approx \sqrt{\left(\frac{4}{3}\frac{d(\rho_p-\rho_f)g}{C_d\rho_f}\right)}$$

d = particle diameter

ρ_p = particle density

ρ_f = fluid density

g = acceleration due to gravity

C_d = dimensionless drag coefficient

- **For small particles (Re_p < 1) -** viscous forces dominate:

$$V_t \approx \left(\frac{\rho_p g d^2}{18\nu}\right)$$

ρ_p = particle density

g = acceleration due to gravity

d = particle diameter

v = kinematic viscosity

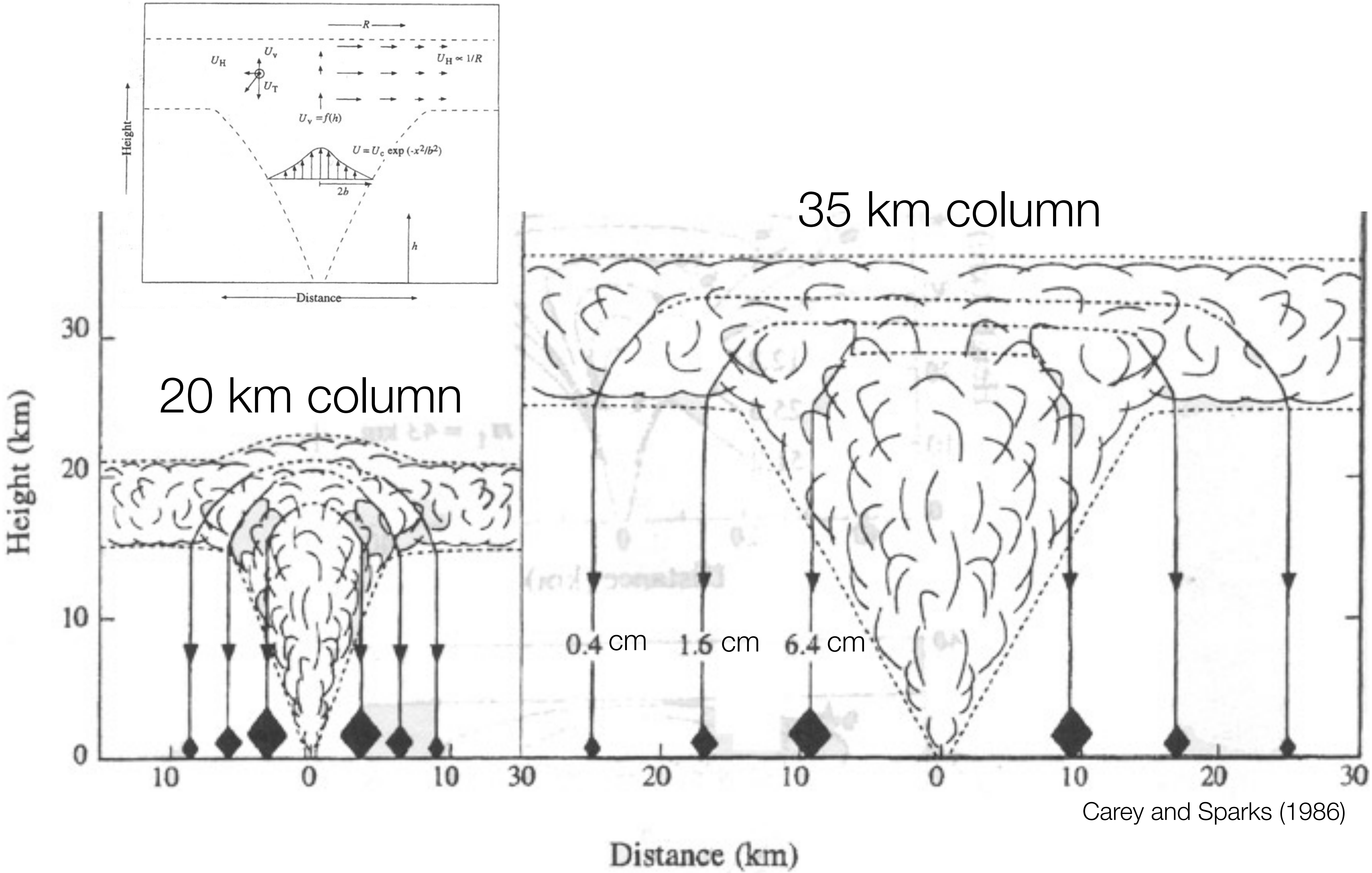

Carey and Sparks (1986)

Proximal fallout

Particle size decreases with distance

Redoubt (Alaska) 2009 Doppler radar observations

(D. Schneider, USGS)

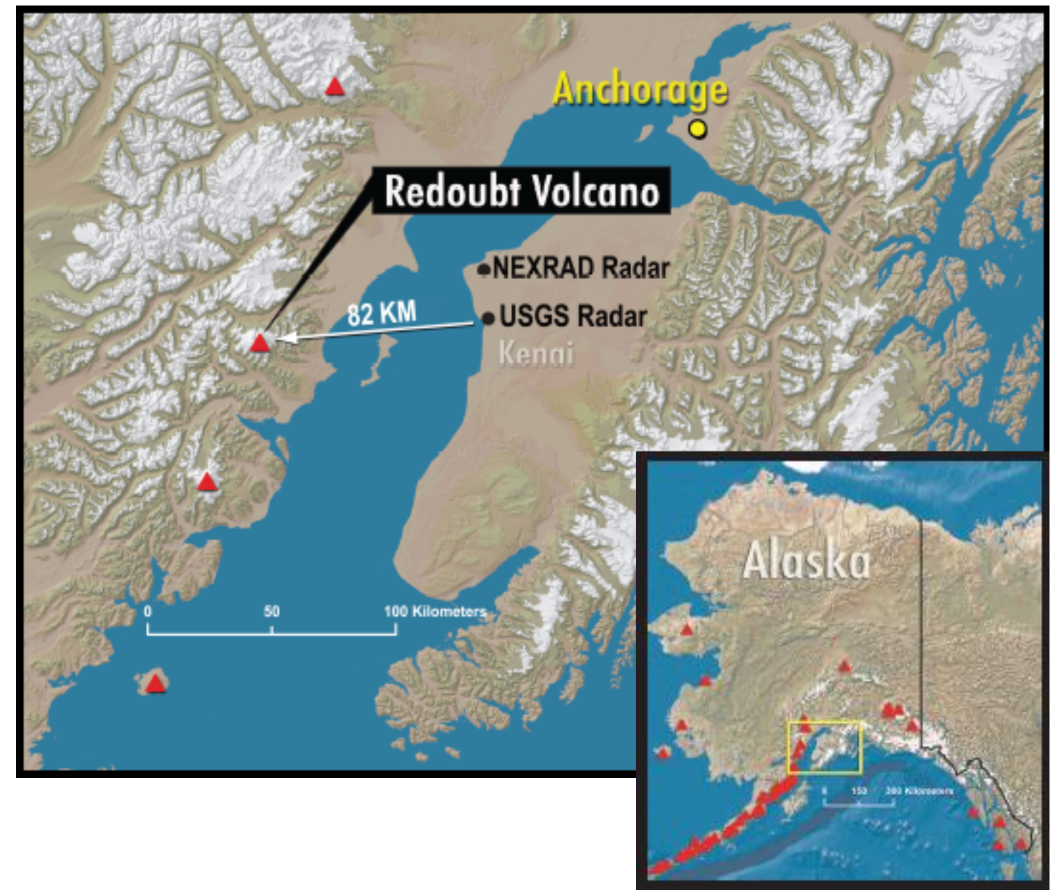

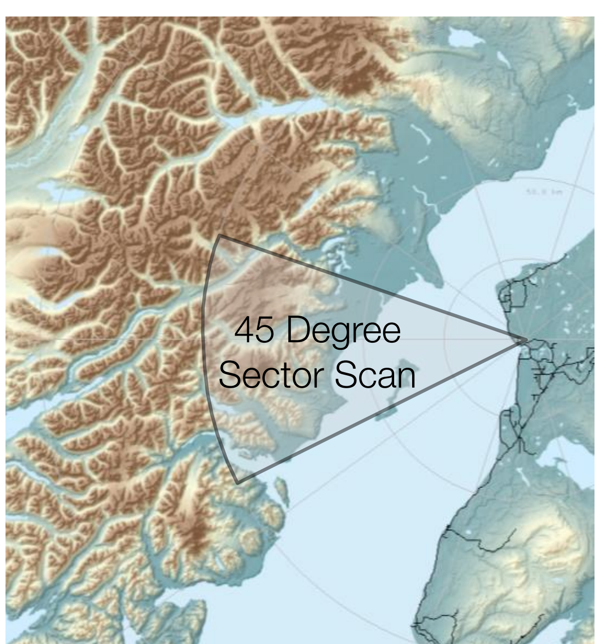

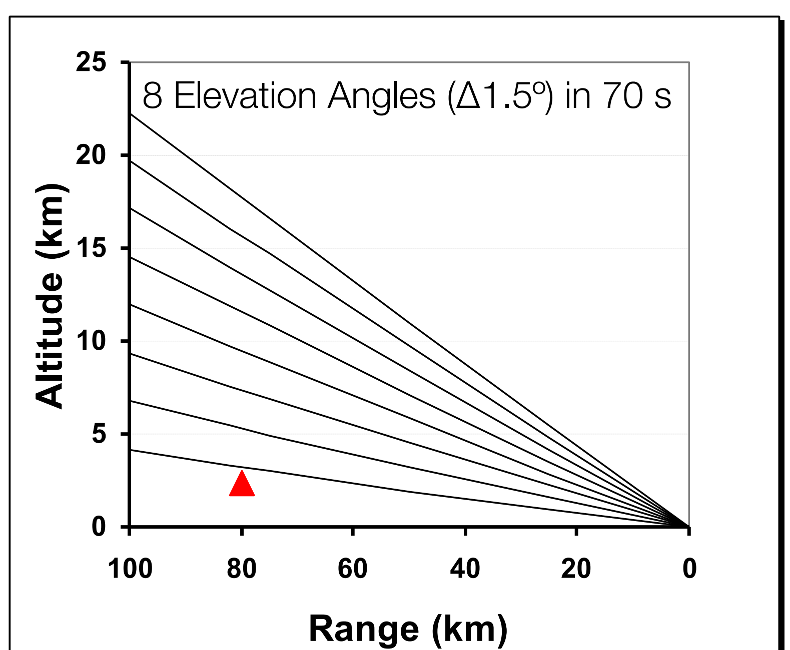

Radial Velocity: 3/23/09 12:31:00 UTC

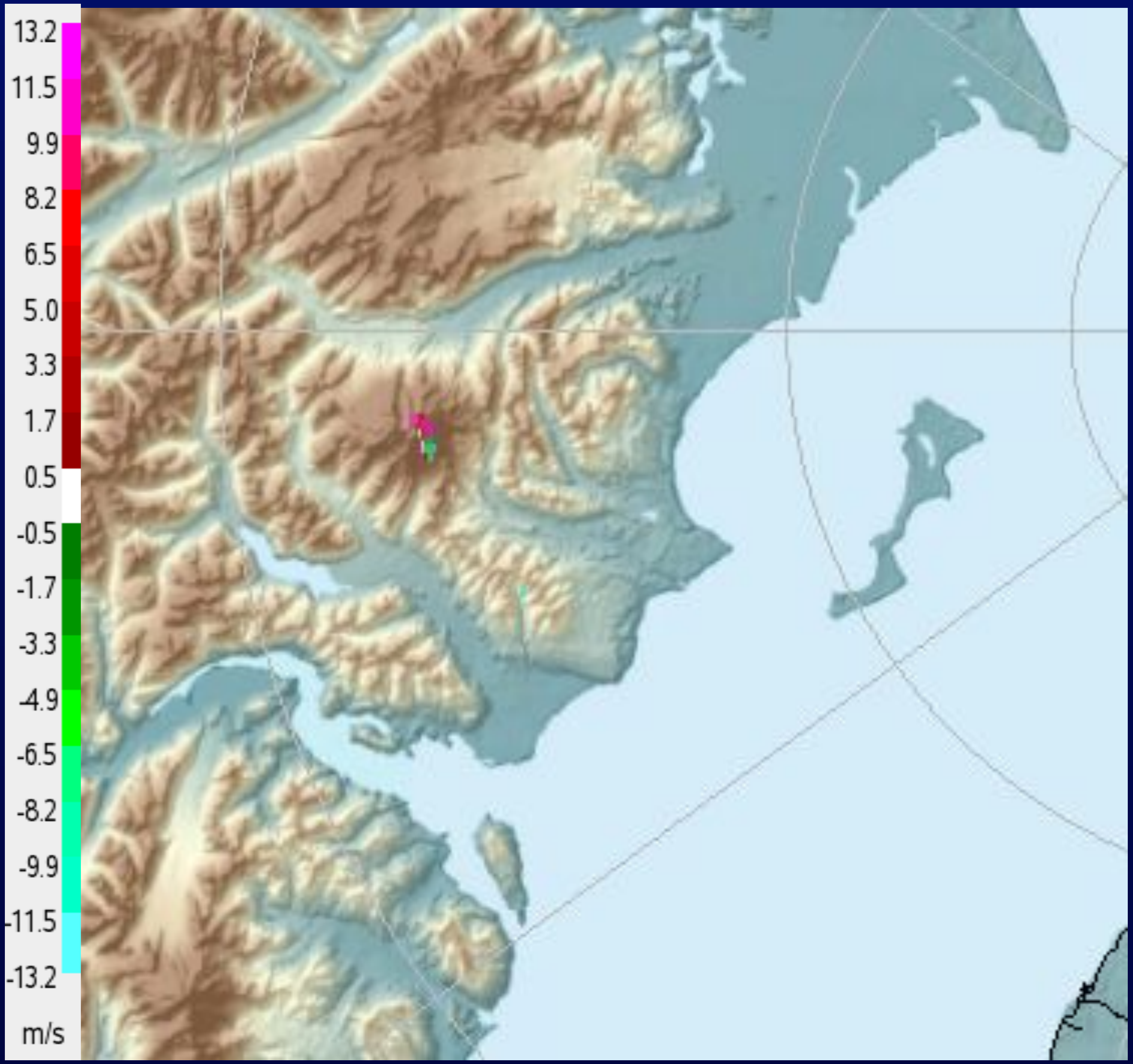

Altitude: 4.7 km asl; 2.3 km above vent

USGS

Radial Velocity: 3/23/09 12:33:30 UTC

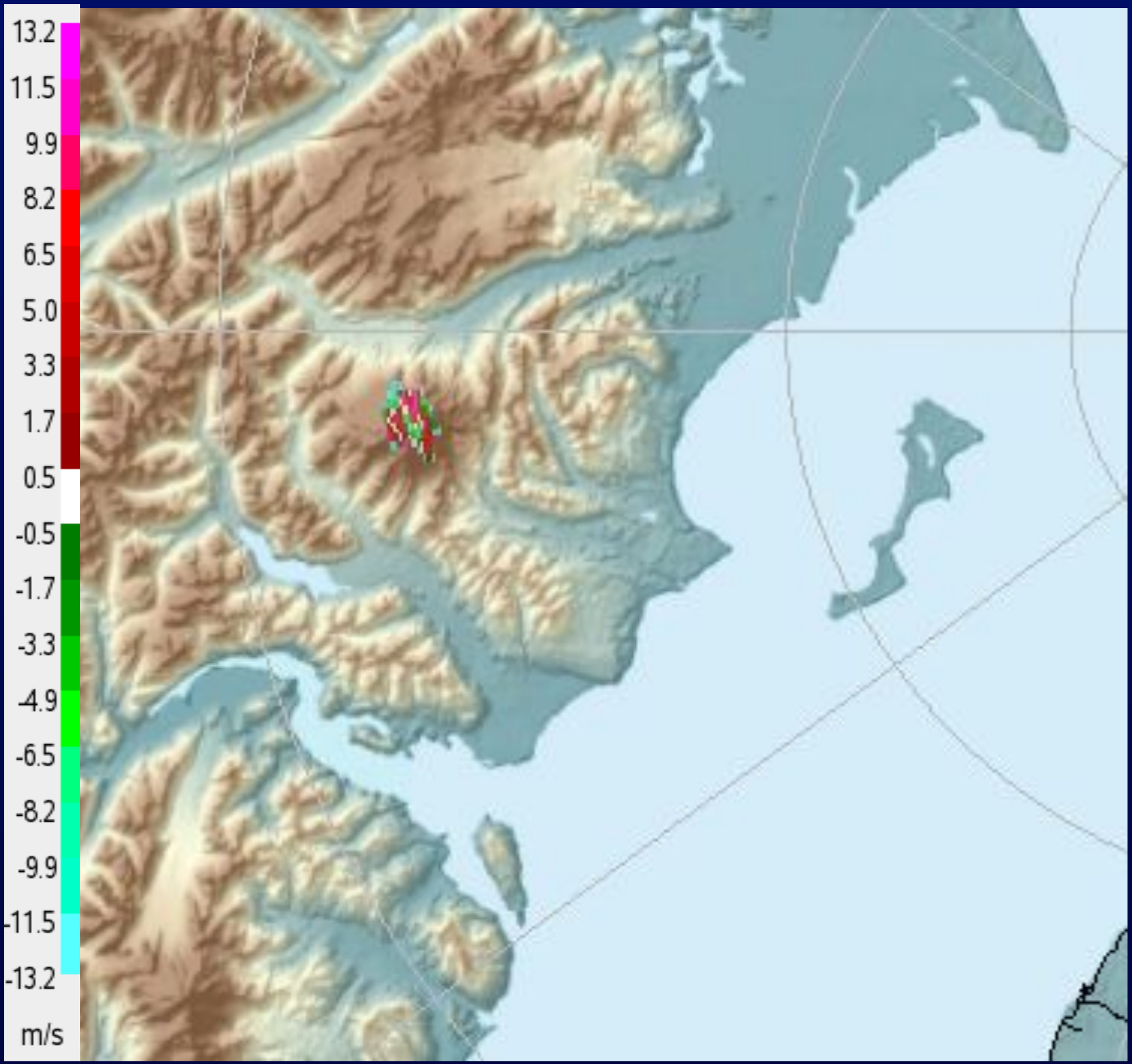

USGS

Altitude: 4.7 km asl; 2.3 km above vent

Radial Velocity: 3/23/09 12:34:00 UTC

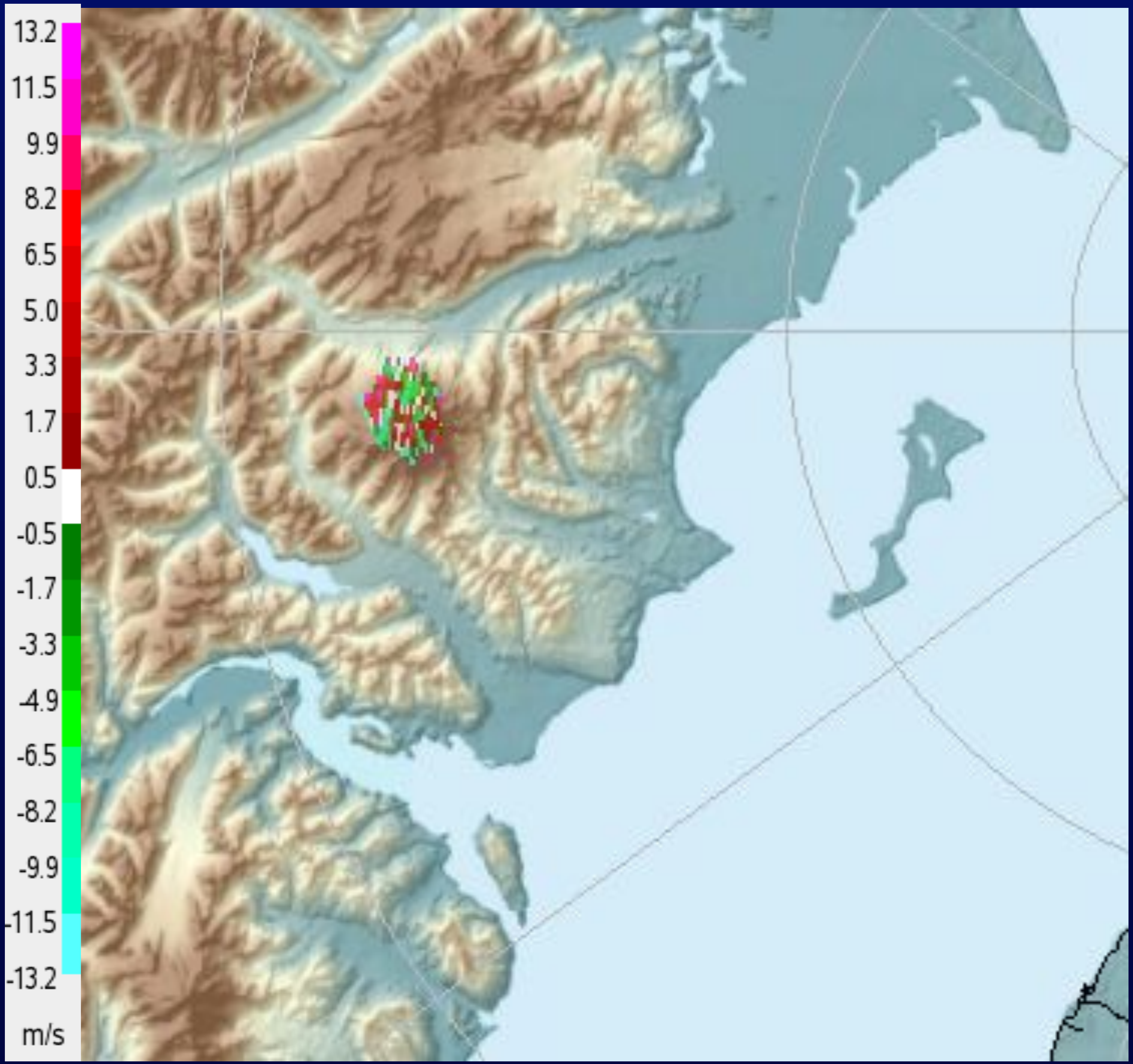

Altitude: 4.7 km asl; 2.3 km above vent

Radial Velocity: 3/23/09 12:35:30 UTC

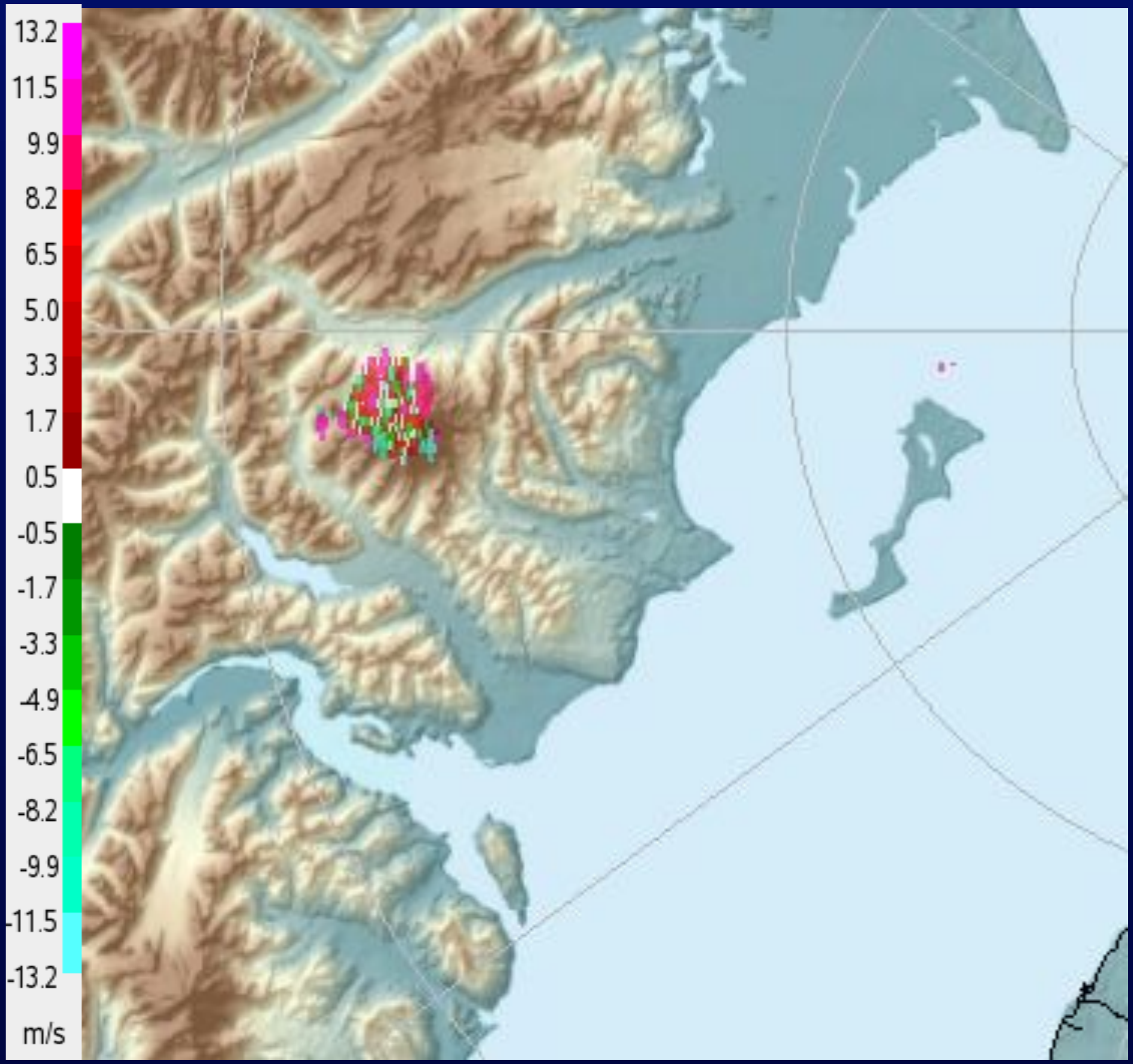

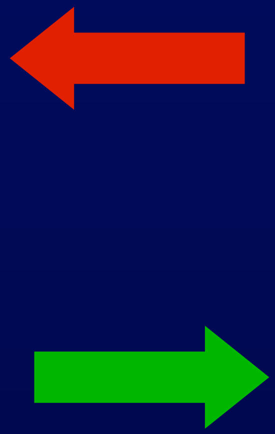

USGS

Altitude: 4.7 km asl; 2.3 km above vent

Radial Velocity: 3/23/09 12:37:00 UTC

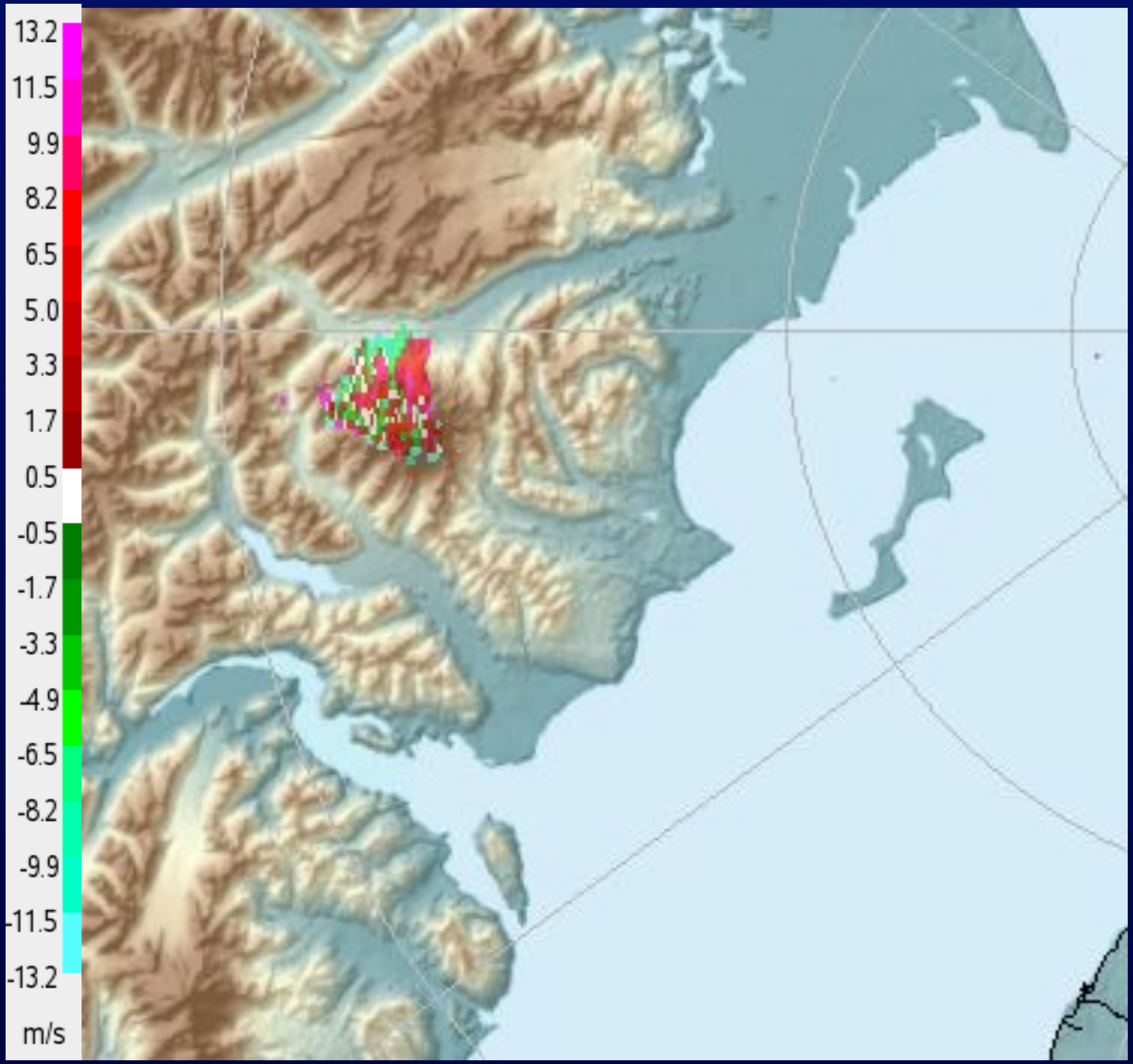

USGS

Altitude: 4.7 km asl; 2.3 km above vent

Radial Velocity: 3/23/09 12:39:30 UTC

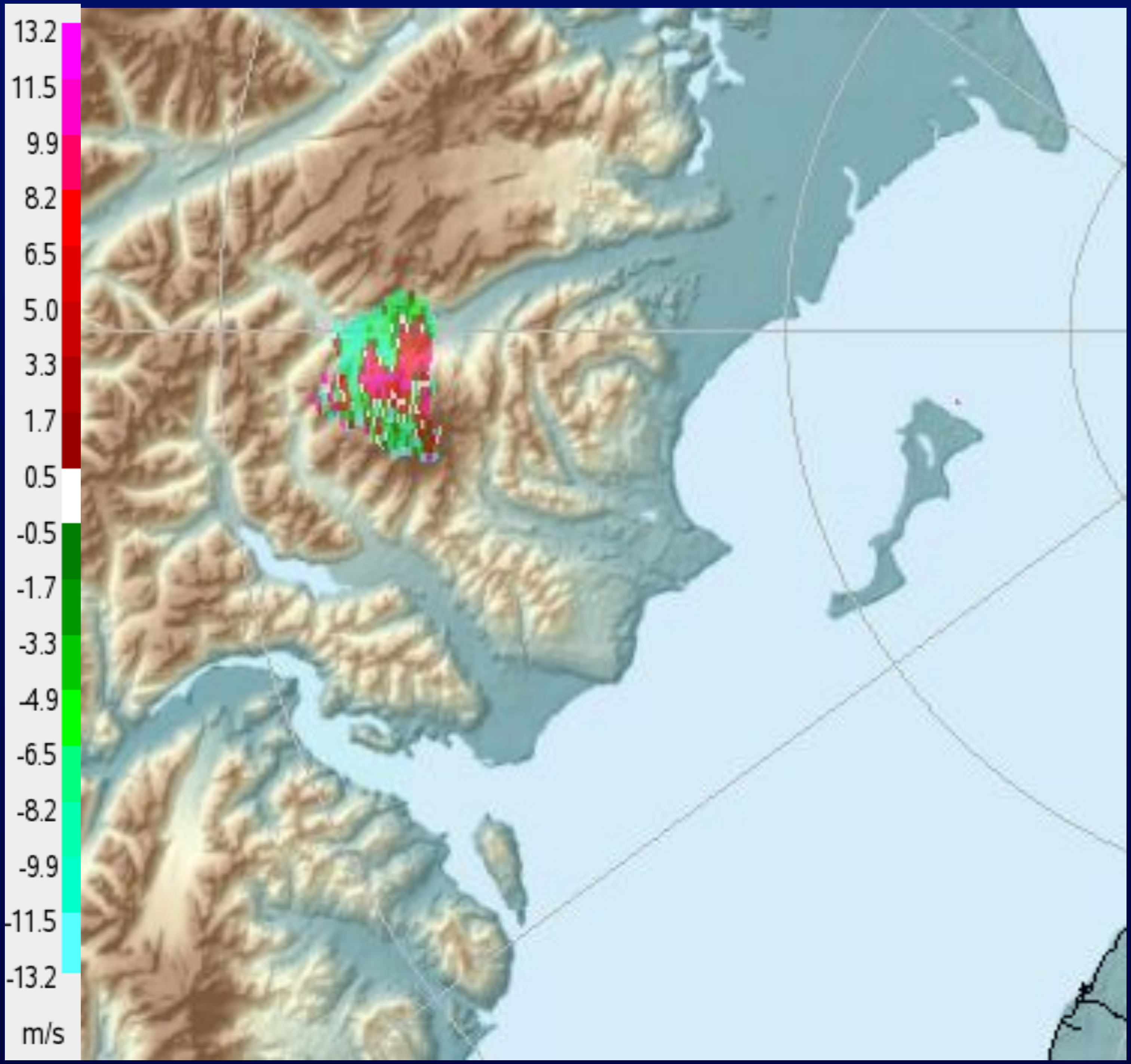

Altitude: 4.7 km asl; 2.3 km above vent

Radial Velocity: 3/23/09 12:40:00 UTC

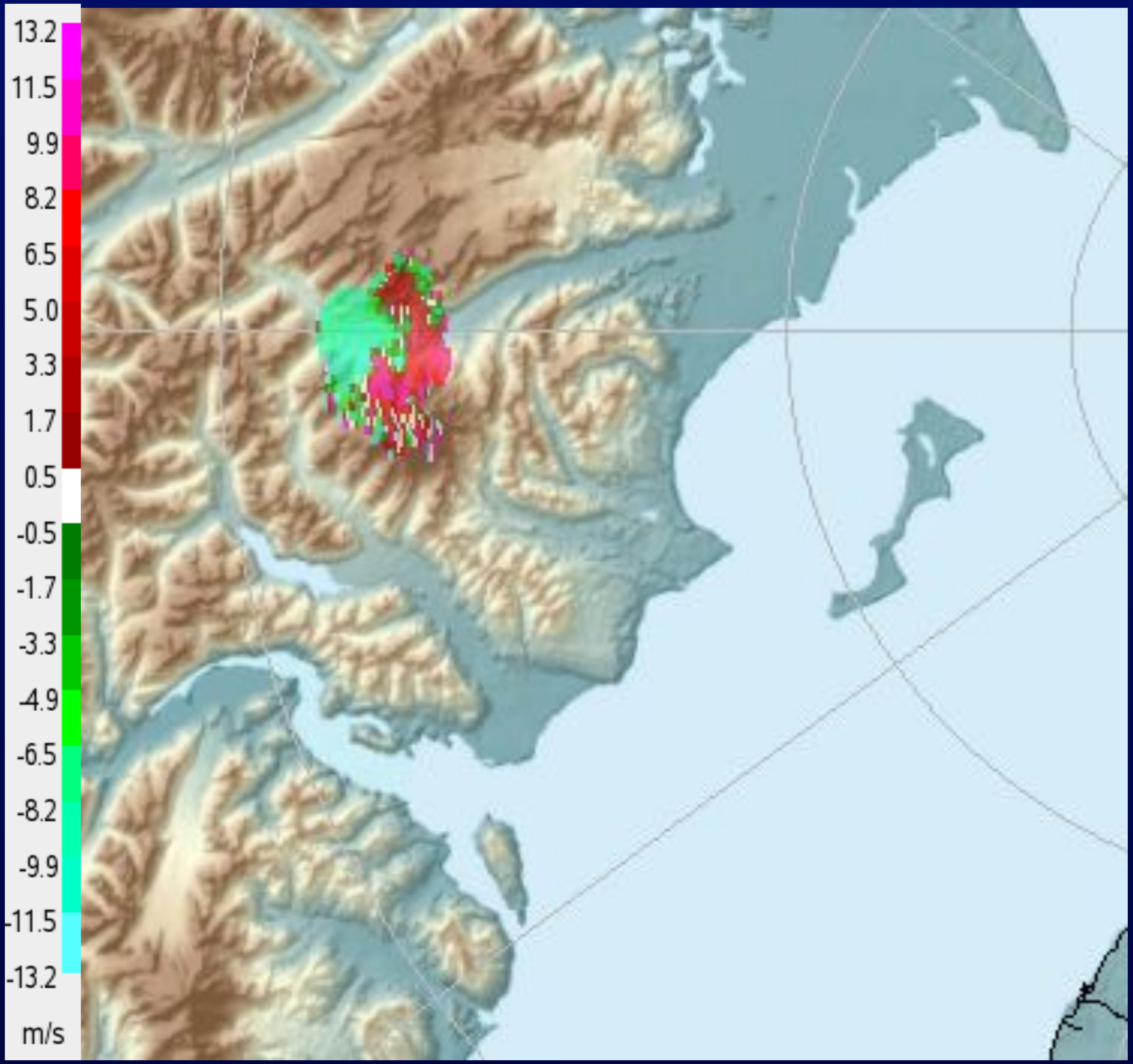

Altitude: 4.7 km asl; 2.3 km above vent

USGS

Radial Velocity: 3/23/09 12:42:30 UTC

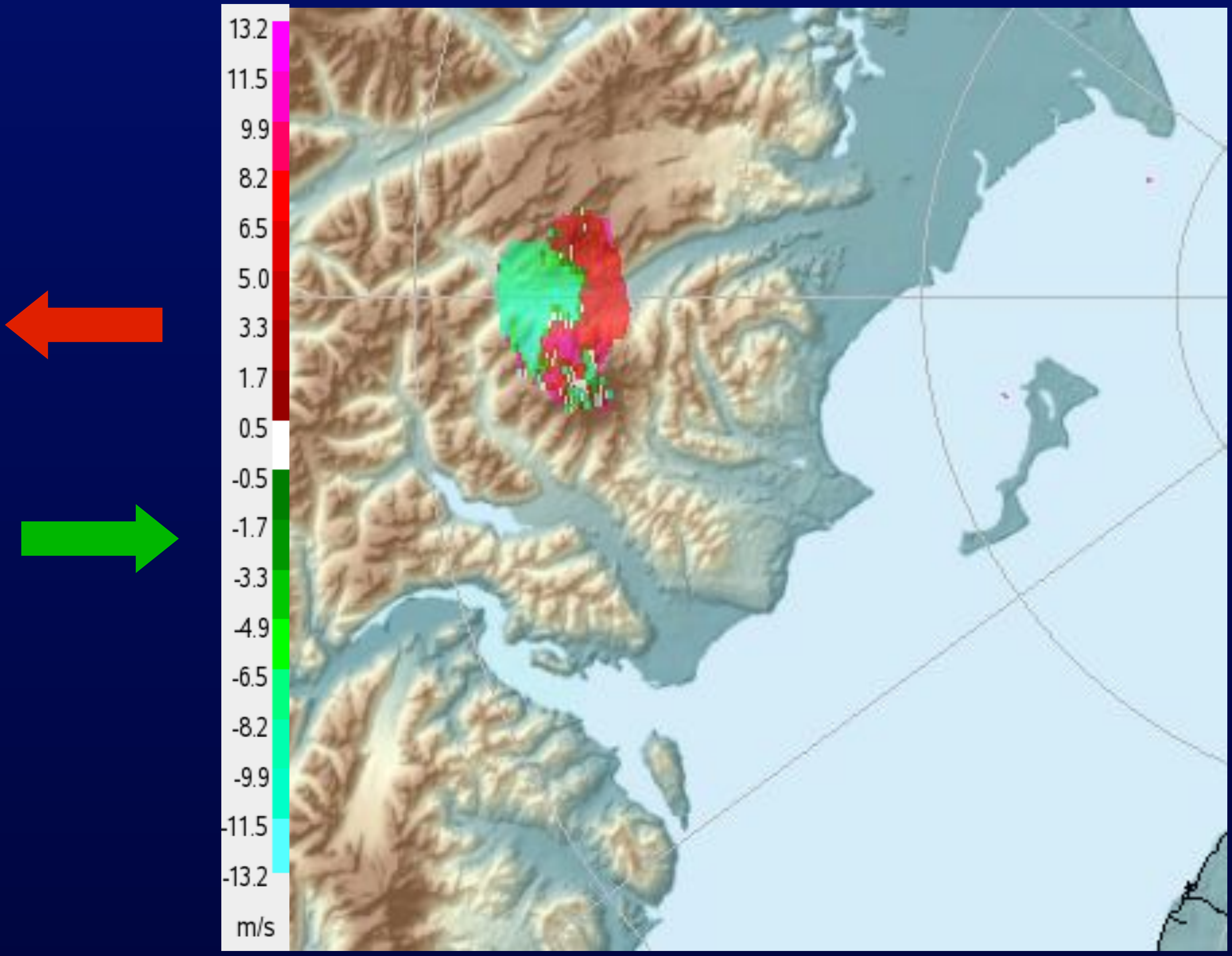

USGS

Altitude: 4.7 km asl; 2.3 km above vent

Radial Velocity: 3/23/09 12:44:00 UTC

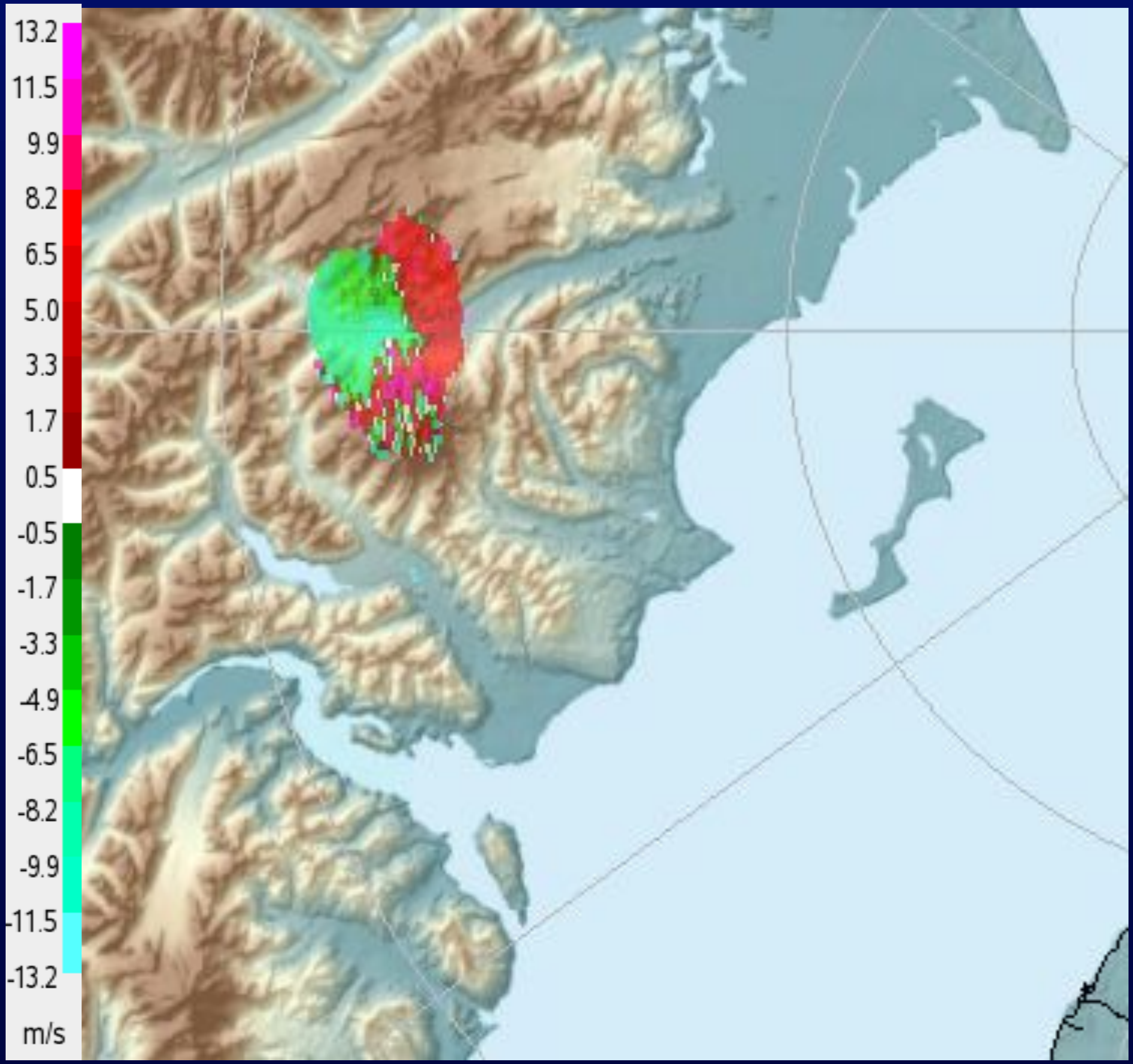

Altitude: 4.7 km asl; 2.3 km above vent

USGS

Radial Velocity: 3/23/09 12:45:30 UTC

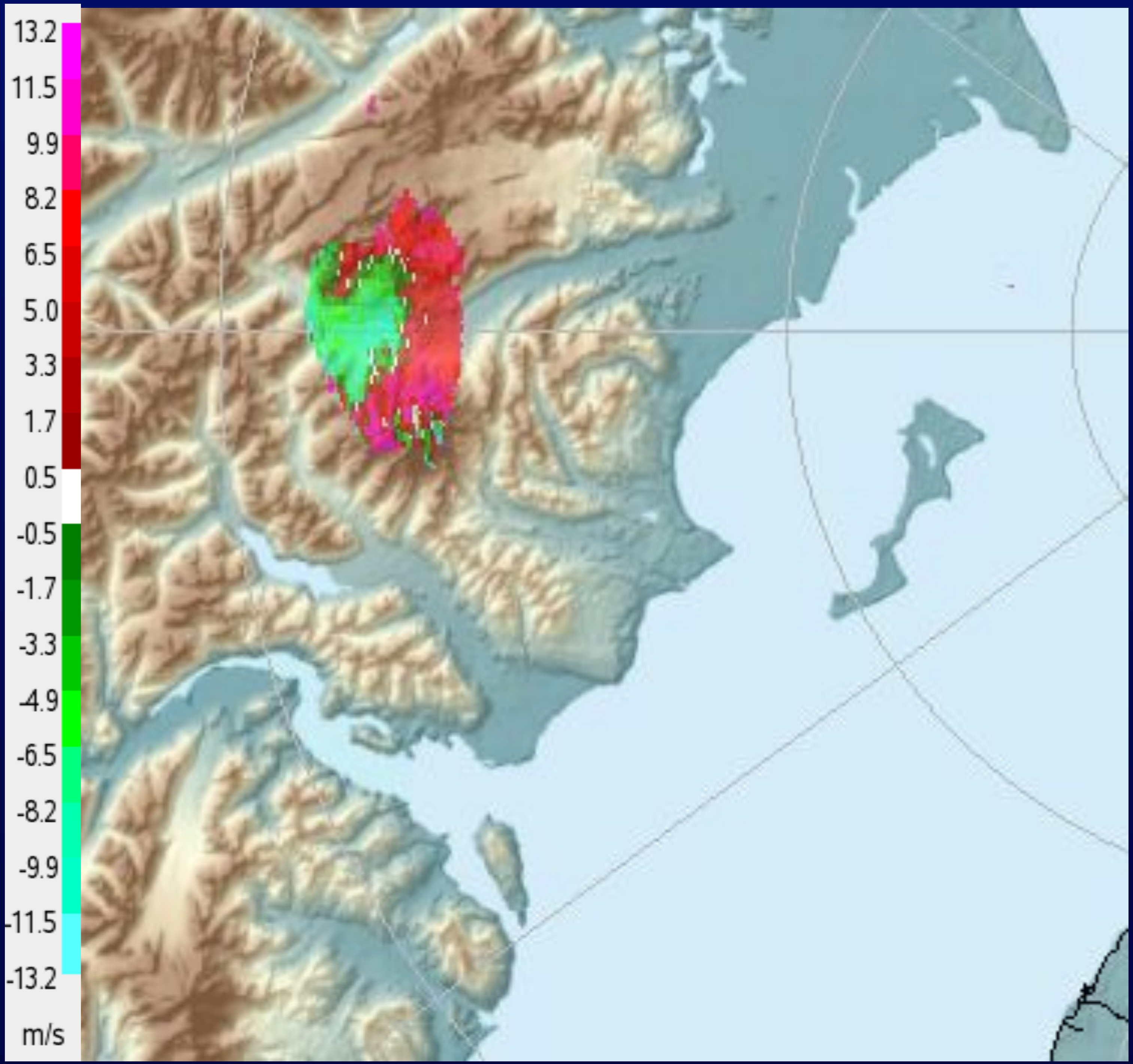

USGS

Altitude: 4.7 km asl; 2.3 km above vent

Aggregate fallout and column height

(C. Wallace; D. Schneider, USGS)

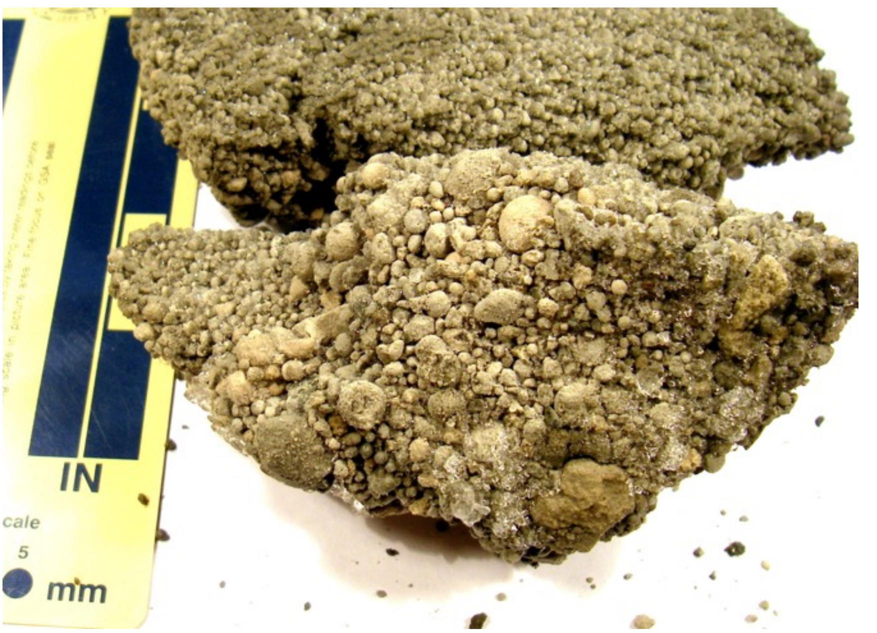

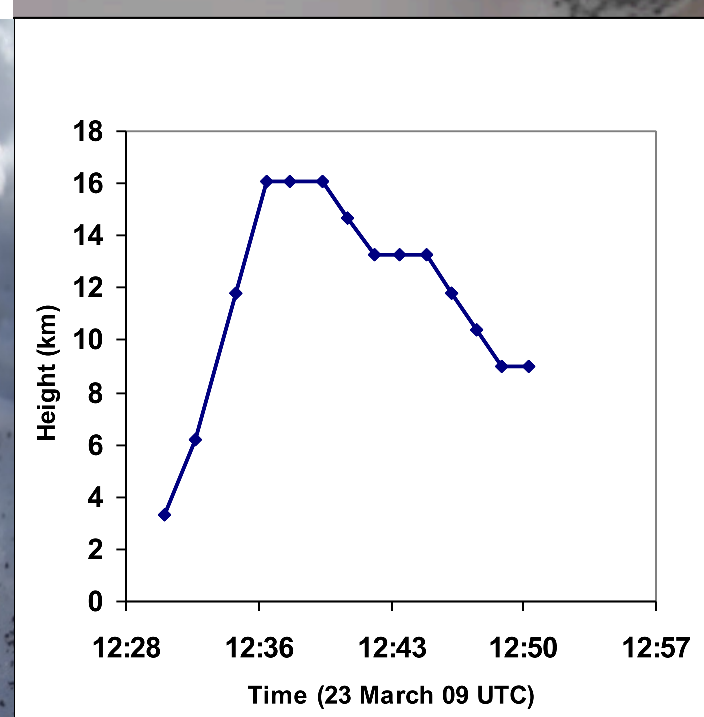

Ash aggregate morphological variability

PARTICLE CLUSTERS

ACCRETIONARY PELLETS

Ash Clusters (PC1)

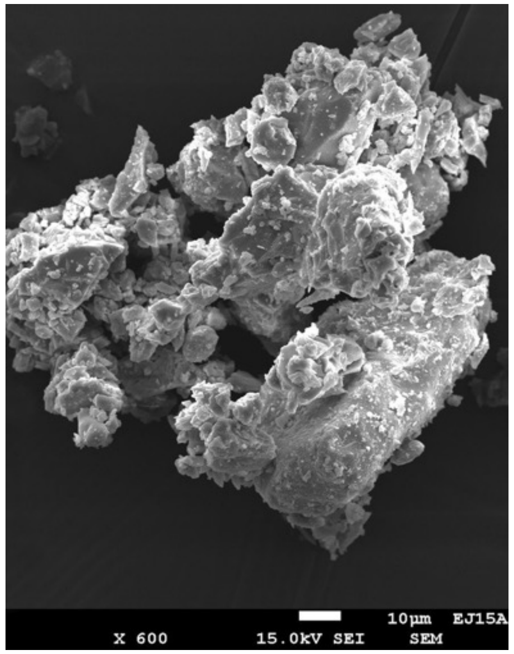

Coated Particles (PC2)

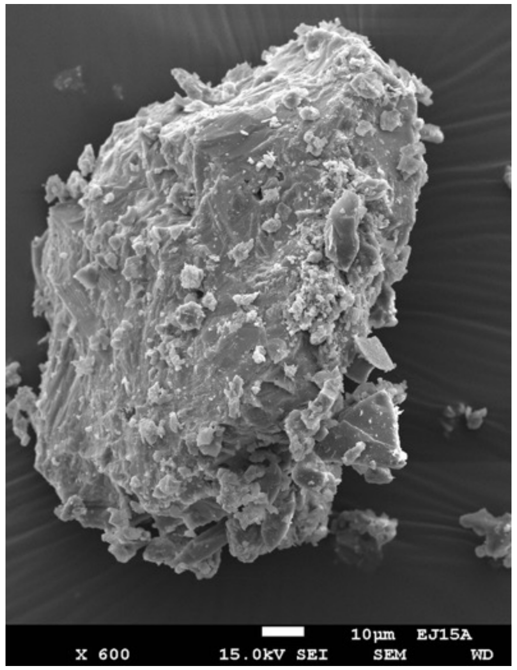

Unstructured pellets (AP1)

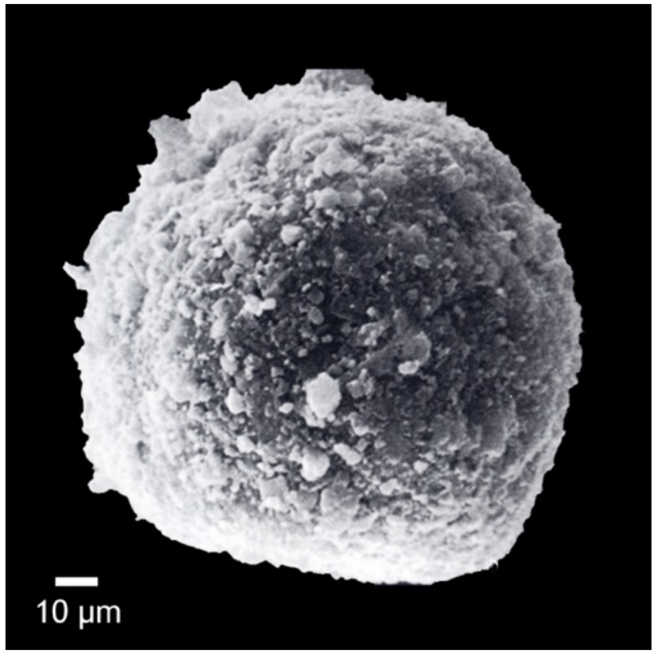

Concentric pellets (AP2)

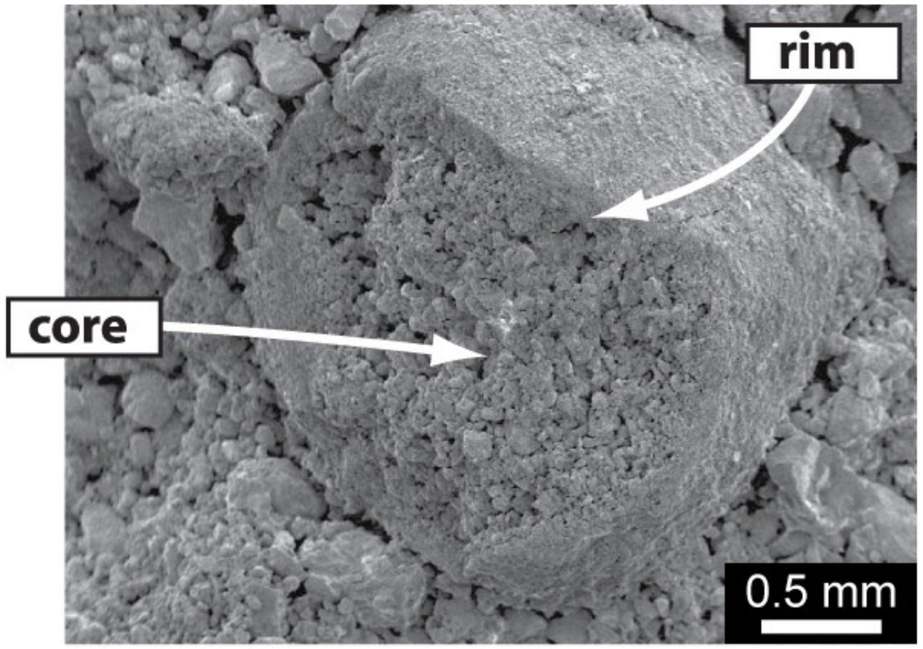

Liquid Pellets (AP3)

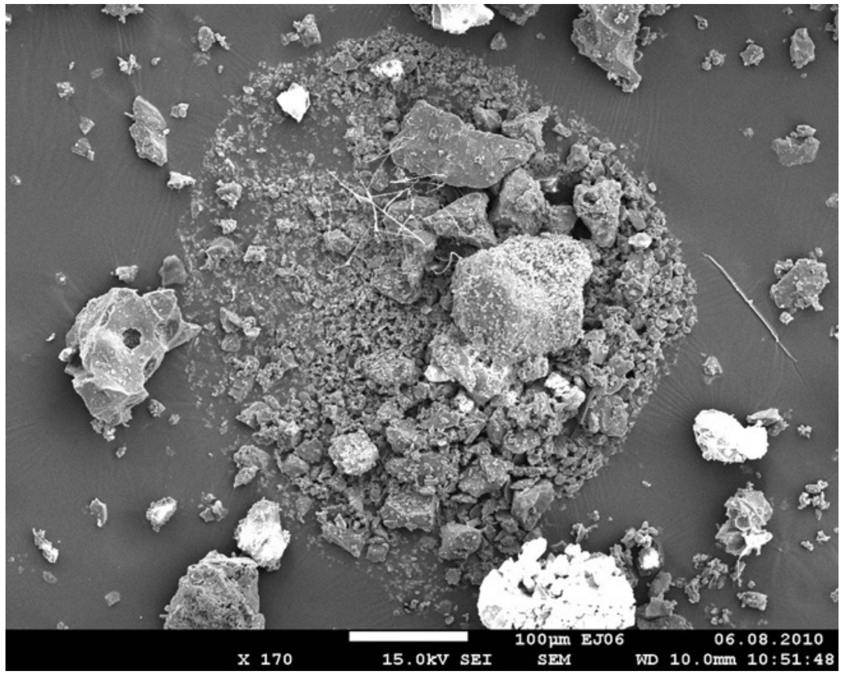

Brown, Bonadonna, Durant (2012),
A review of volcanic ash aggregation,
Phys. Chem. Earth., 45-46, 65-78.

Eyjafjallajokull, Iceland, 2010 eruption: proximal <50 km (Data and SEM images from C. Bonadonna)

Particle clusters

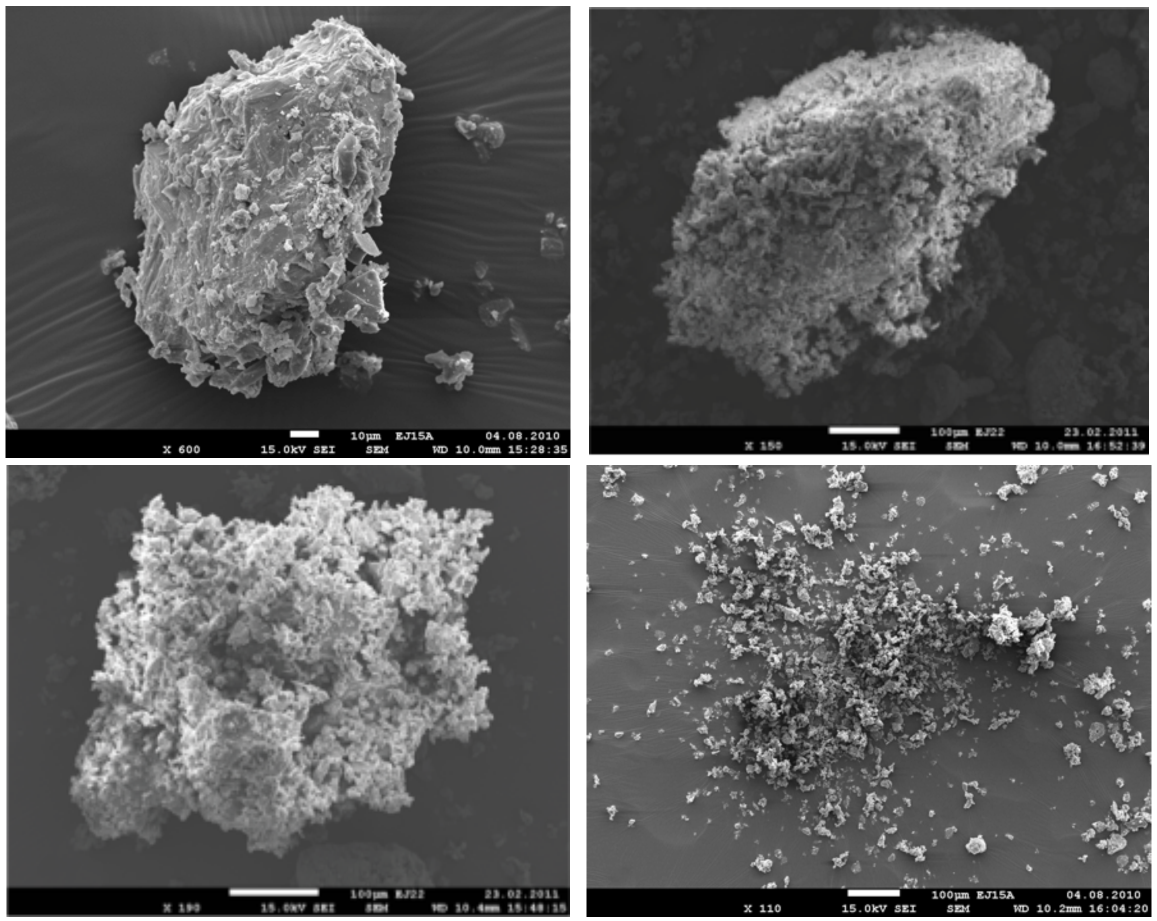

Accretionary pellets

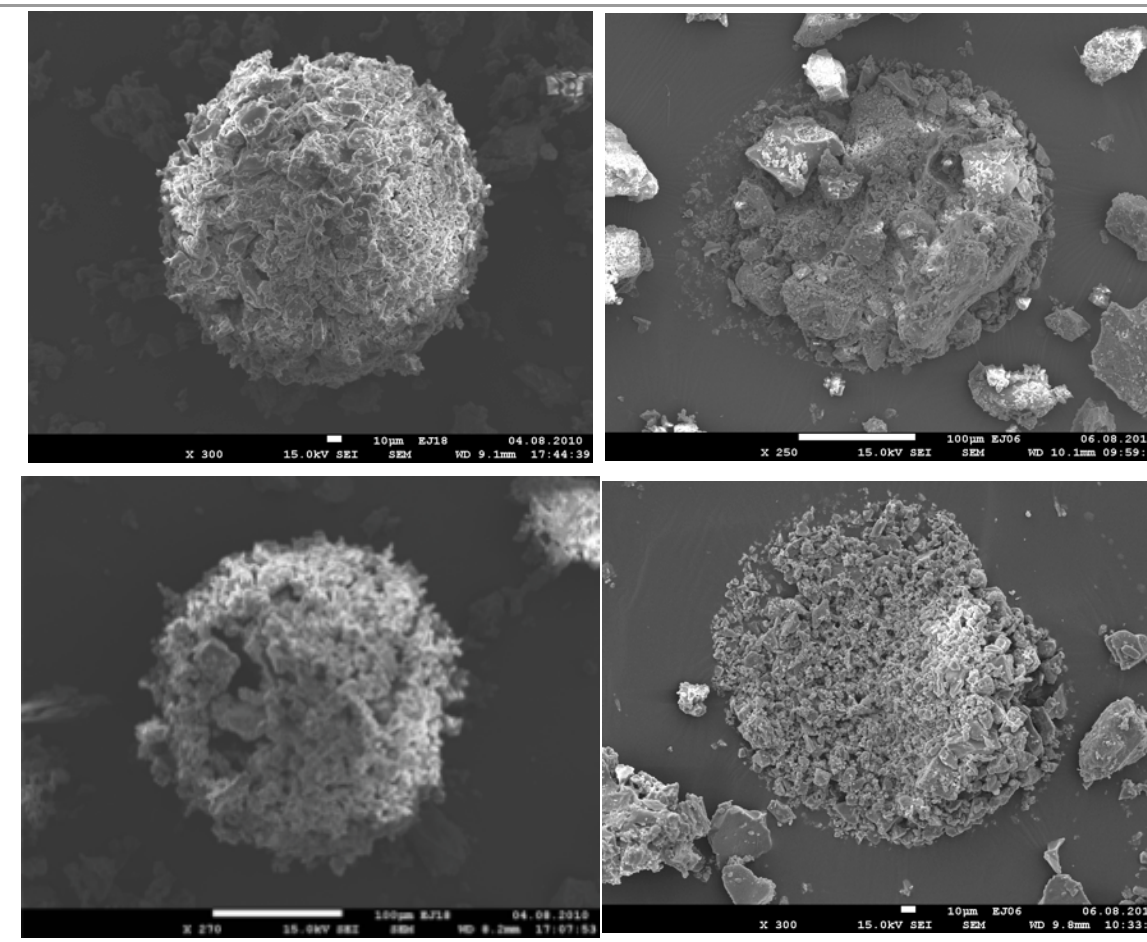

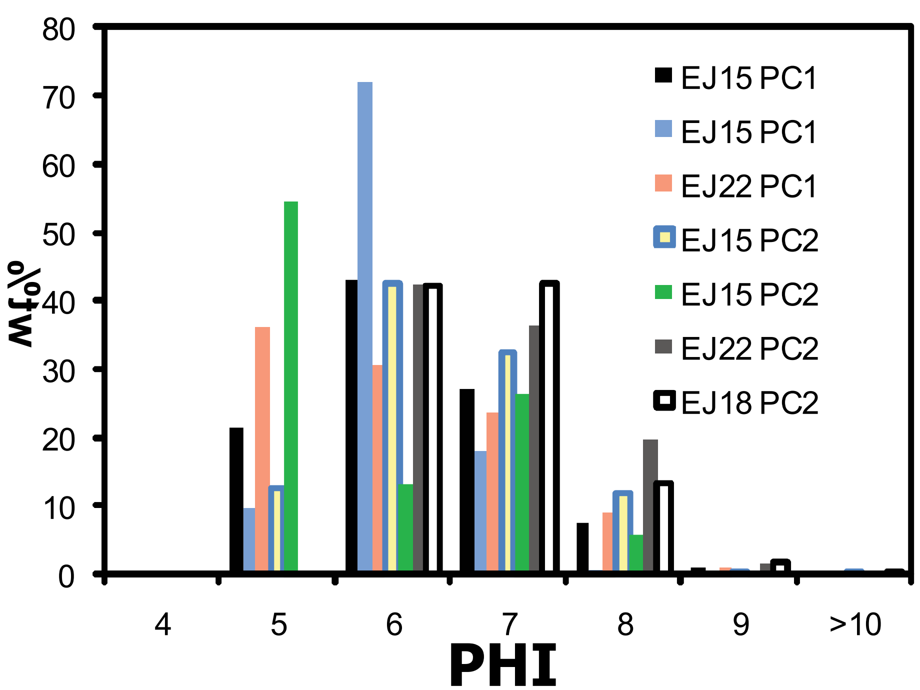

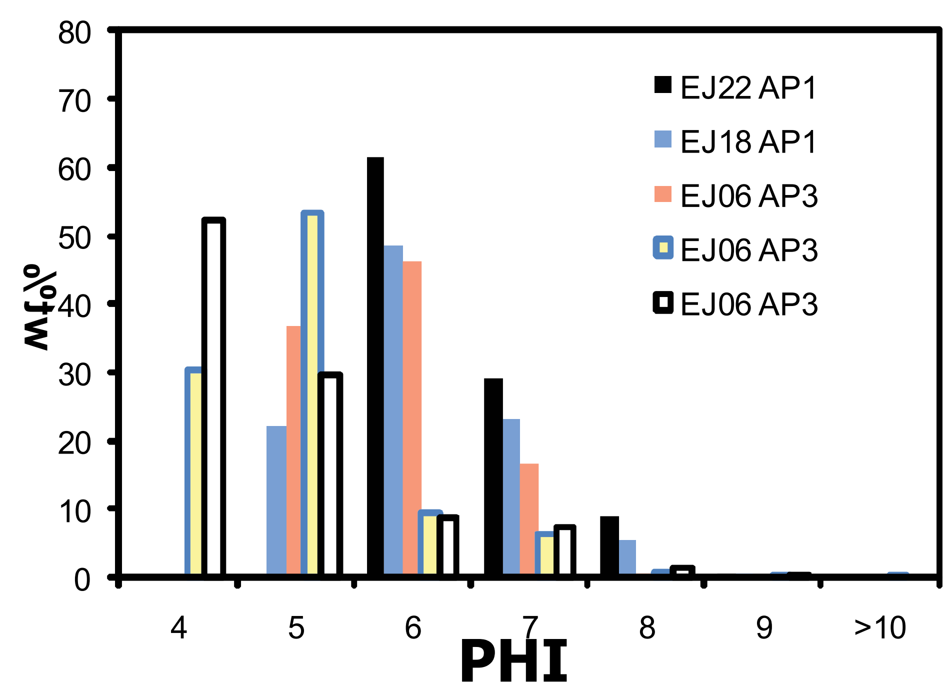

Distal fallout (>1000 km) from recent Icelandic eruption clouds

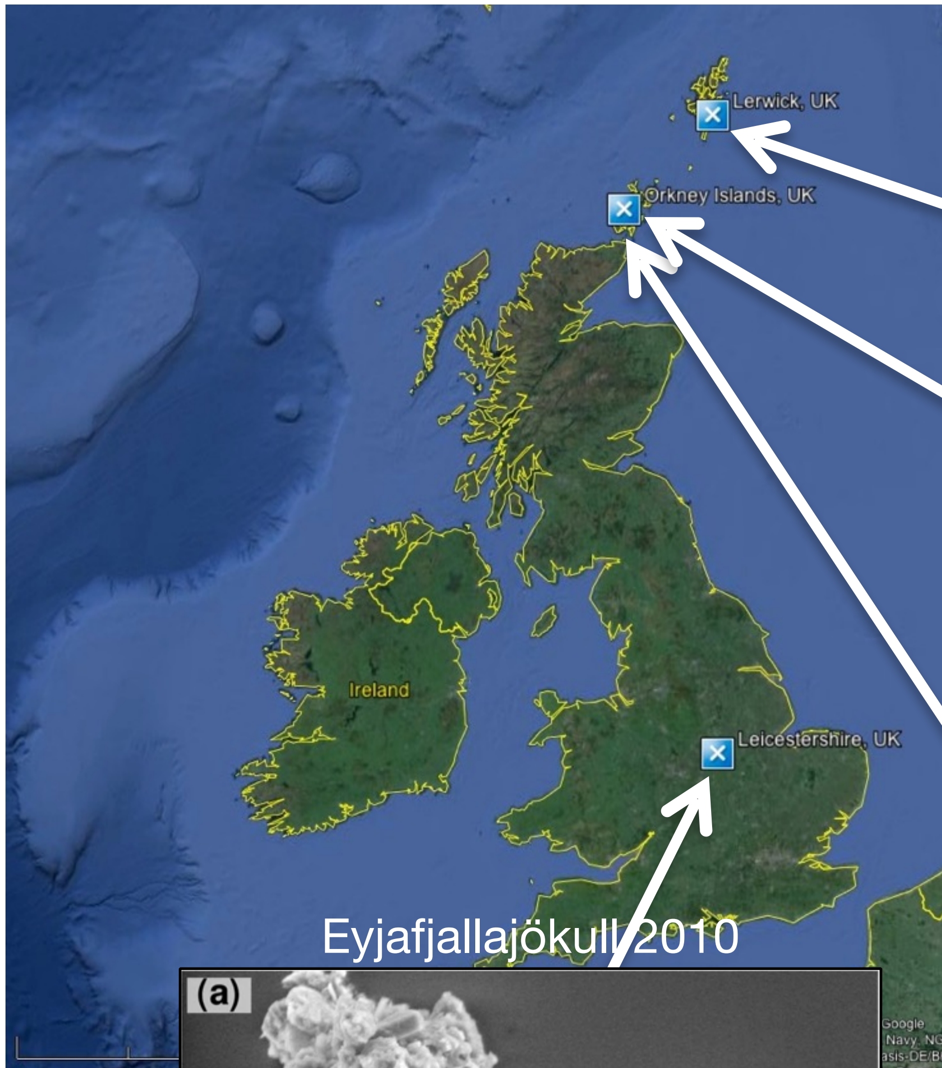

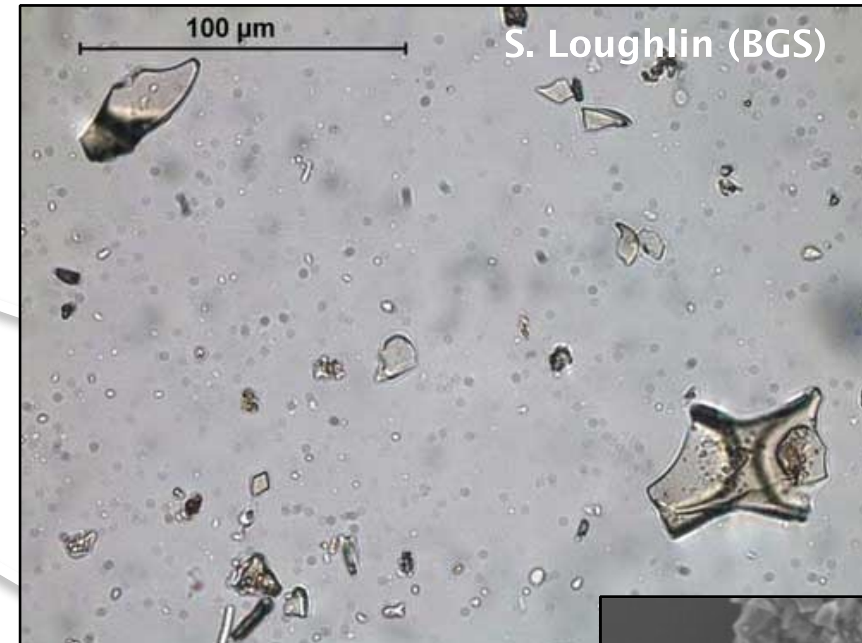

Stevenson, J. A., S. C. Loughlin, A. Font, G. W. Fuller, A. MacLeod, I. W. Oliver, B. Jackson, C. J. Horwell, T. Thordarson, and I. Dawson (2013), **UK monitoring and deposition of tephra from the May 2011 eruption of Grímsvötn, Iceland**, J. App. Volcanol., 2(1), 3, doi: 10.1186/2191-5040-2-3.

Eyjafjallajökull 2010

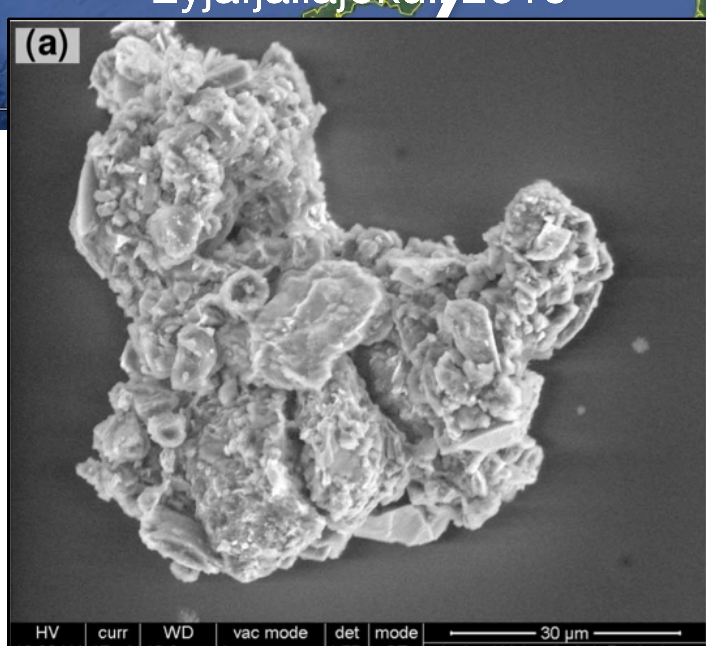

Grímsvötn 2011

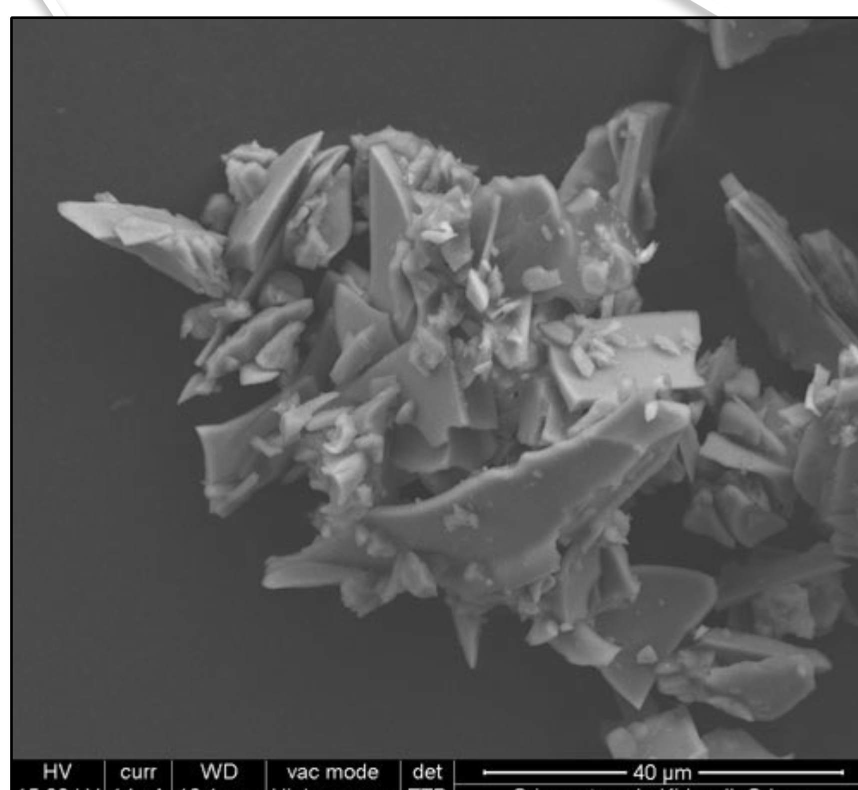

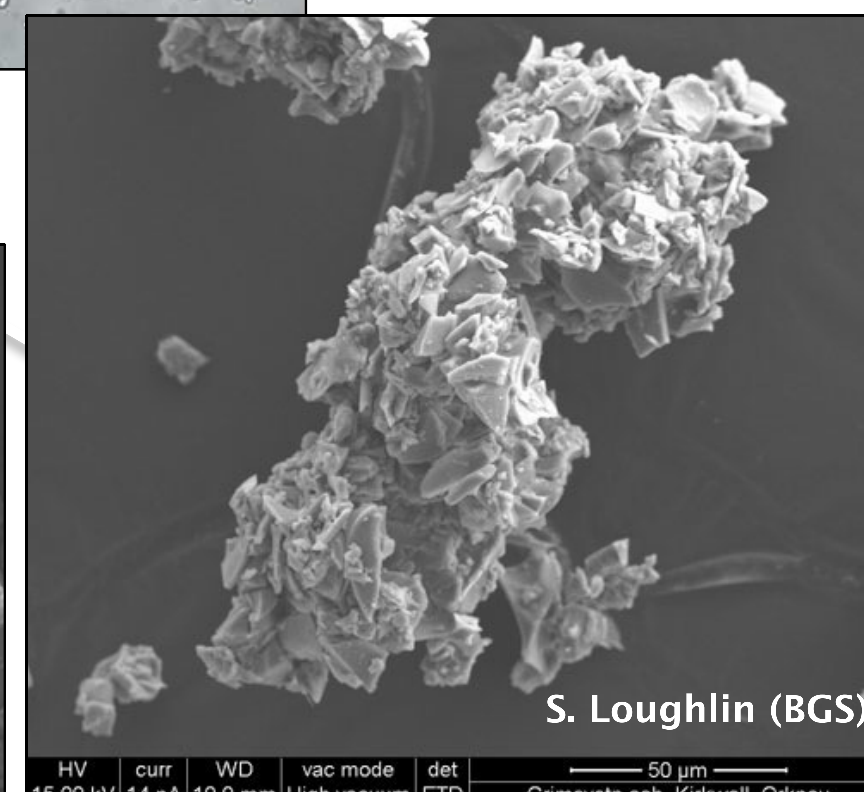

Stevenson, Loughlin, Rae, et al. (2012), **Distal deposition of tephra from the Eyjafjallajökull 2010 summit eruption**, J. Geophys. Res., 117(B9), B00C10

Deviations from “classical” theory

Hydrometeors, turbulence and instabilities

Distal ash deposition anomalies

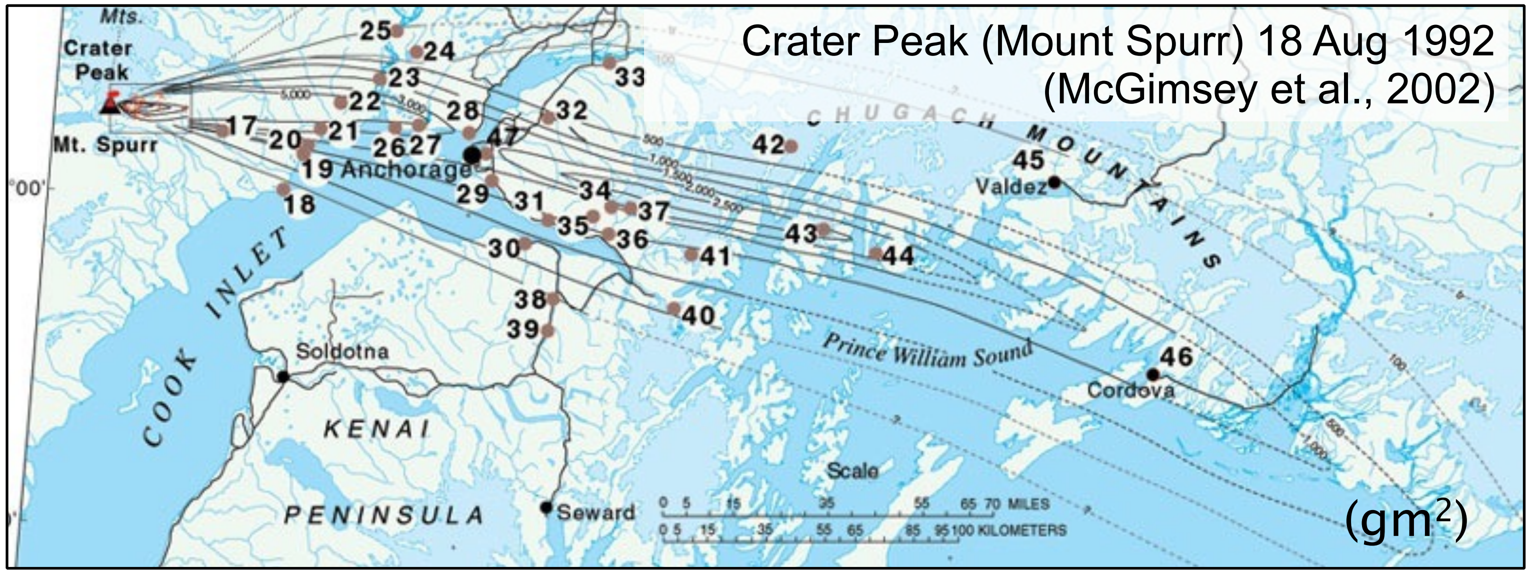

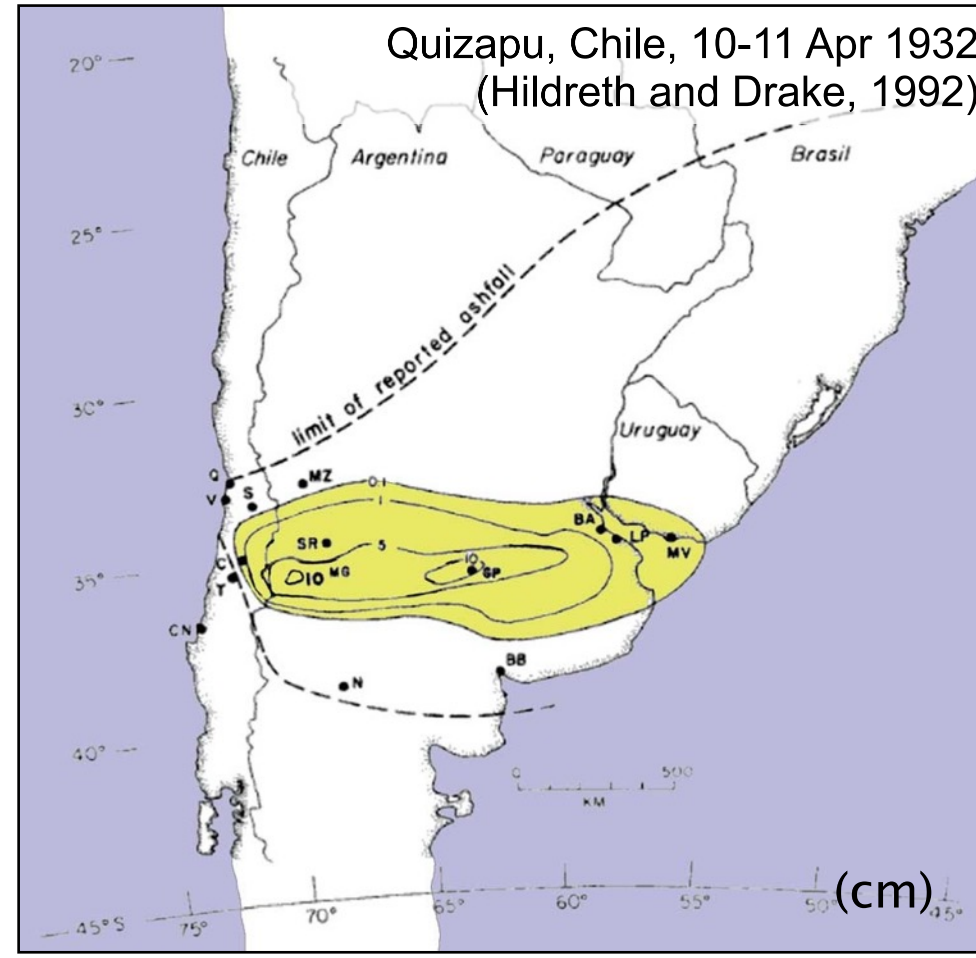

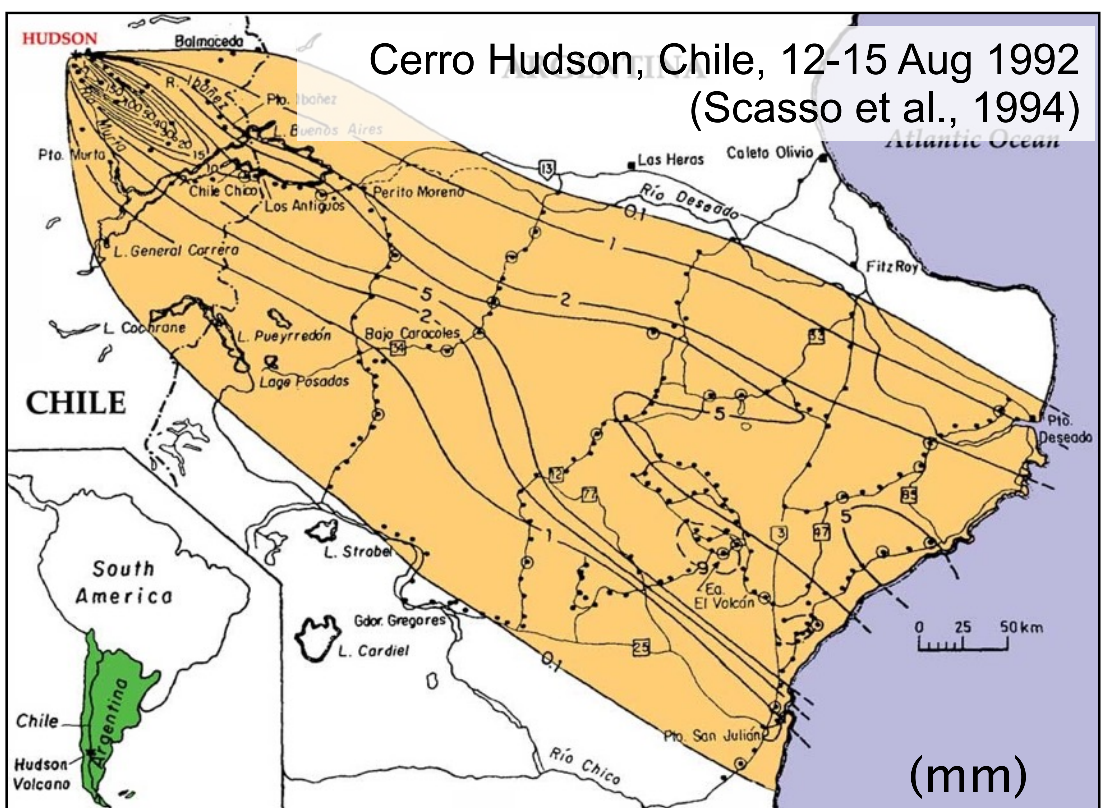

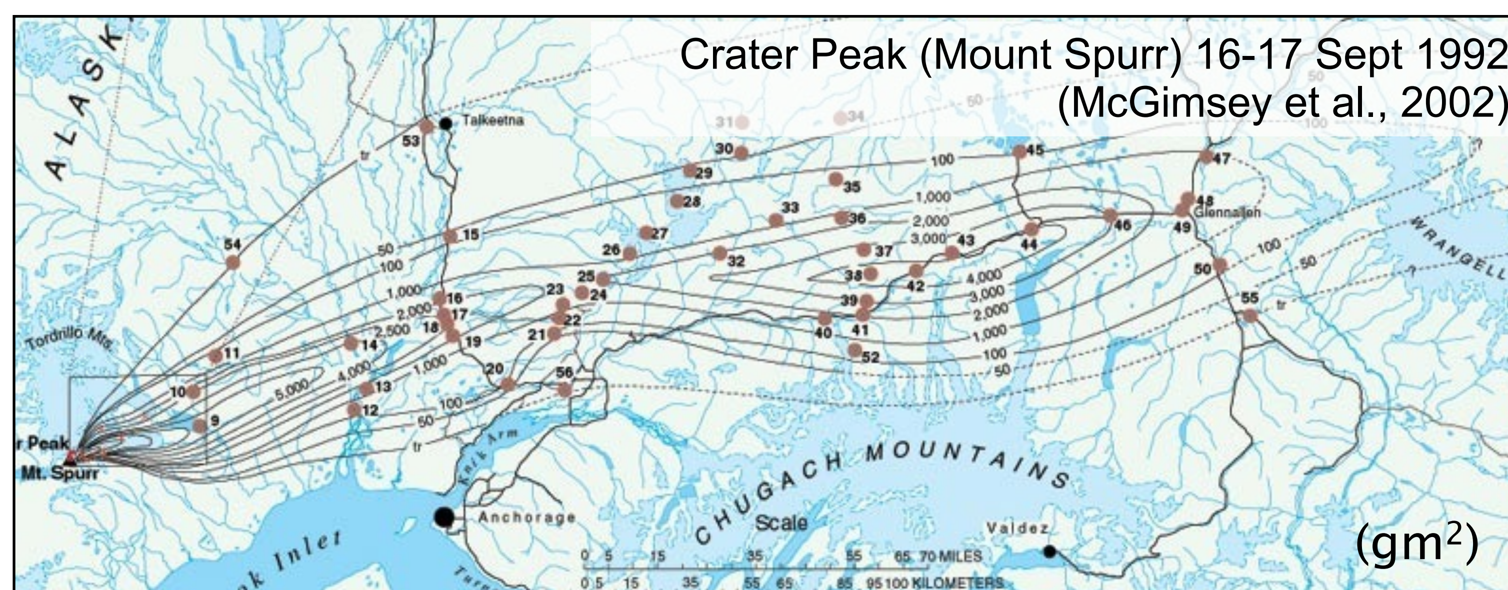

Mount St. Helens, USA, 18 May 1980

(Durant et al., *J. Geophys. Res.*, 2009)

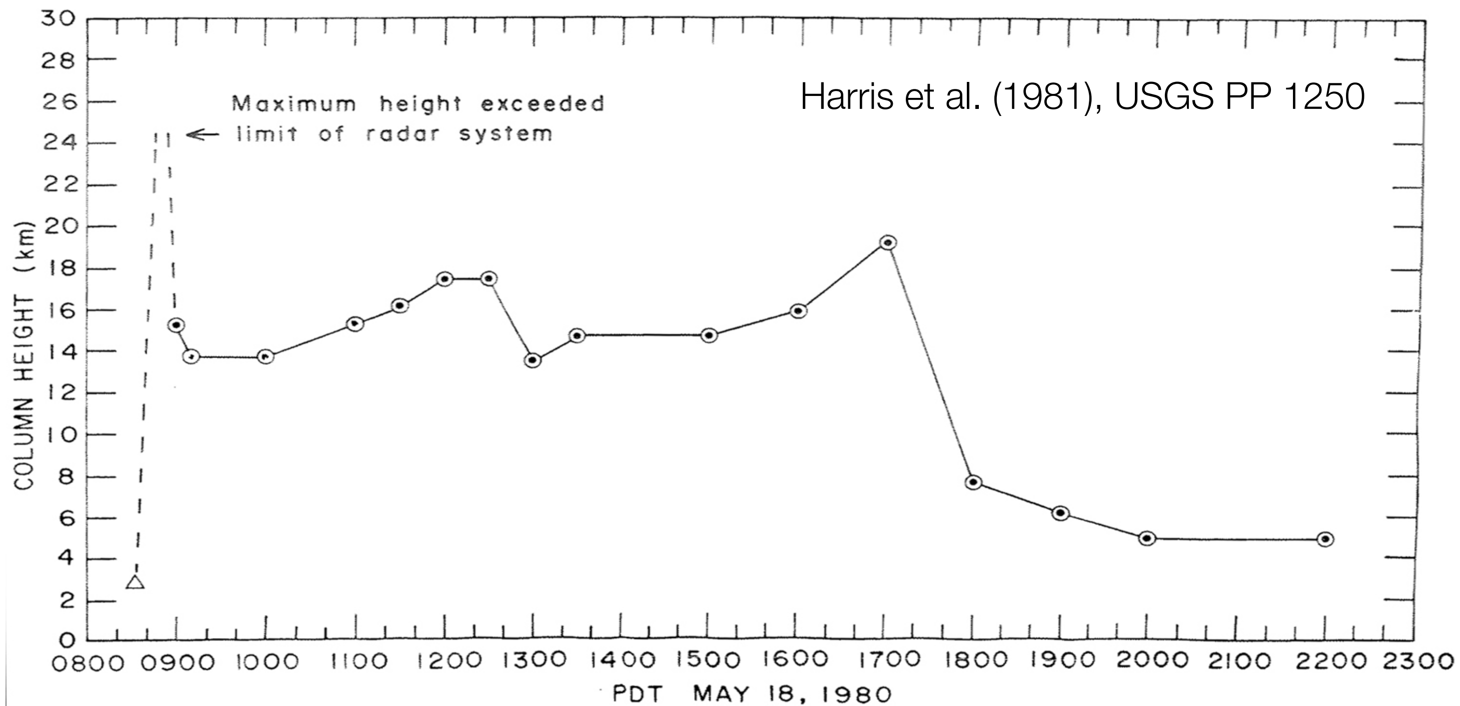

FIGURE 1.3. Height of the 18 May 1980 Plinian eruption column near Mount St. Helens, as determined by Portland WS radar. Triangle represents elevation of Mount St. Helens vent at the onset of eruption. Heights are relative to sea el. From Harris et al., 1981a.

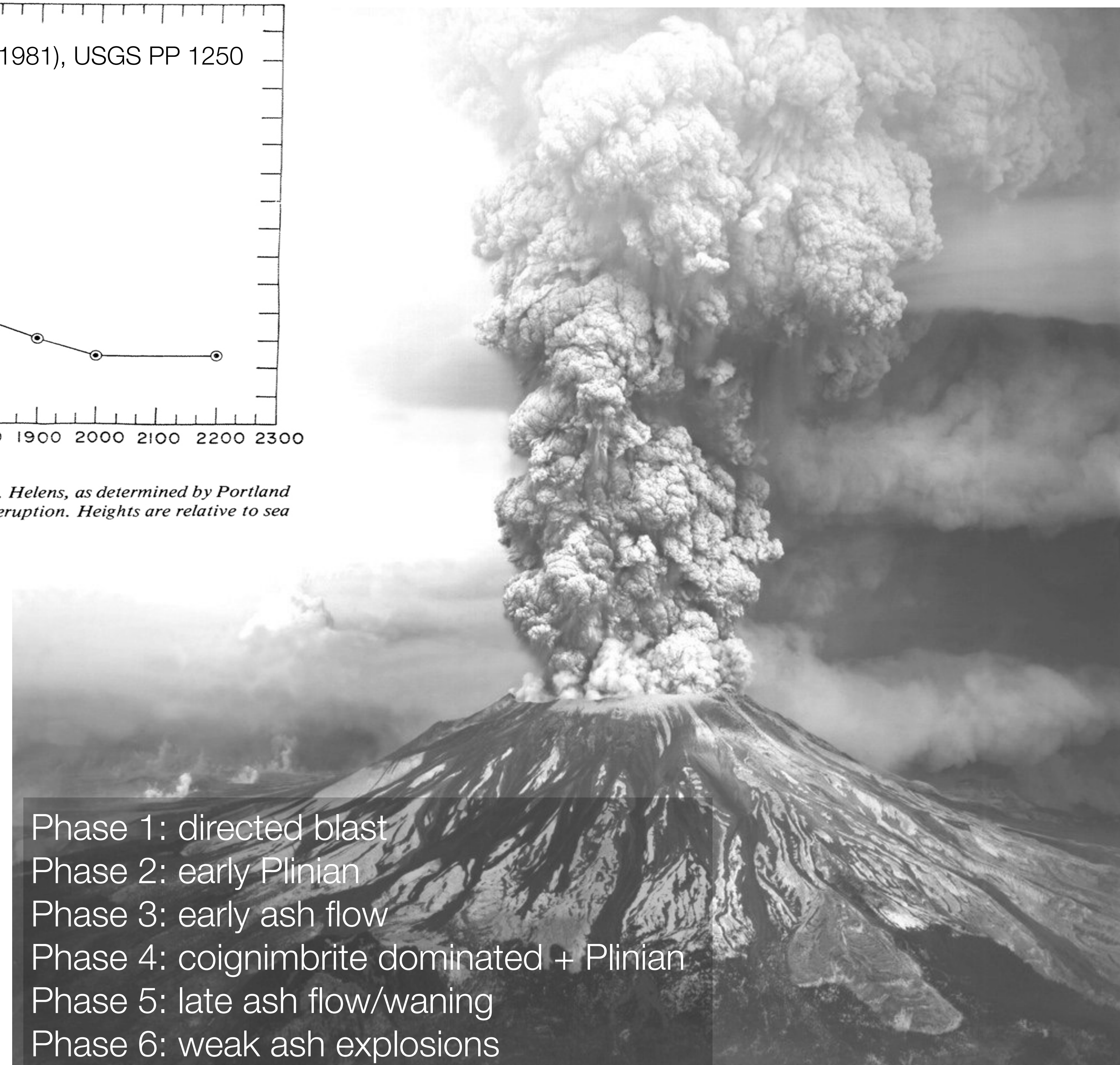

MSH 18 May 1980 distal ash ~600 km from source

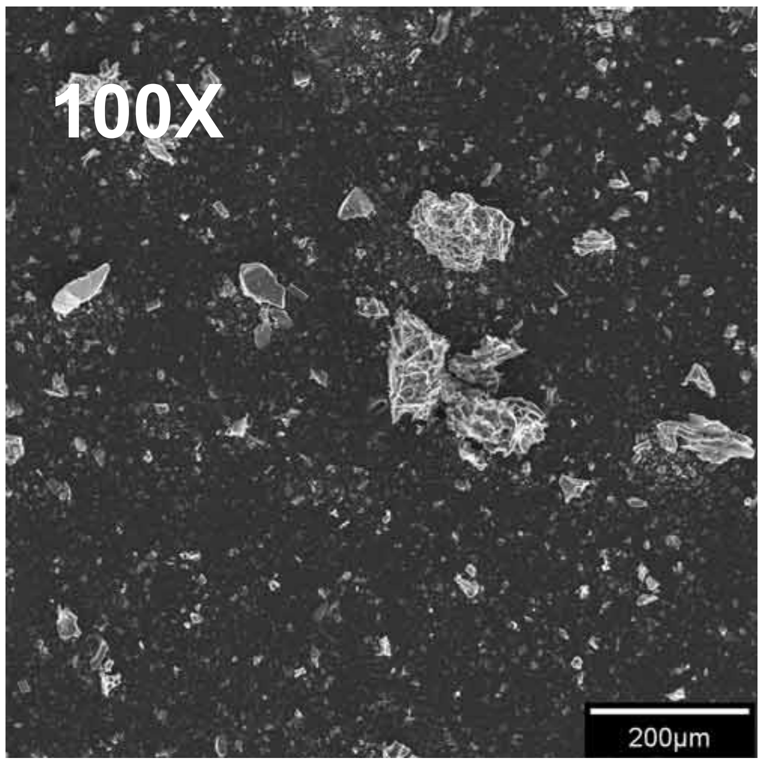

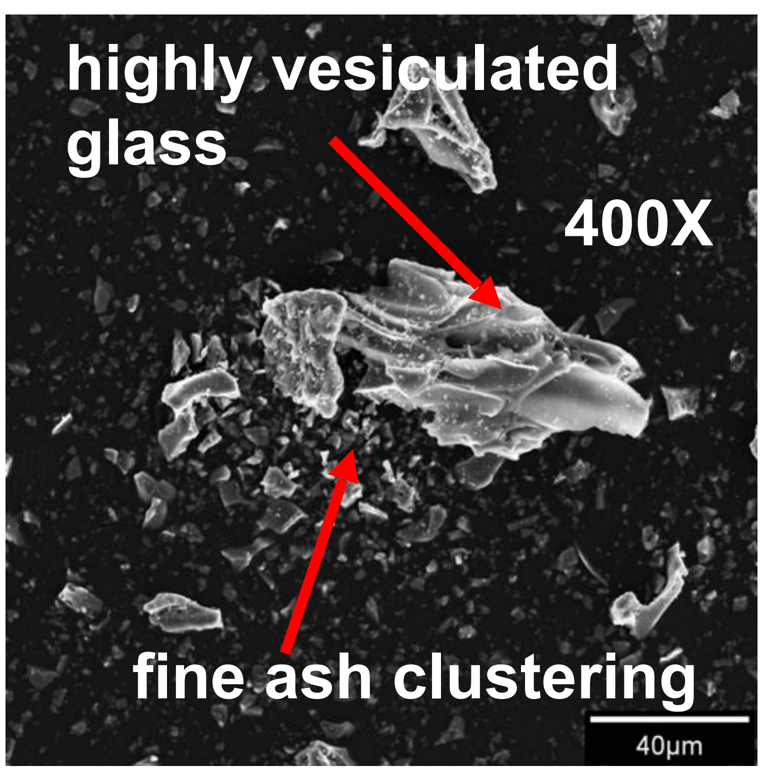

very fine ash binding to large ash particle

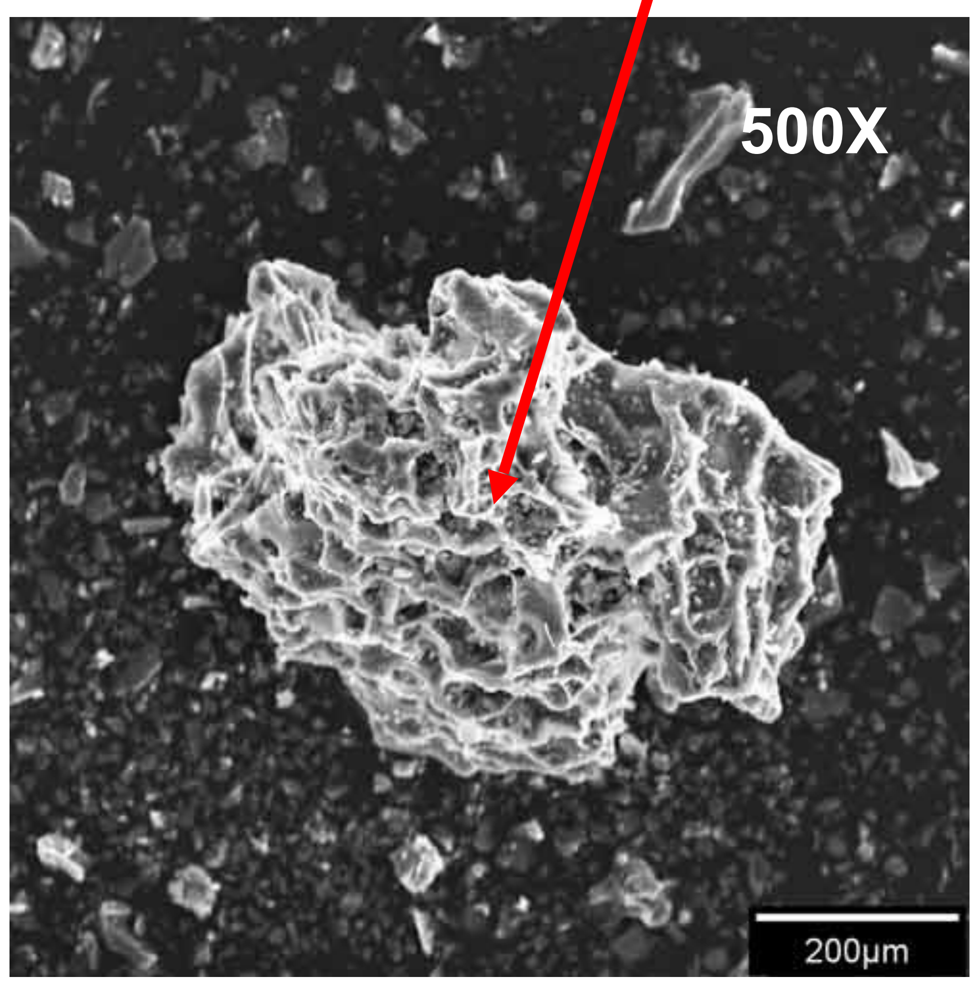

MSH80 aggregates

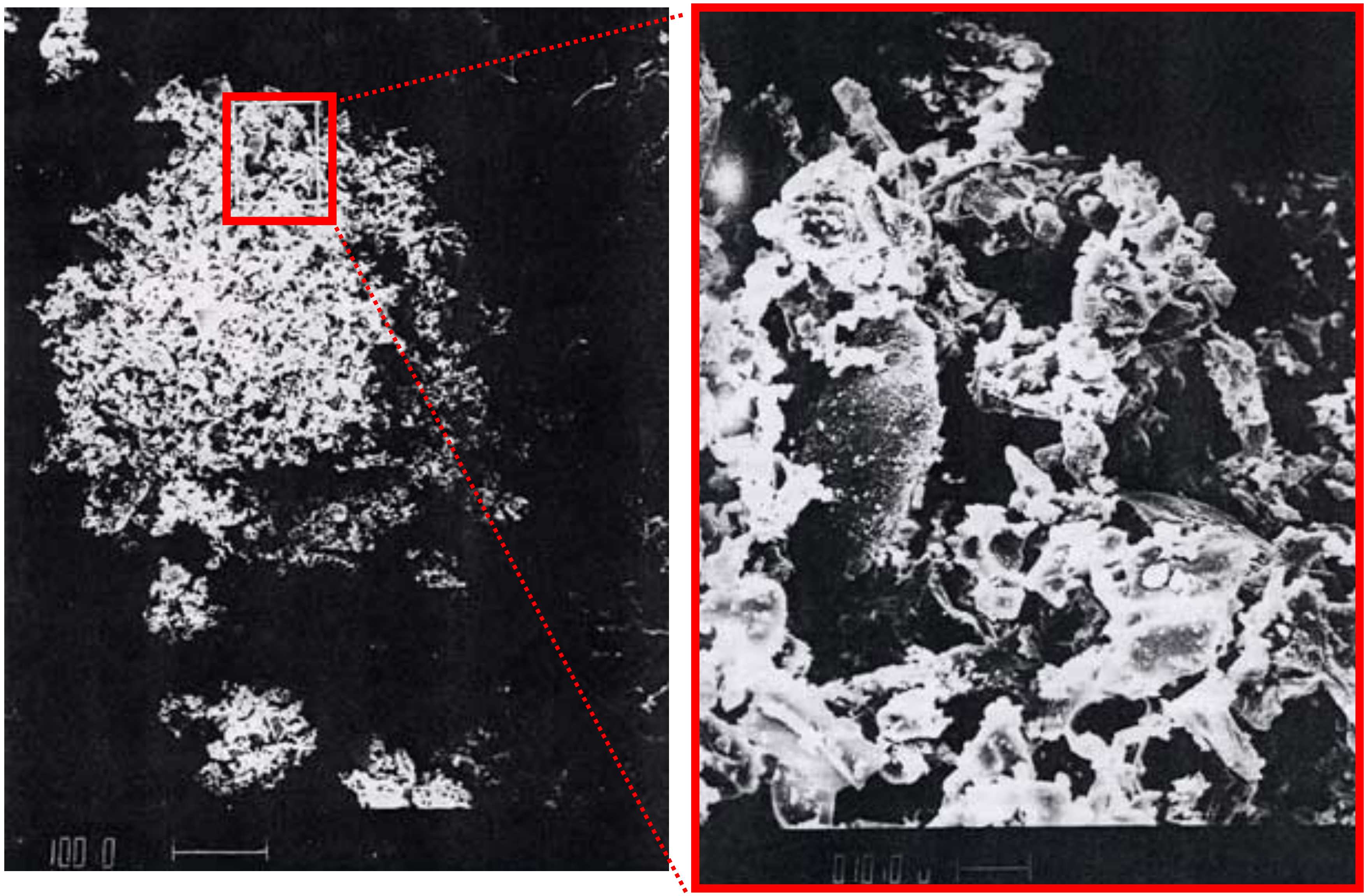

MSH May 18th 1980 ash cluster

from Sorem 1982

Particle size ranges from sub-μm to >40 μm

Large ash particles rafted to more distal areas by aggregated fine ash; fine ash prematurely settled out

break up on deposition

"…loosely bound ash clusters…" *Sorem 1982*

"…with high porosities and fragile structures." *Gilbert & Lane 1994*

Distal aggregation influences deposit sedimentology

(Durant et al., *J. Geophys. Res.*, 2009)

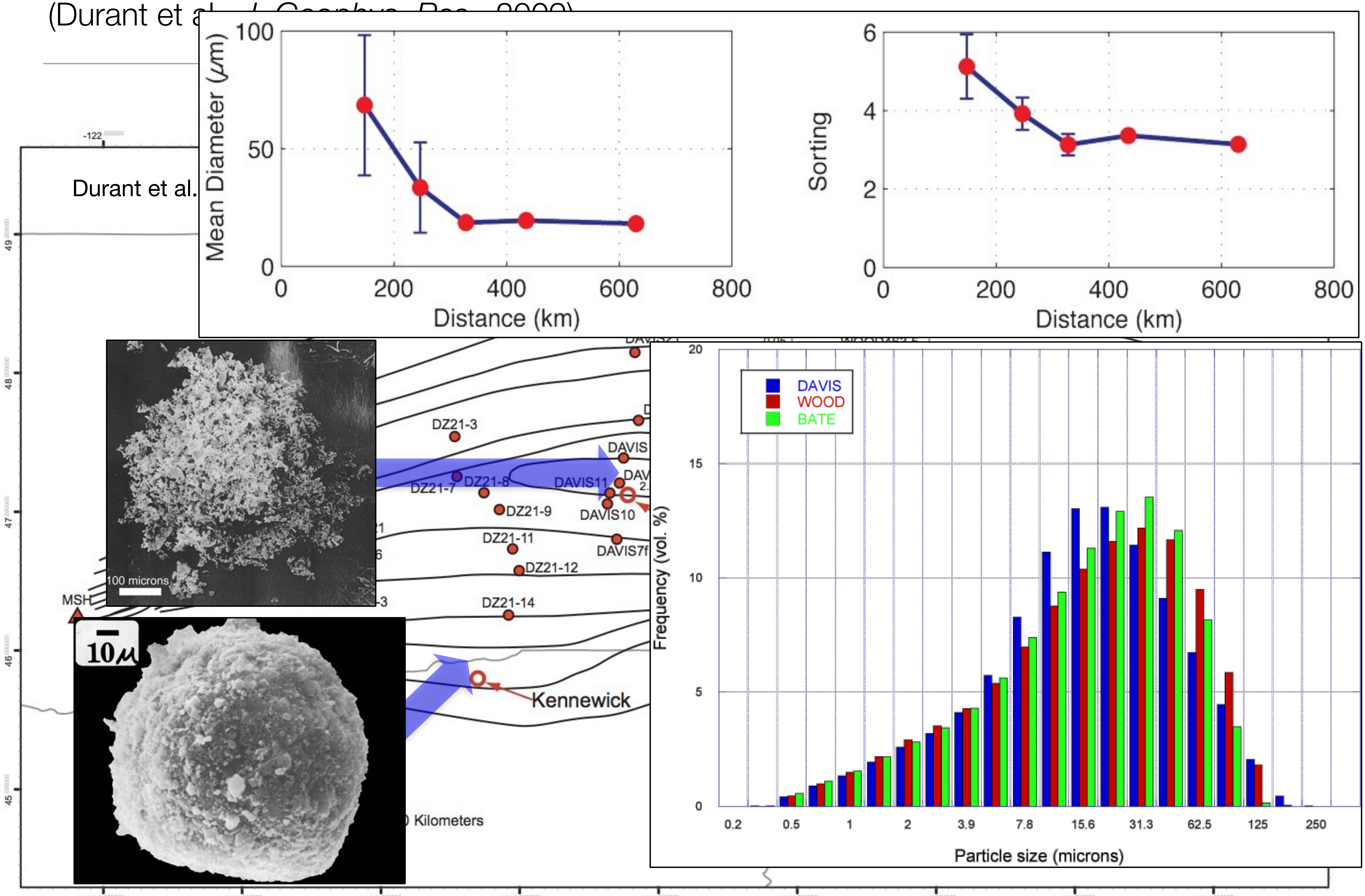

Very fine particle size classes remain constant with distance

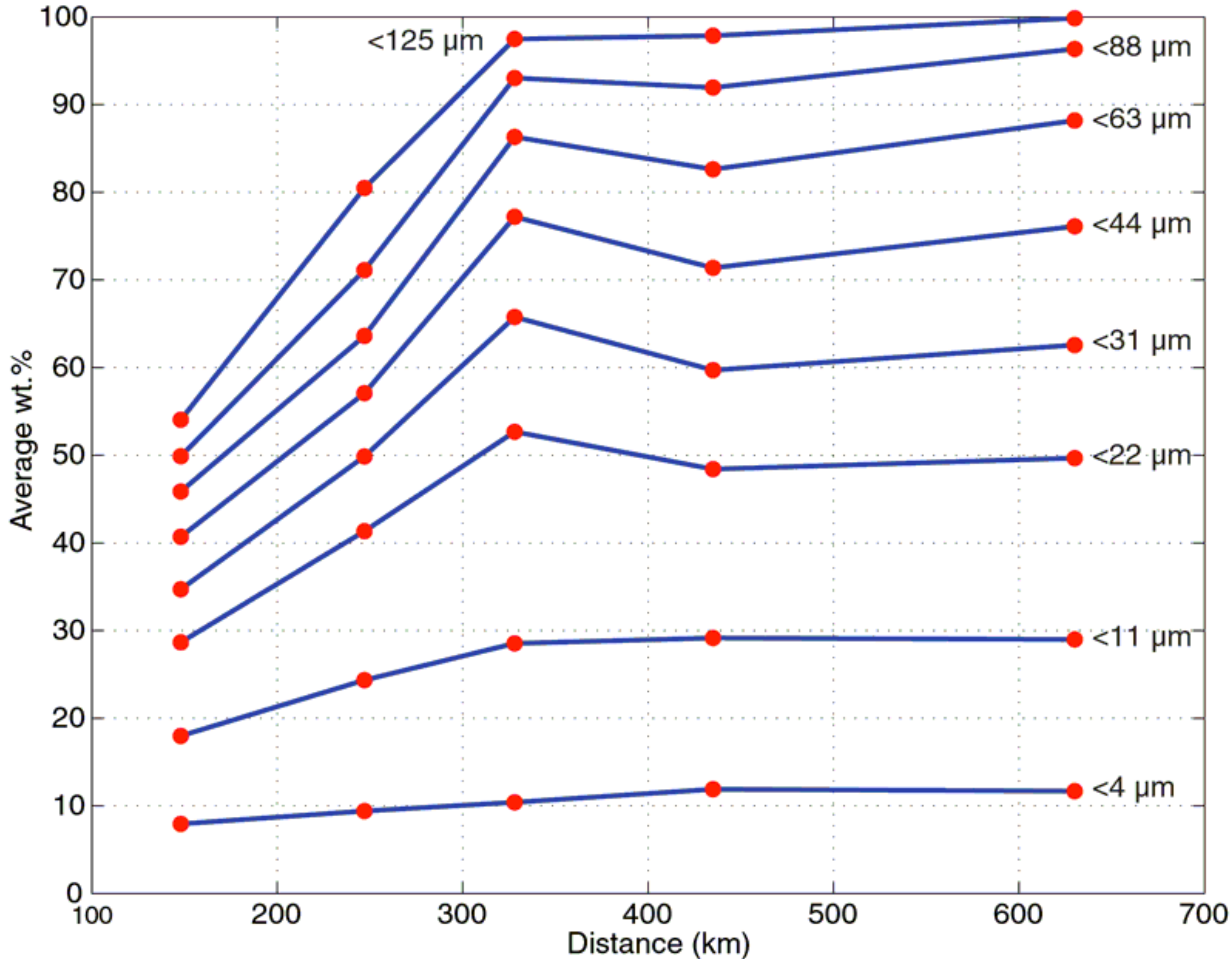

Particle size subpopulations: proxy for ash particle involvement in cloud microphysical processes

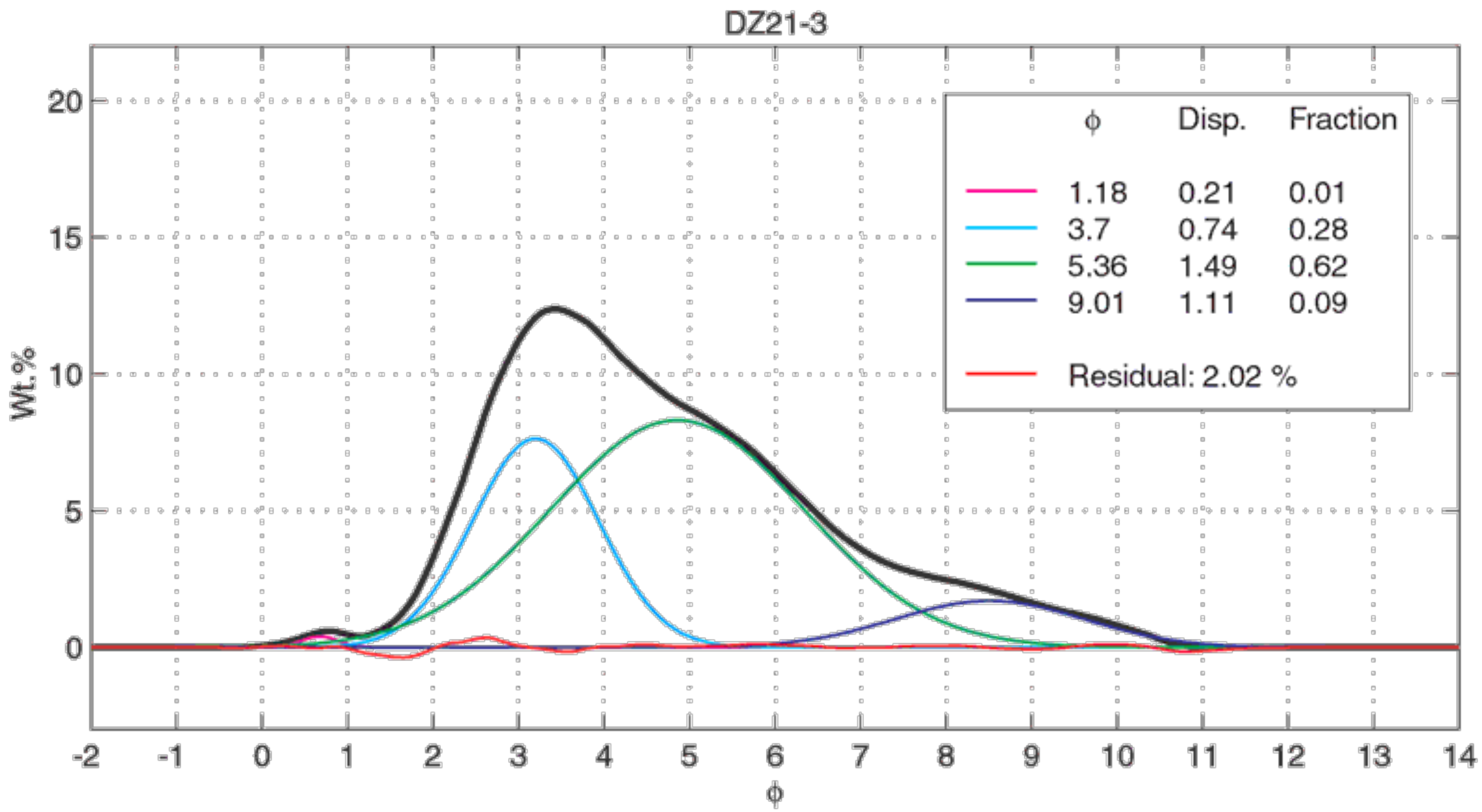

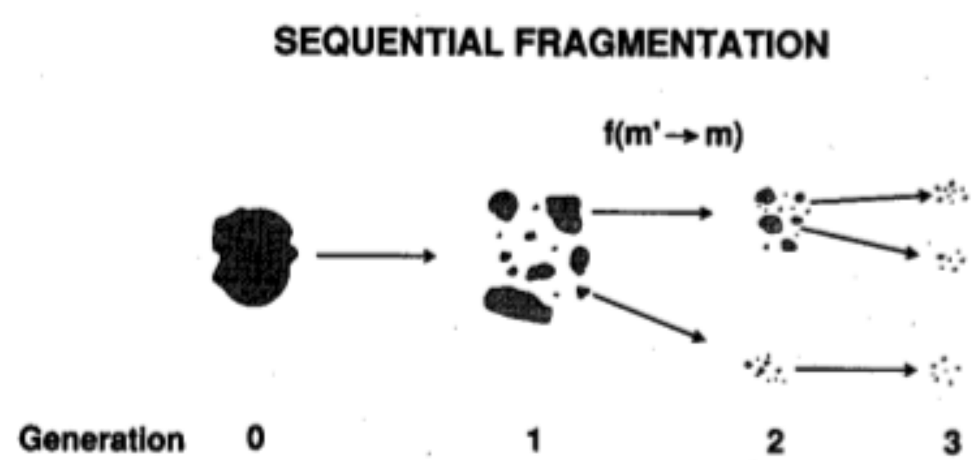

Wohletz KH, Sheridan MF, Brown WK (1989) Particle-Size Distributions and the Sequential Fragmentation Transport-Theory Applied to Volcanic Ash. *Journal of Geophysical Research-Solid Earth and Planets 94(B11):15703-15721*

Particle size subpopulations

(Durant et al., *J. Geophys. Res.*, 2009; Durant et al., *Phys. Chem. Earth*, 2011)

Chaiten 2008

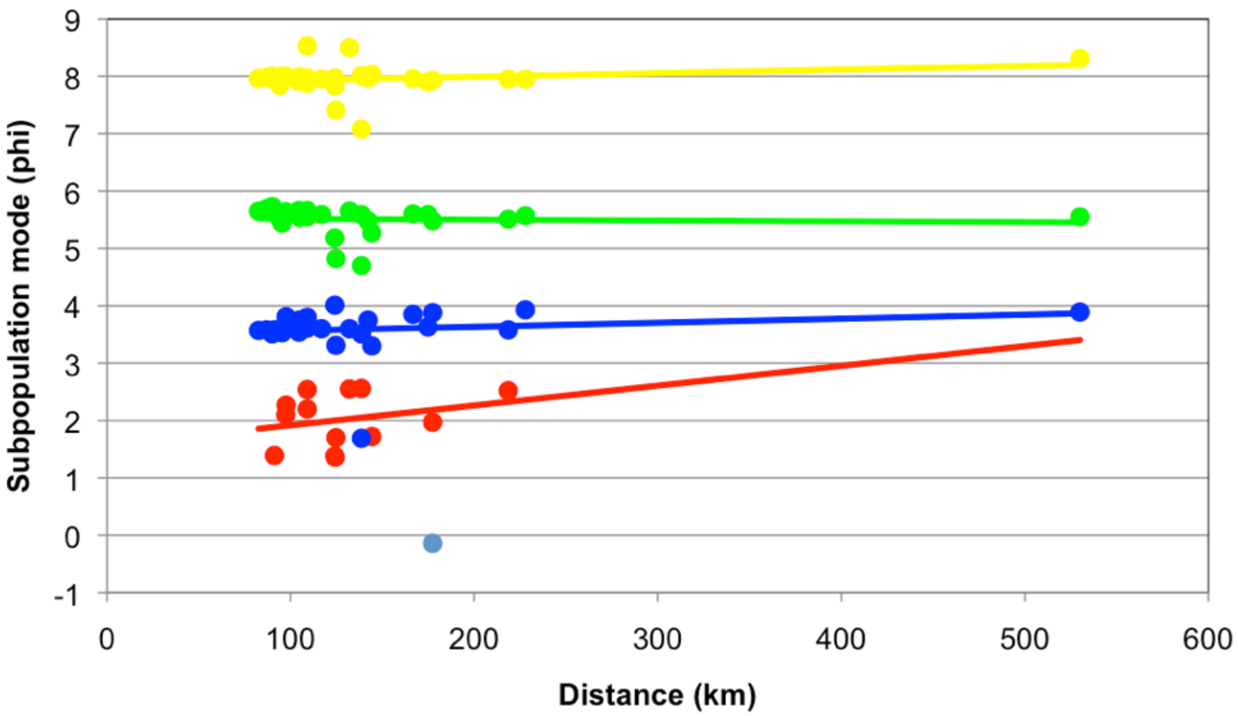

Mount St. Helens 1980

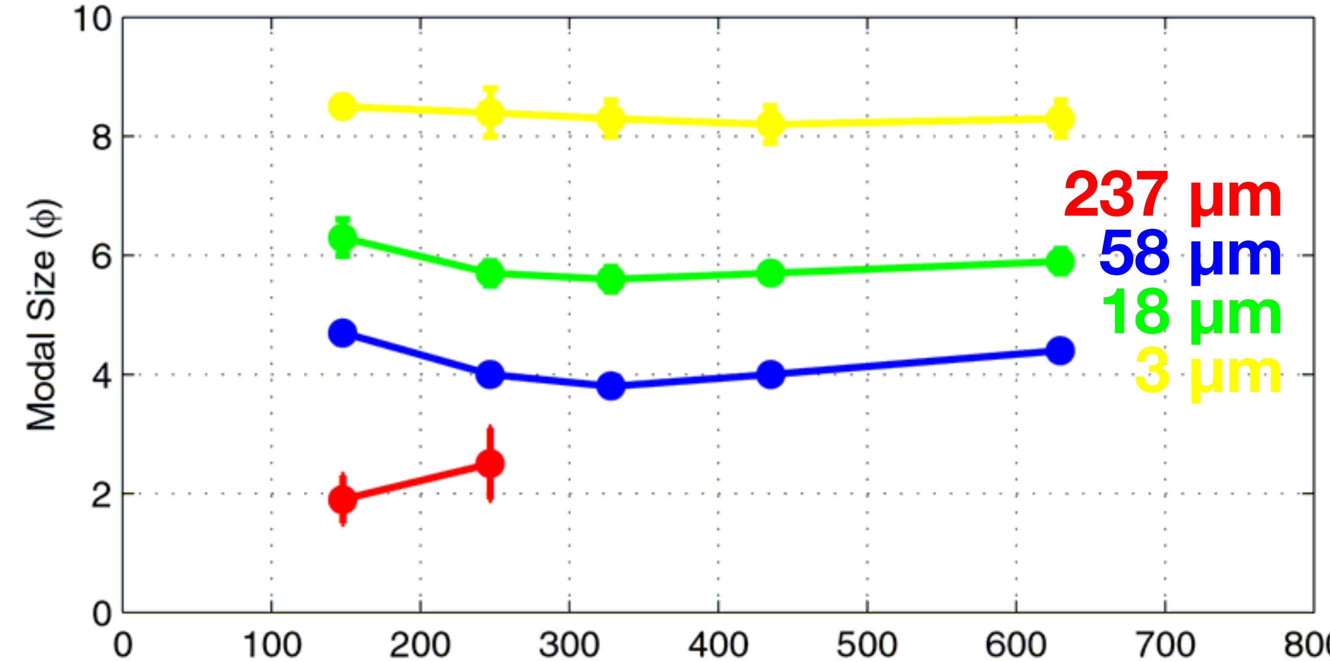

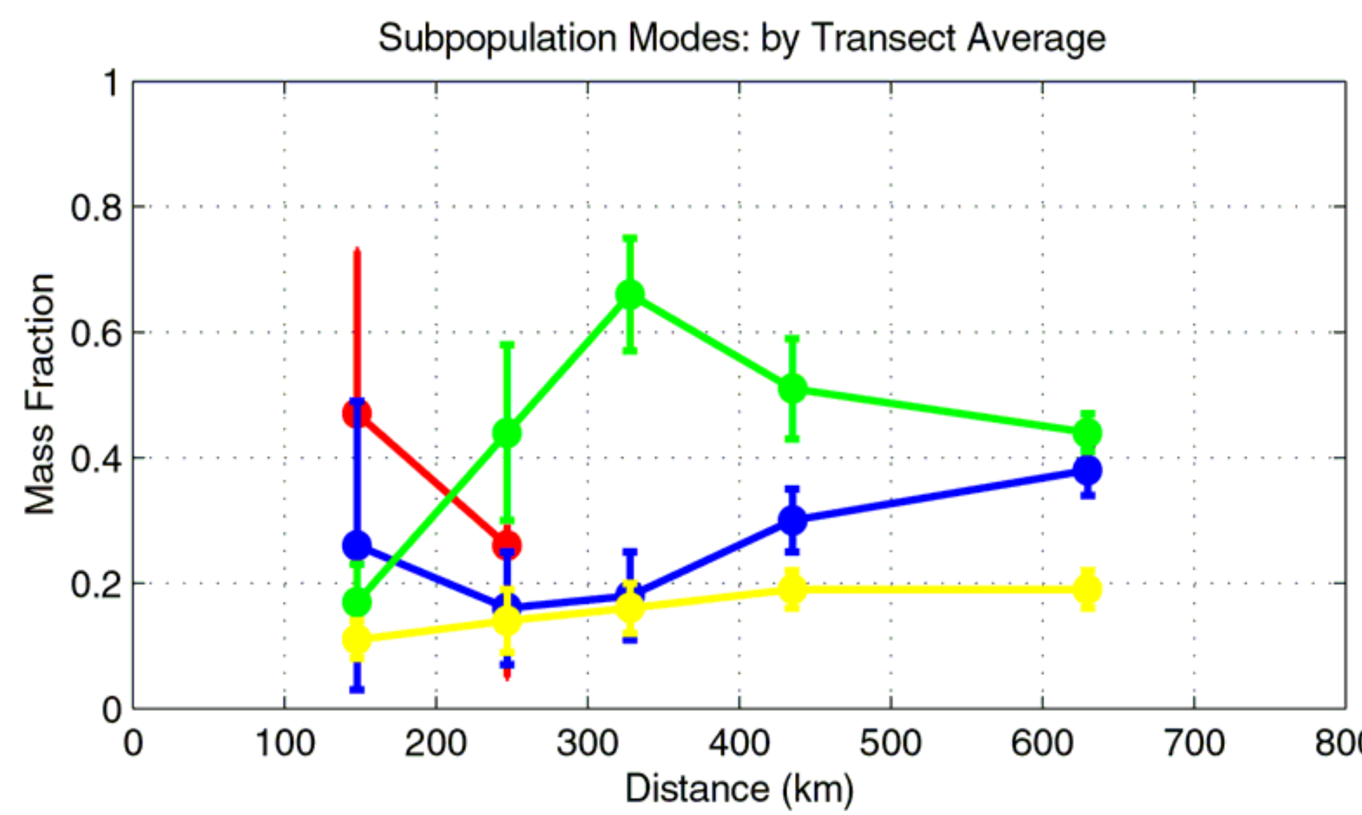

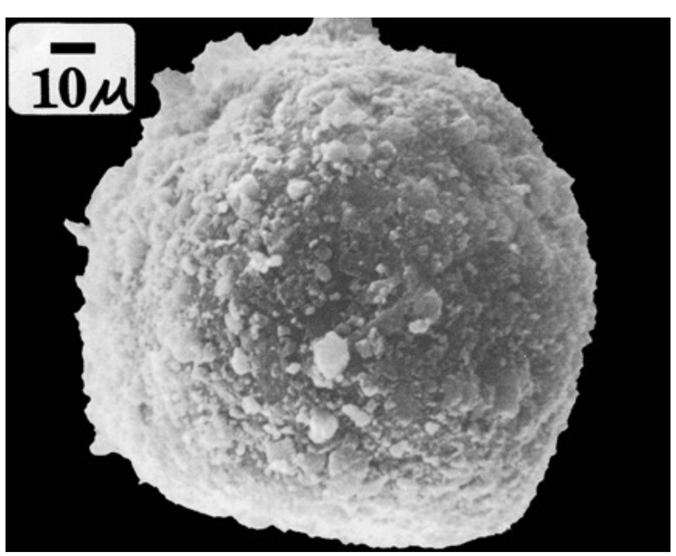

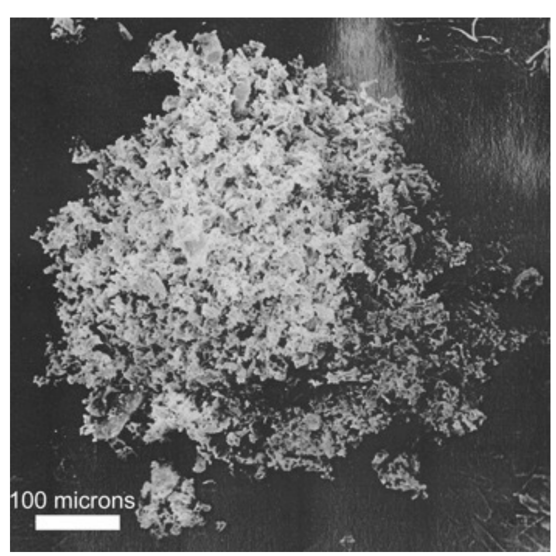

LINK TO CLOUD MICROPHYSICS

Temperature, water content and wind speed varies with height in the atmosphere

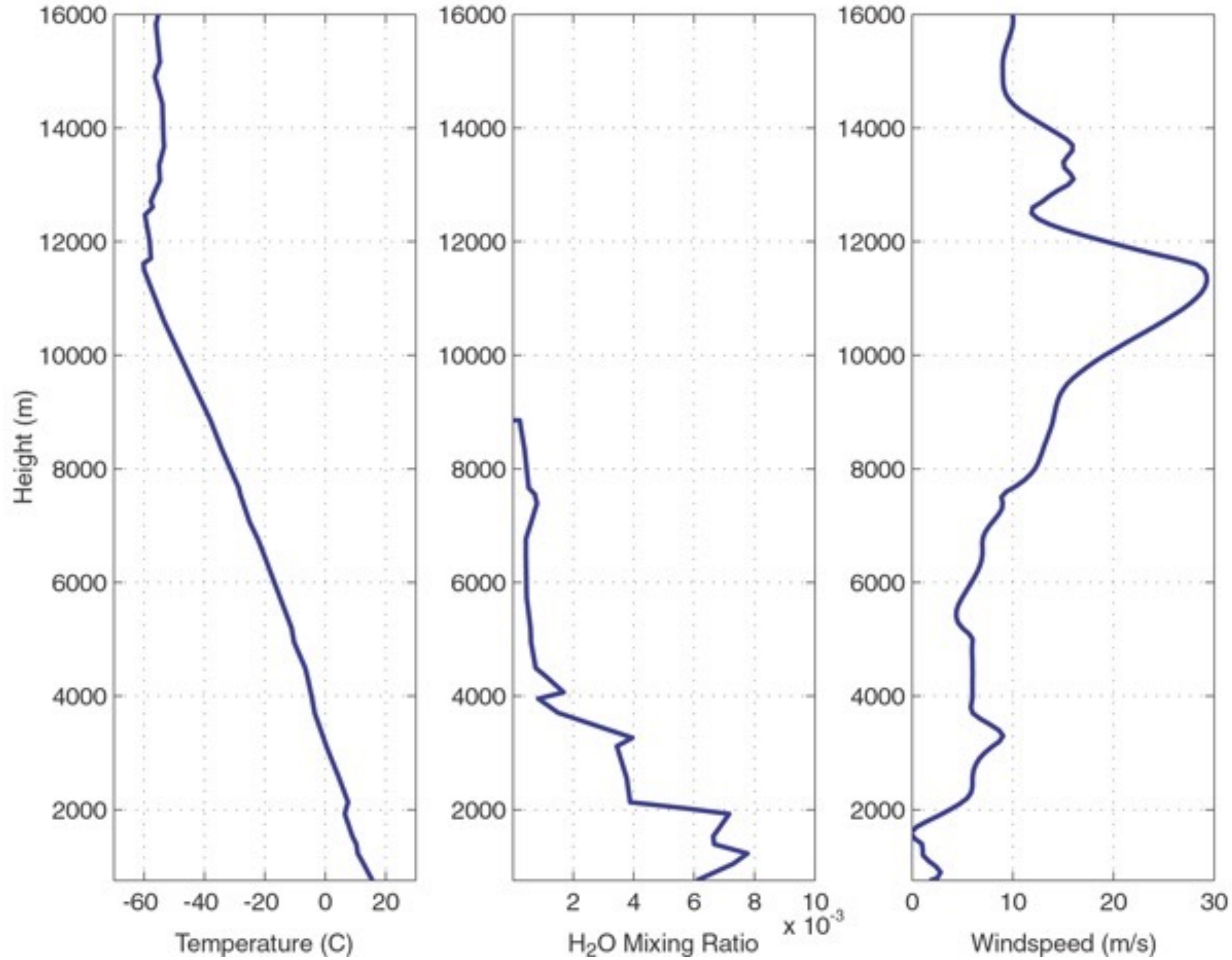

Environmental parameters determined from the radiosonde sounding taken at Spokane International Airport at 1800 UTC on 18 May 1980. (Durant et al., *J. Geophys. Res*., 2009)

Water phase stability varies as a function of temperature and pressure

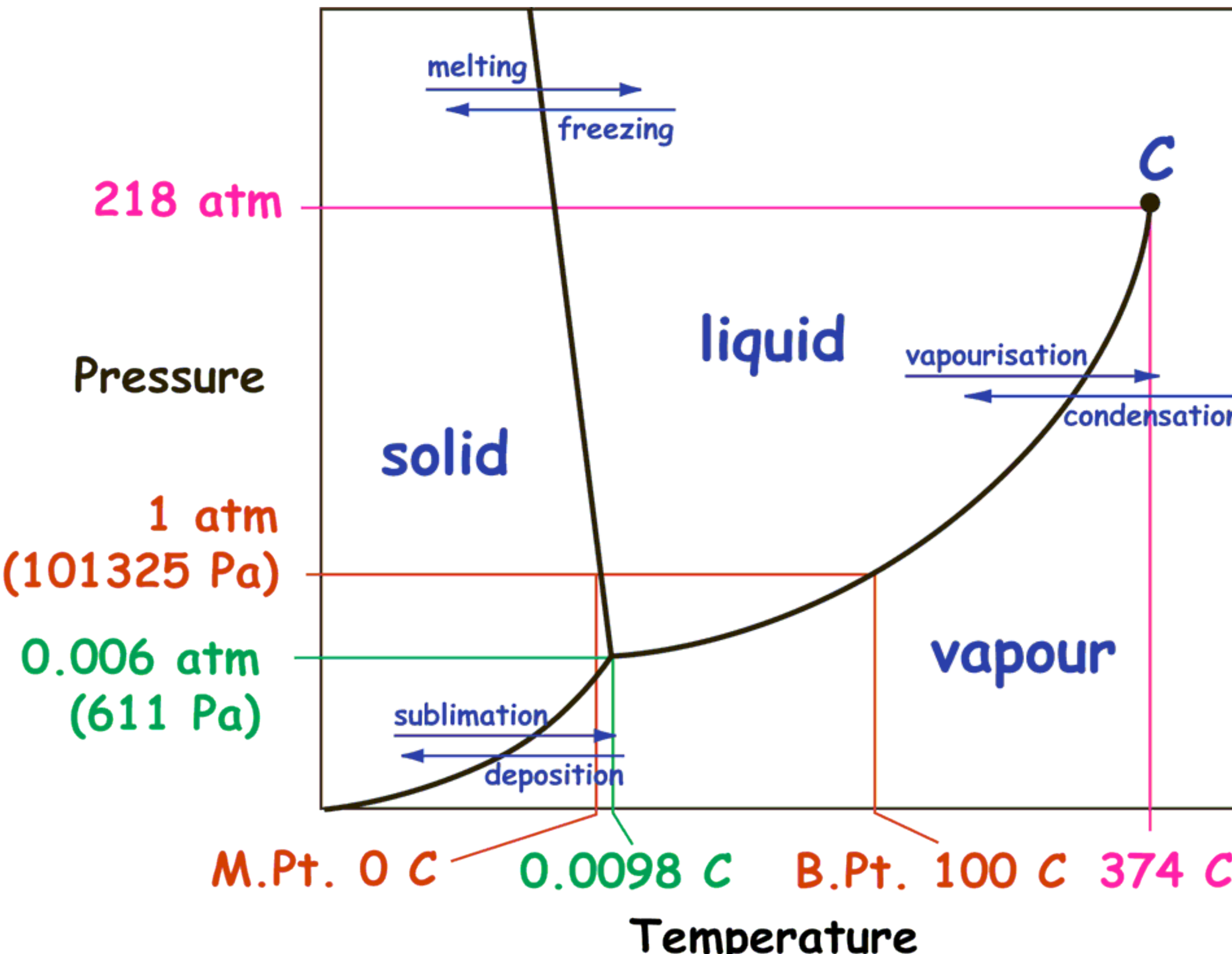

Hydrometeors are products of condensation or freezing of water

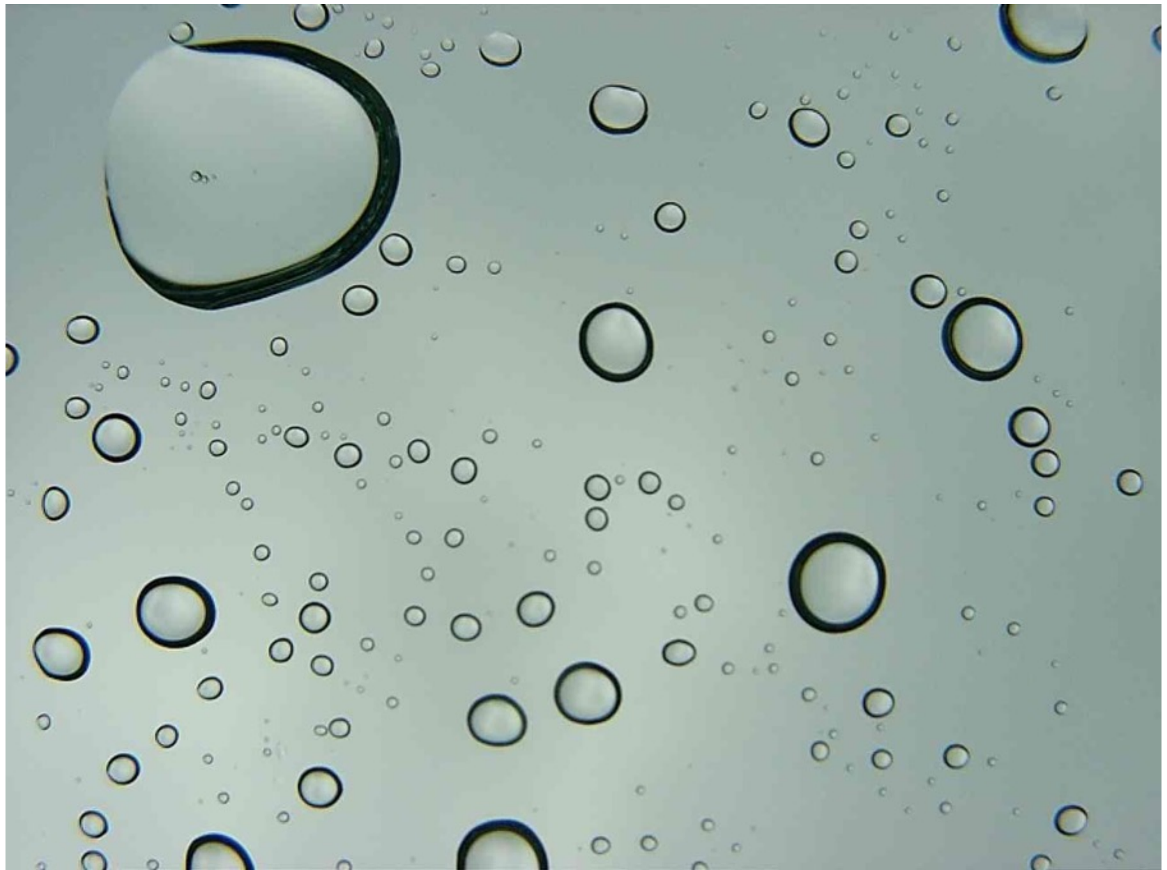

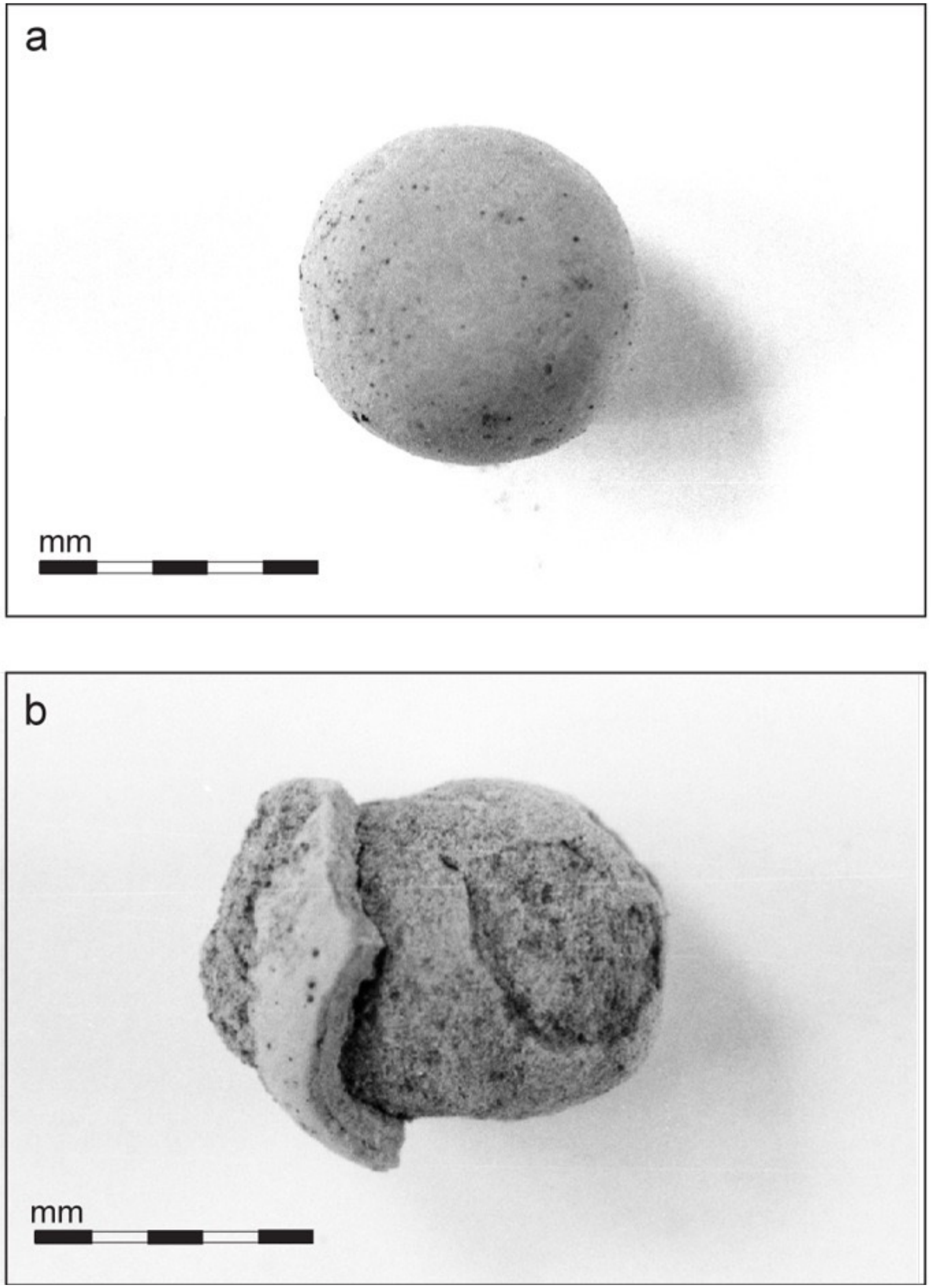

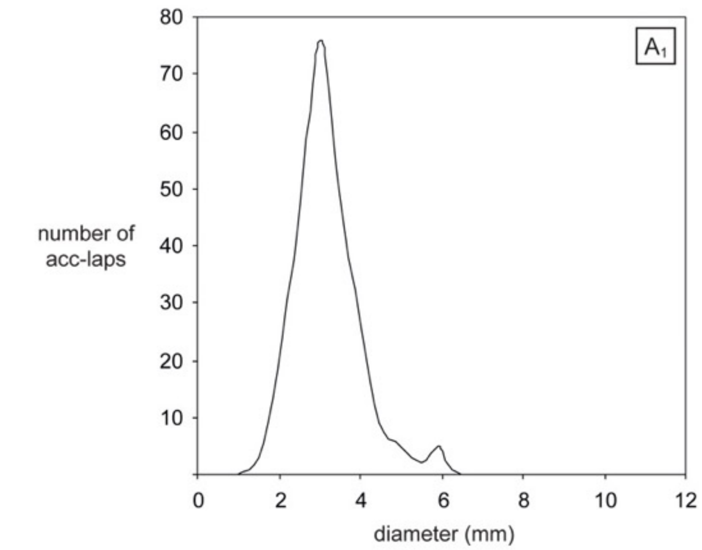

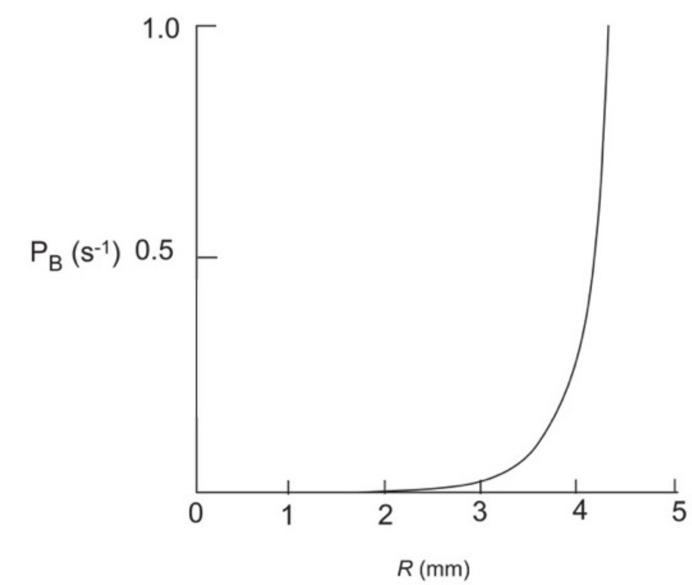

Houze (1994)

AP2 from the Upper Scoriae 1 deposit, Santorini, Greece, have a size distribution that resembles raindrops

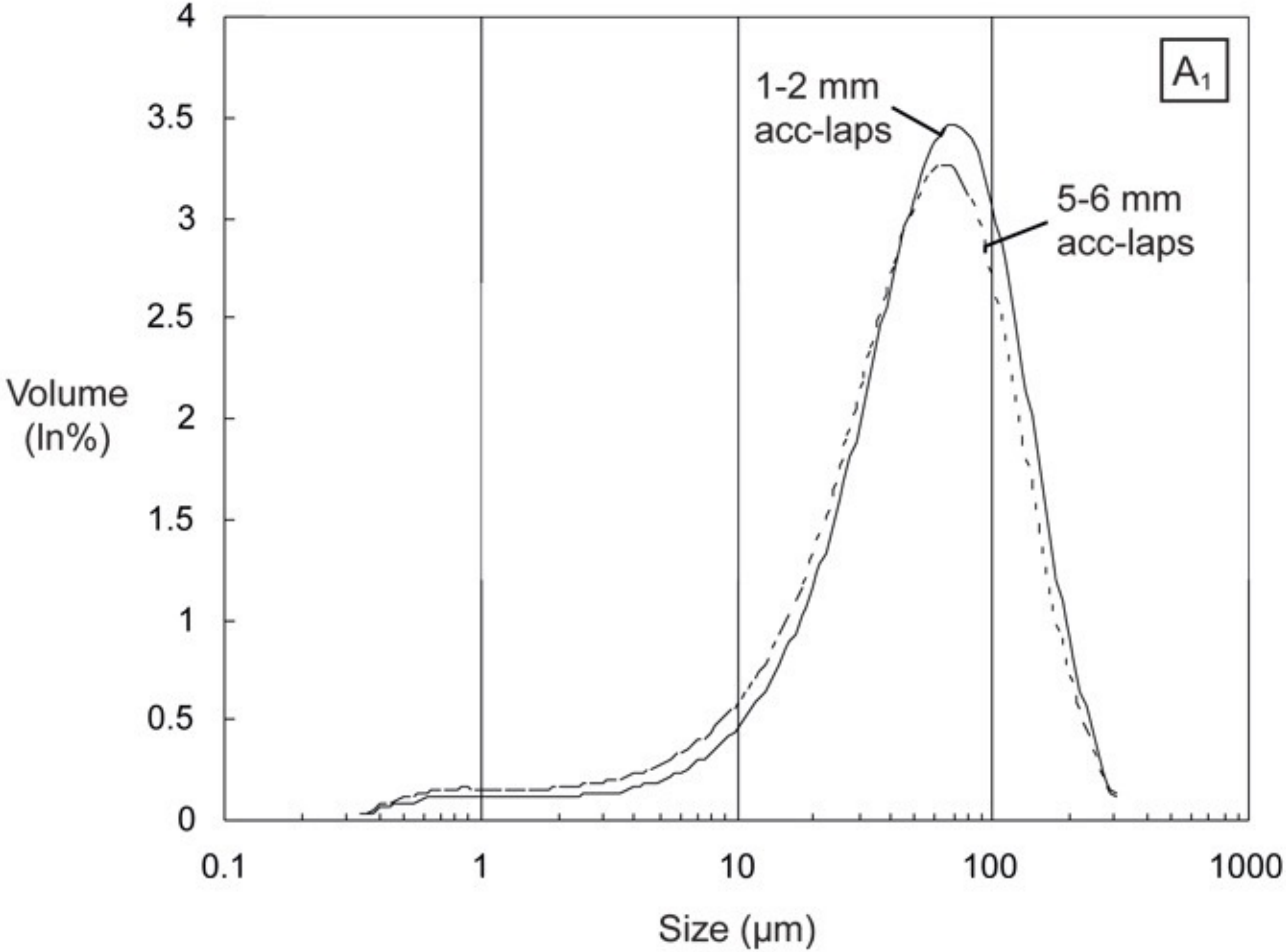

Constituent particle size distribution

Upper Scoriae 1, Santorini, Greece

Empirically-derived aggregation coefficient

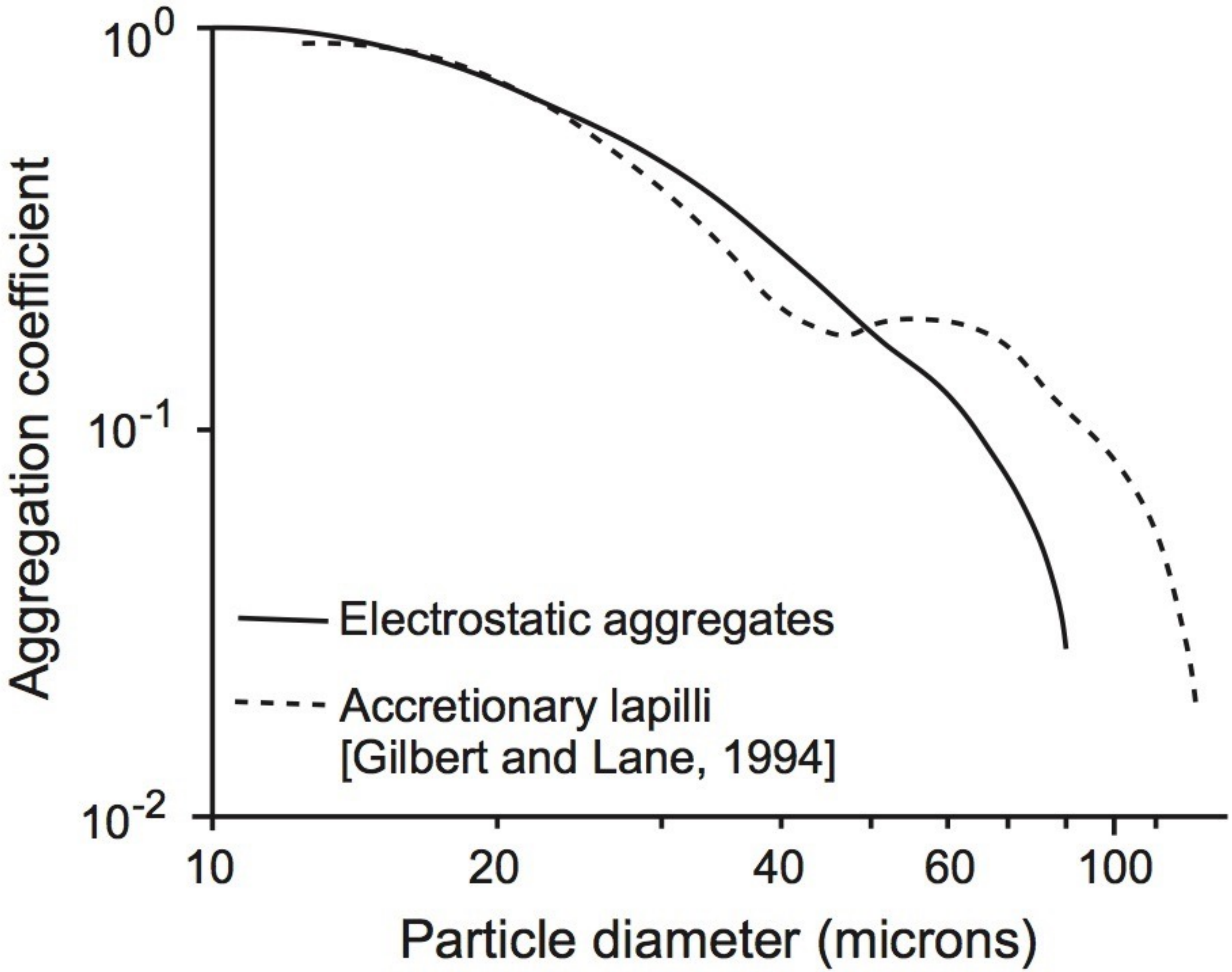

May 2011 Grímsvötn, Iceland, eruption through Vatnajökull ice sheet

Volcanogenic frozen water drops fell within 20 km of the volcano

Heterogeneous ice nucleation by volcanic ash occurs over a broad temperature range (-10C to -20C)

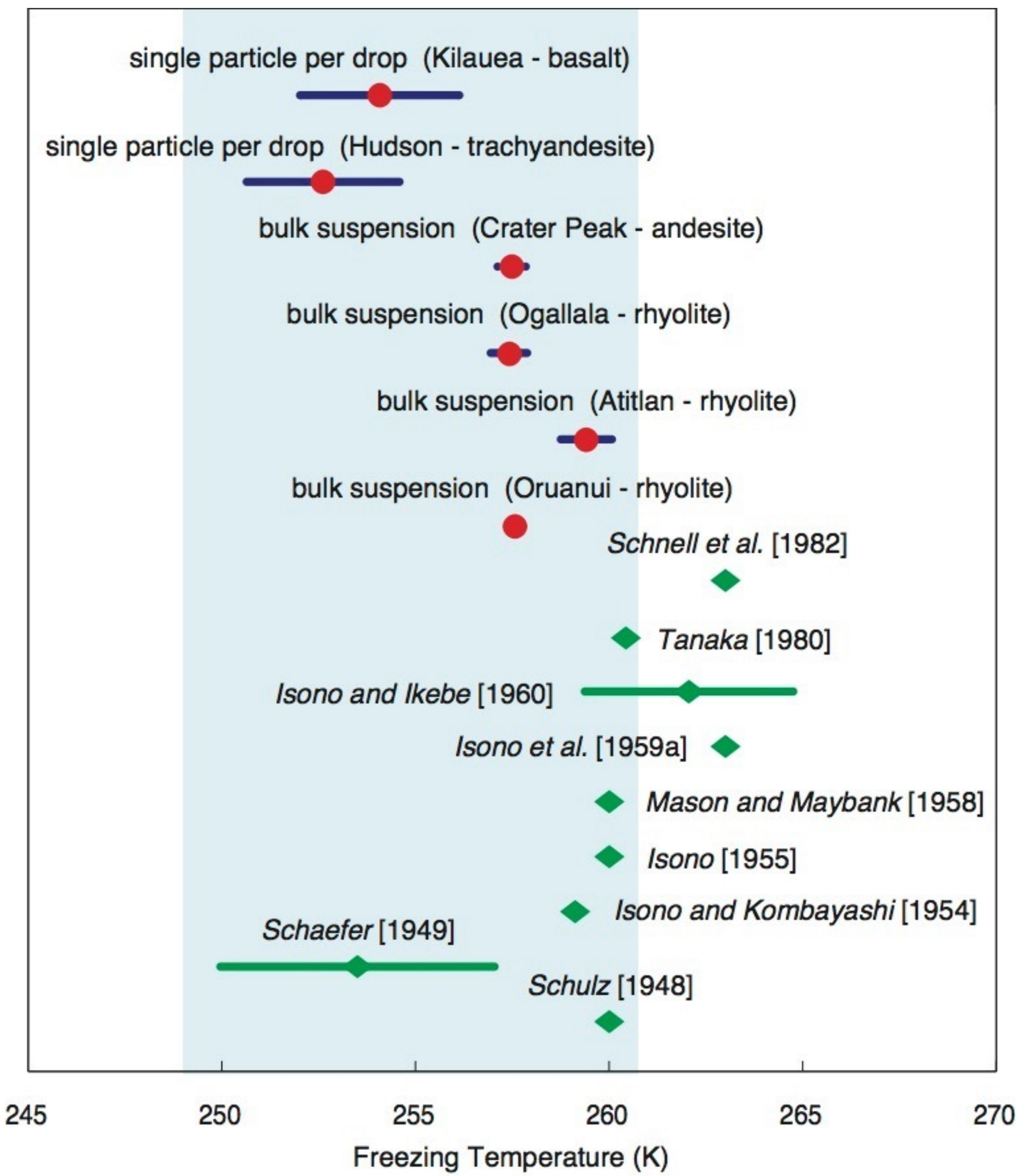

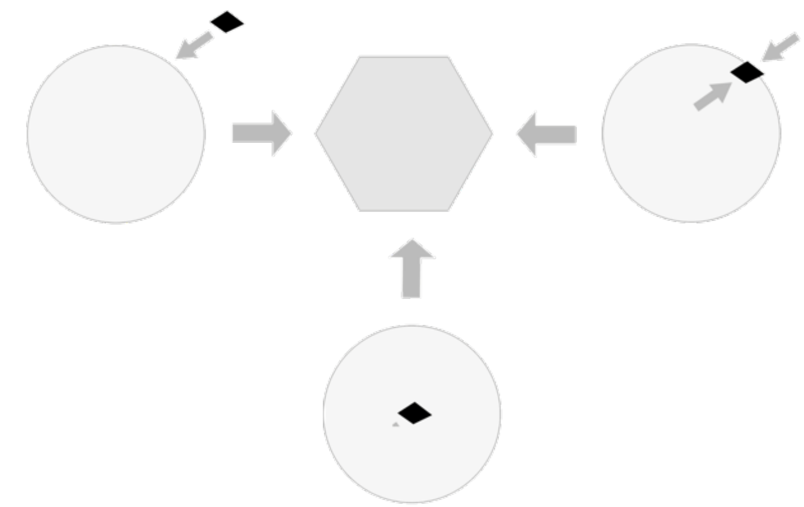

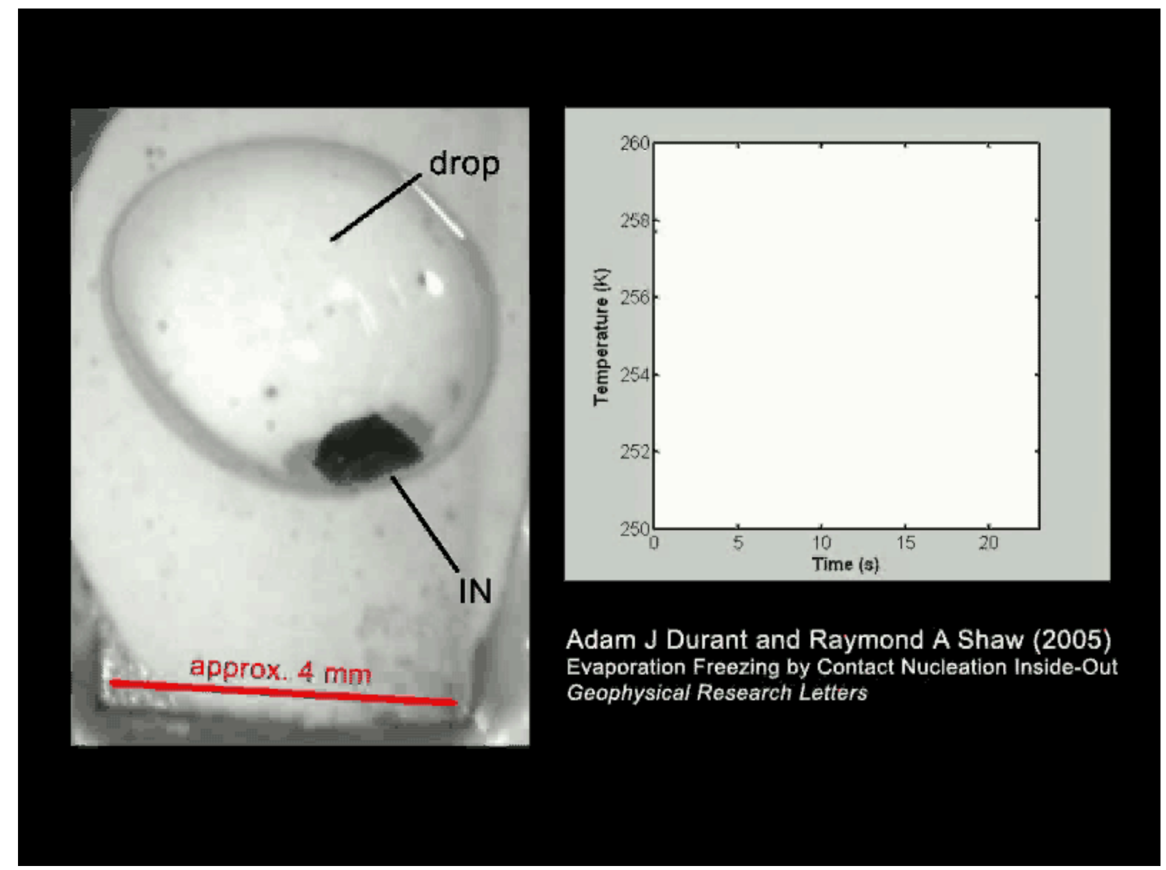

Durant AJ, Shaw RA, Rose WI, Mi Y, Ernst GGJ (2008), **Ice nucleation and overseeding of ice in volcanic clouds**, *Journal of Geophysical Research-Atmospheres* 113(D9):doi: 10.1029/2007JD009064

AP1 and AP2 aggregates in deposits often have bubble voids preserved - evidence for freezing?

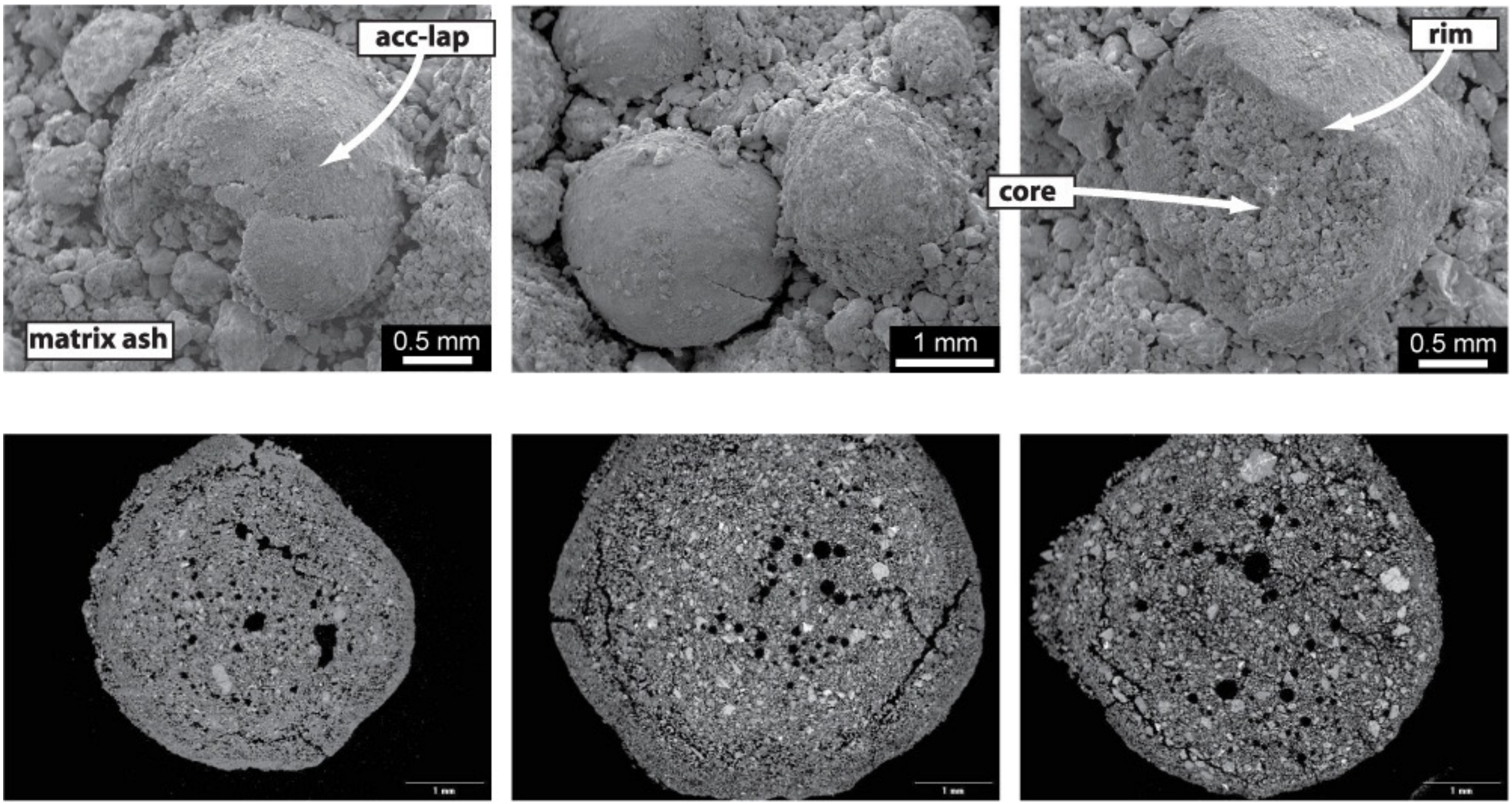

(Keanakak’oi Ash, Kilauea, Hawai’i)

Conceptual model of “proximal” ash aggregation: many different aggregate types

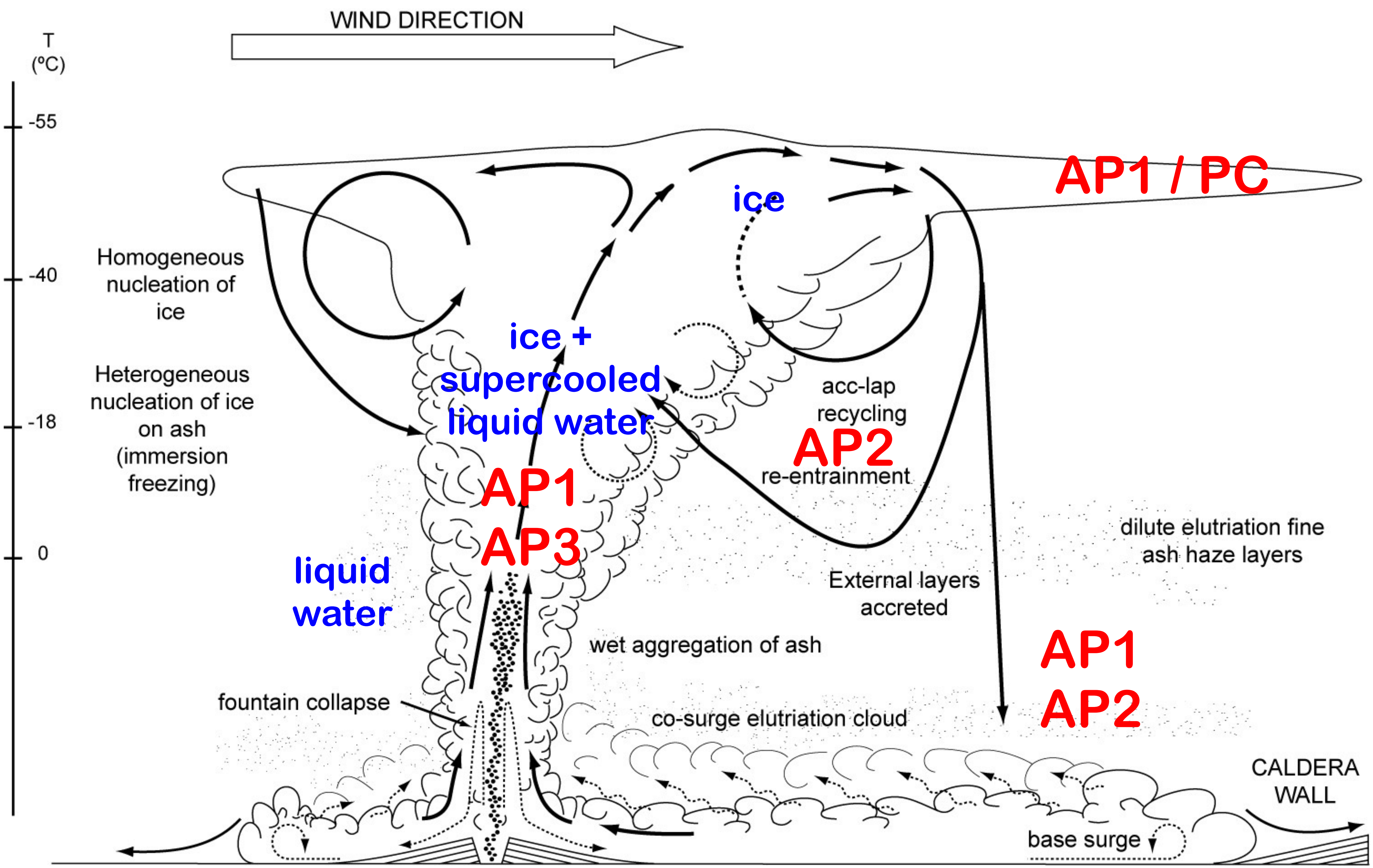

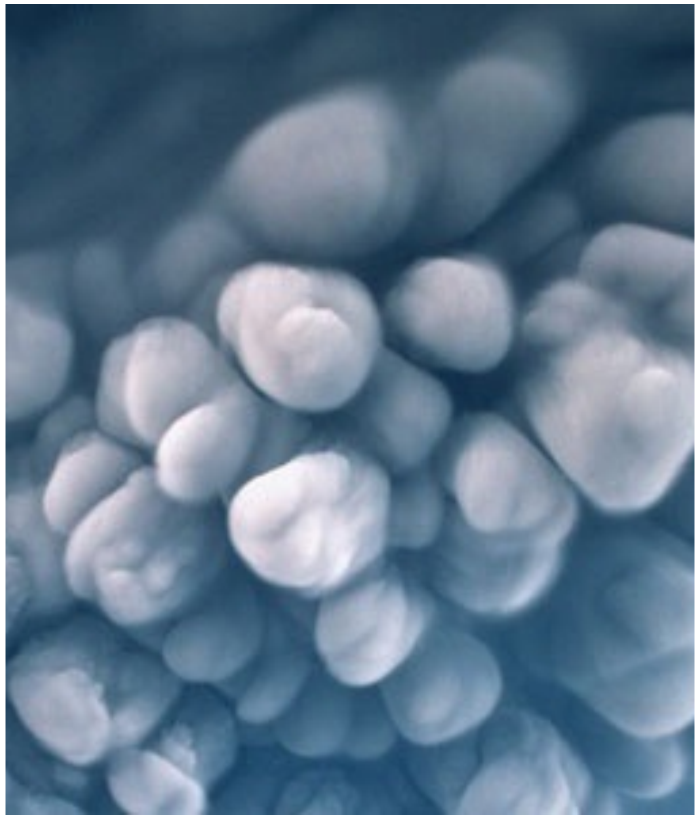

Schultz DM, Kanak KM, Straka JM, Trapp RJ, Gordon BA, Zrnic DS, Bryan GH, Durant AJ, Garrett TJ, Klein PM, Lilly DK (2006), The mysteries of mammatus clouds: observations and formation mechanisms, J. Atmos. Sci., 63(10), 2409-2435

Distal aggregation processes and volcanic mammatus

(a) Cumulonimbus anvil mammatus: 25 Mar 2005, Salt Lake City, UT (b) Mammatus with ragged edges: 29 Jun 2004, Norman, OK (c) Well-developed cumulonimbus anvil mammatus lobes: 29 May 2004, near Belleville, KS (d) Cumulonimbus anvil mammatus arranged in lines, showing blue sky between lobes: 8 May 2005, Norman, OK (e) Stratocumulus mammatus: 3 Aug 2003, Ouachita National Forest, OK. (f) Mammatus that formed on a cumulonimbus anvil that had all nearly evaporated except for the leading edge: 2047 CDT 7 Jun 2004, Norman, OK (g) Mammatus exhibiting breaking Kelvin–Helmholtz waves: 2 Aug 1992, Norman, OK ((h) Mammatus in the ash cloud from the Mount St. Helens eruption at 0832 Pacific daylight time (PDT) 18 May 1980: picture taken at about 0900 PDT 18 May 1980, Richland, WA.

Mammatus

Cloud features commonly observed on cumulonimbus clouds

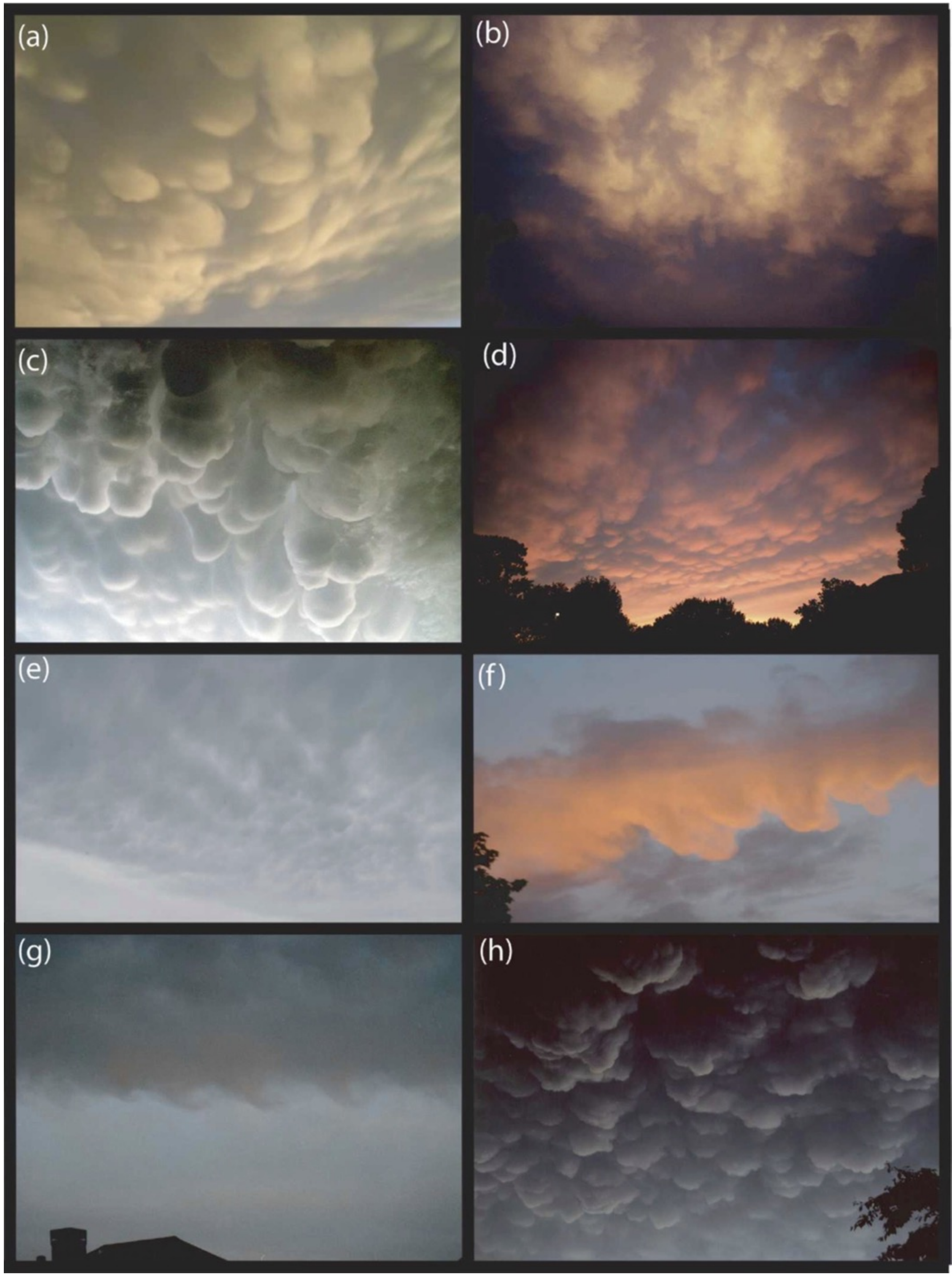

Schultz DM, Kanak KM, Straka JM, Trapp RJ, Gordon BA, Zrnic DS, Bryan GH, Durant AJ, Garrett TJ, Klein PM, Lilly DK (2006), The mysteries of mammatus clouds: observations and formation mechanisms, *J. Atmos. Sci.,* 63(10), 2409-2435

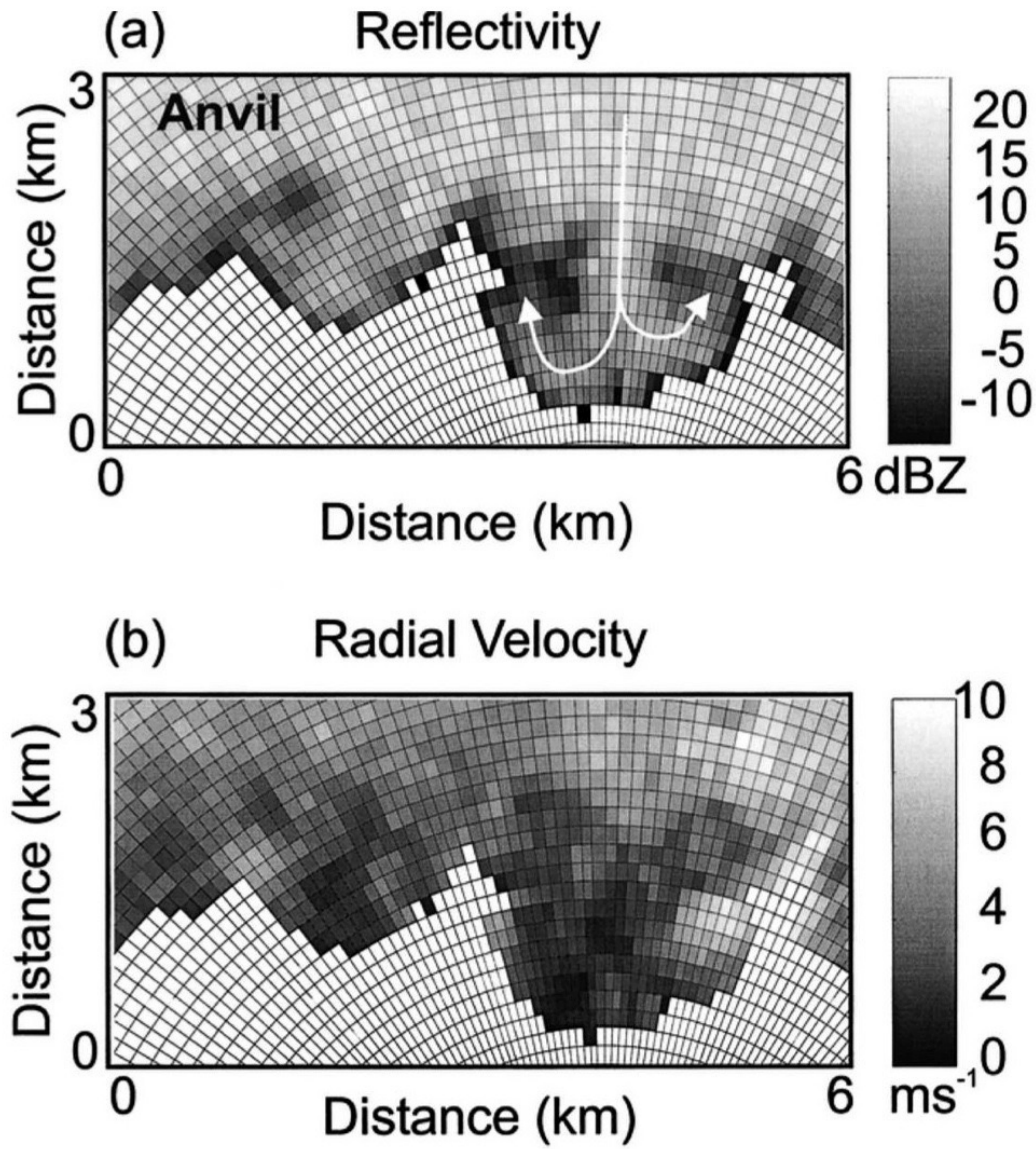

Vertical-directed aircraft Doppler radar

(Schultz et al., *J. Atmos. Sci.*, 2006)

RHI: reflectivity and radial velocity profiles

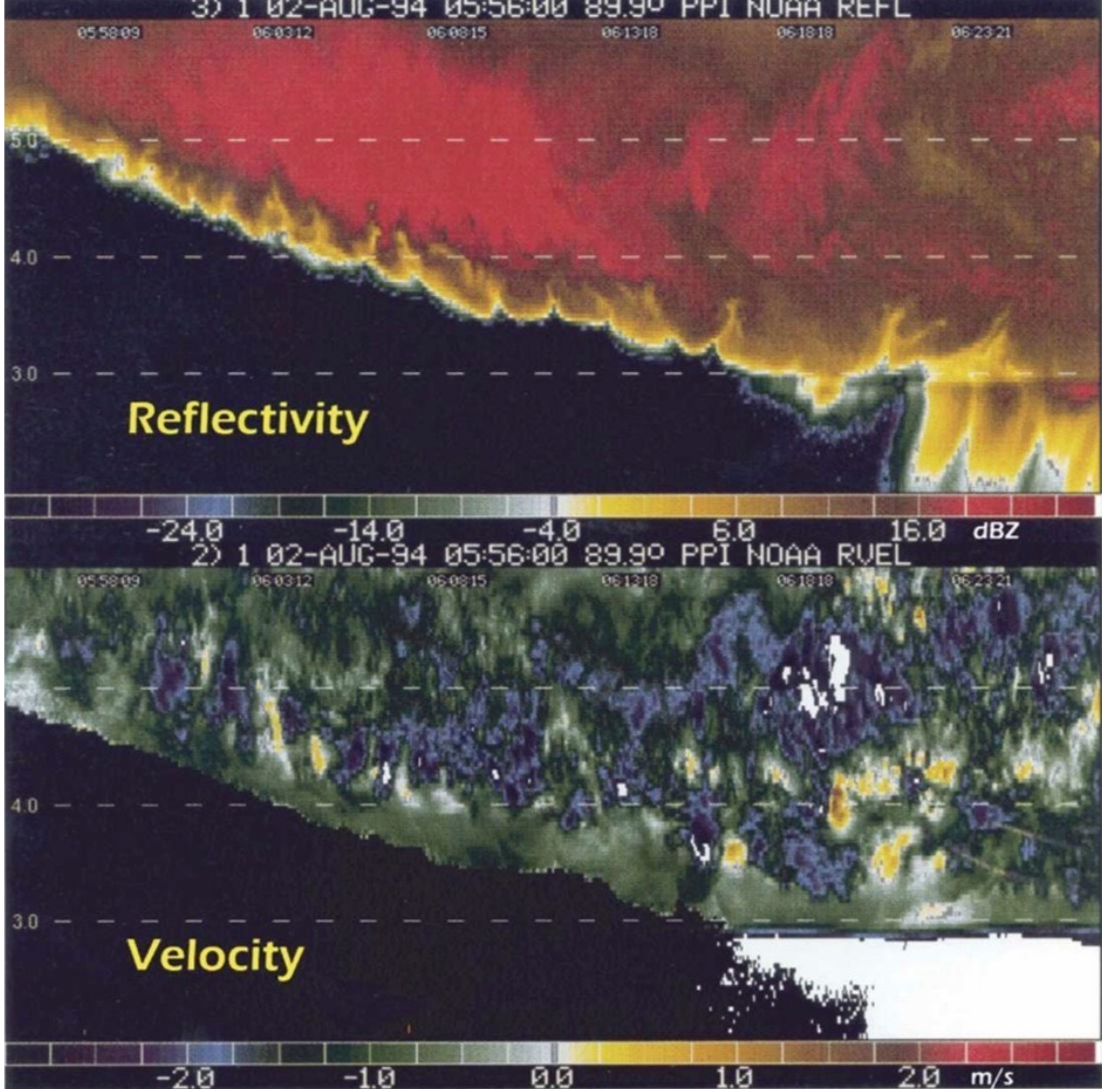

Vertical Doppler radar

(Schultz et al., *J. Atmos. Sci.*, 2006)

Cumulonimbus anvil

Cloud polarisation lidar

(Schultz et al., *J. Atmos. Sci.*, 2006)

Mamas first developed at cirrus heights then evolved into a mature anvil

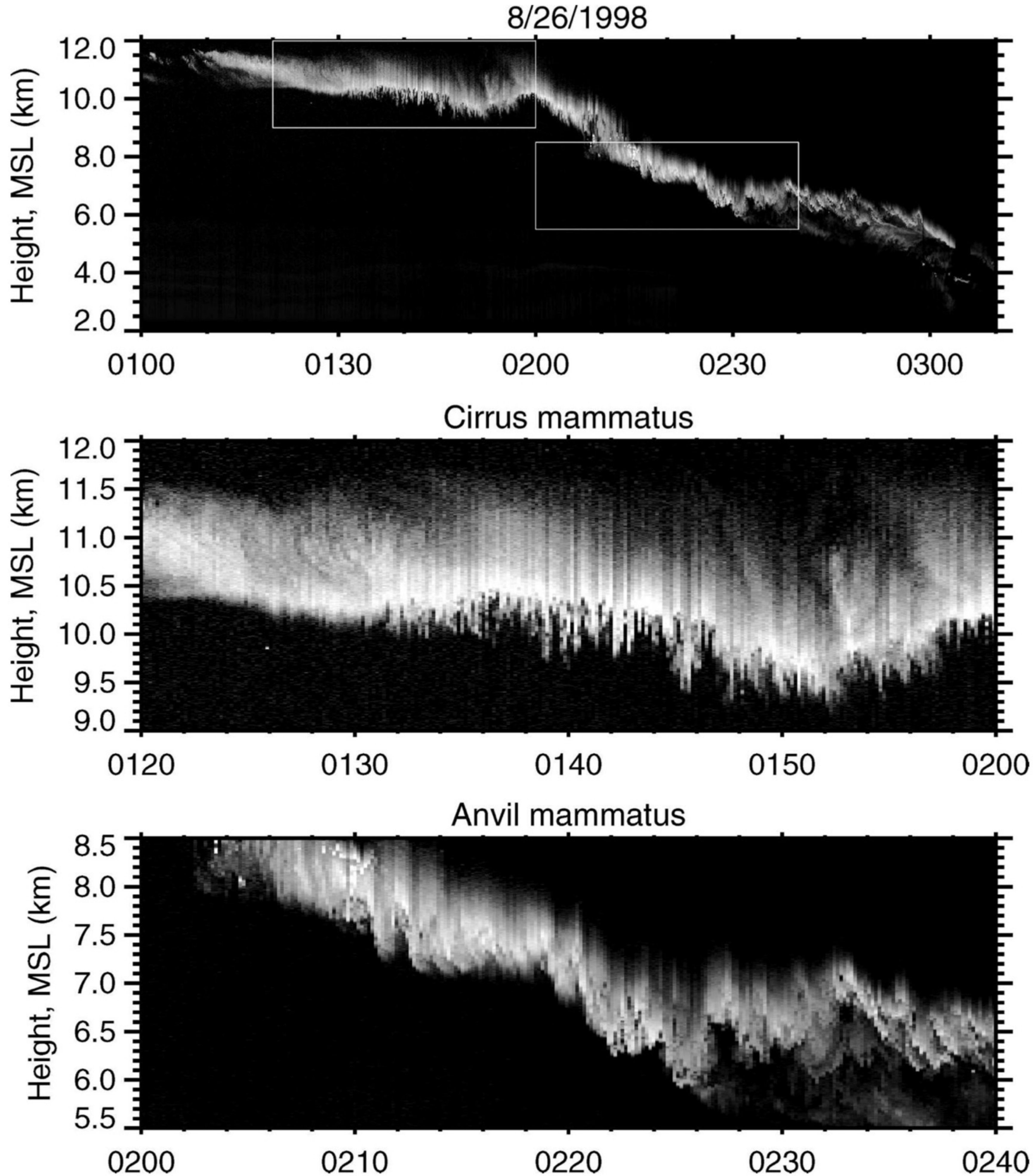

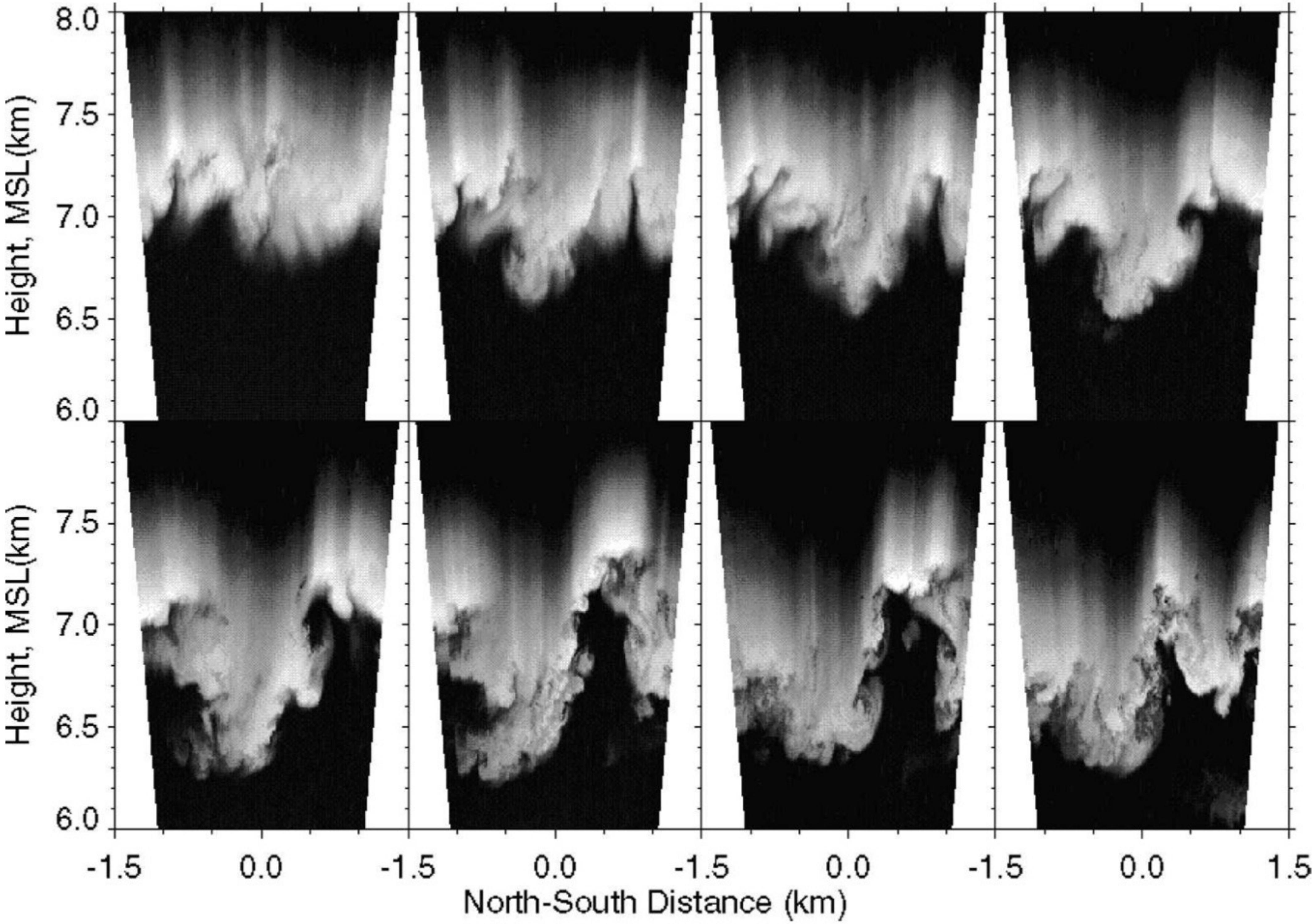

High resolution consecutive lidar scans (10s)

(Schultz et al., *J. Atmos. Sci.*, 2006)

Turbulent cumulonimbus anvil mammatus

Mammatus formation mechanisms

(Schultz et al., *J. Atmos. Sci.*, 2006)

- Large-scale anvil subsidence
- Subcloud evaporation/sublimation
- Melting
- Local-scale hydrometeor fallout
- Cloud-base detrainment instability
- Radiative effects
- Gravity waves
- Kelvin–Helmholtz instability
- Rayleigh–Taylor instability
- Reverse Rayleigh–Bénard-like convection

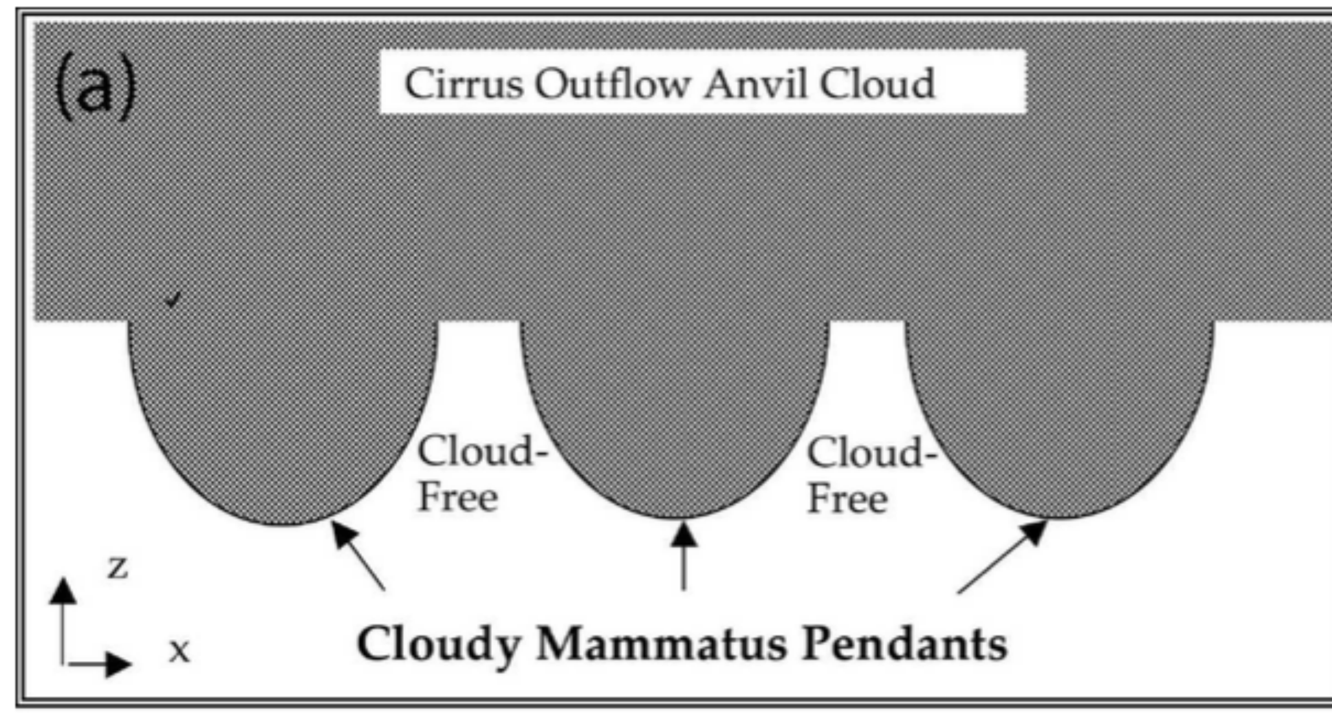

Cumulonimbus outflow anvil cirrus mammatus simulation (Kanak and Straka, *Atmos. Sci. Let.*, 2006)

snowflake-induced aggregation

Simulation time:
30 minutes

Cloud subsidence rate:
~6.5 ms^{-1}

10 µm ice crystal settling rate:
$<10^{-2}$ ms^{-1}

Total vertical distance:
6000 m

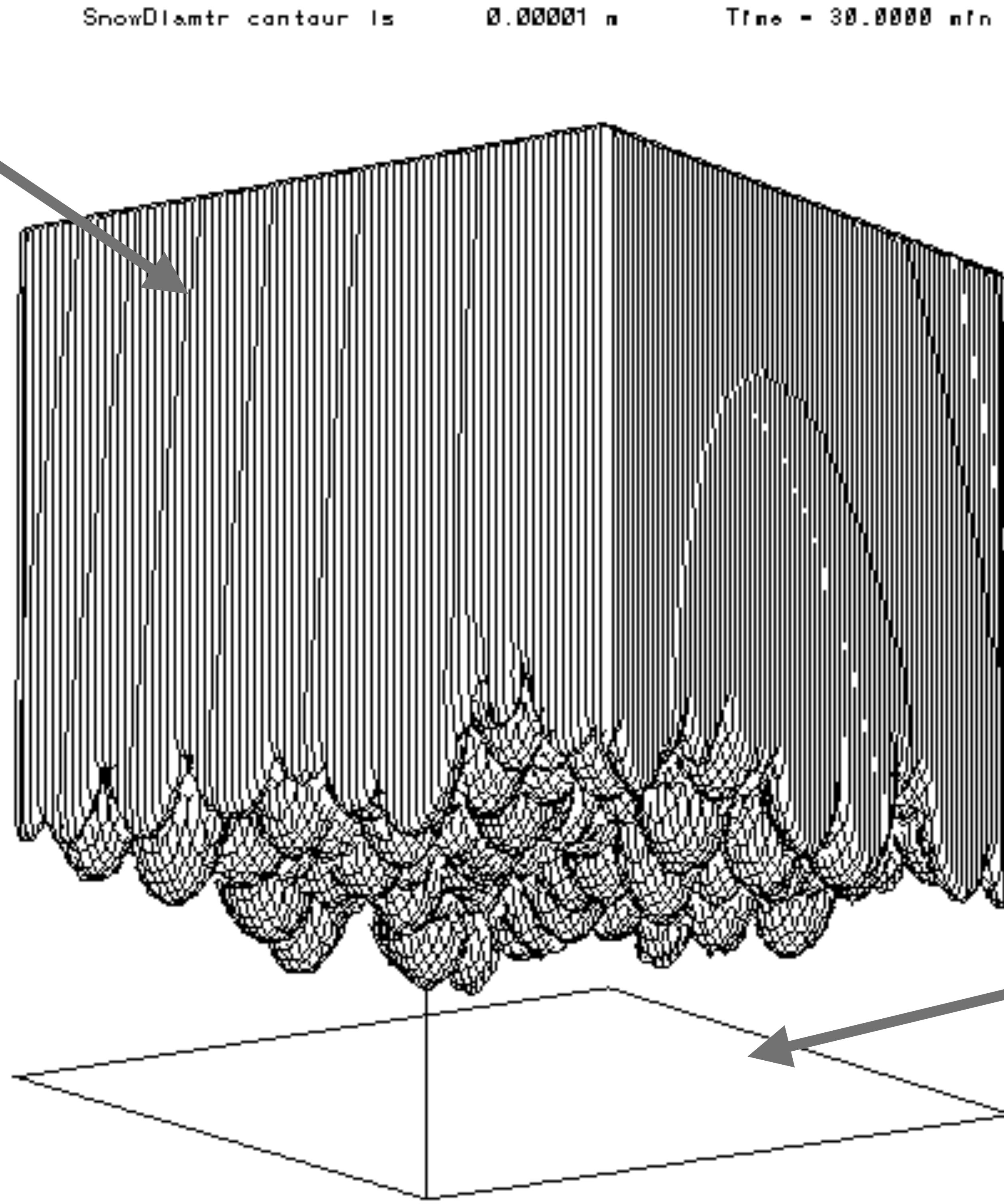

10 µm snow aggregate diameter contours

dry sub-cloud layer

Mount St. Helens radar observations

(Harris et al., *USGS Prof. Paper 1250,* 1981)

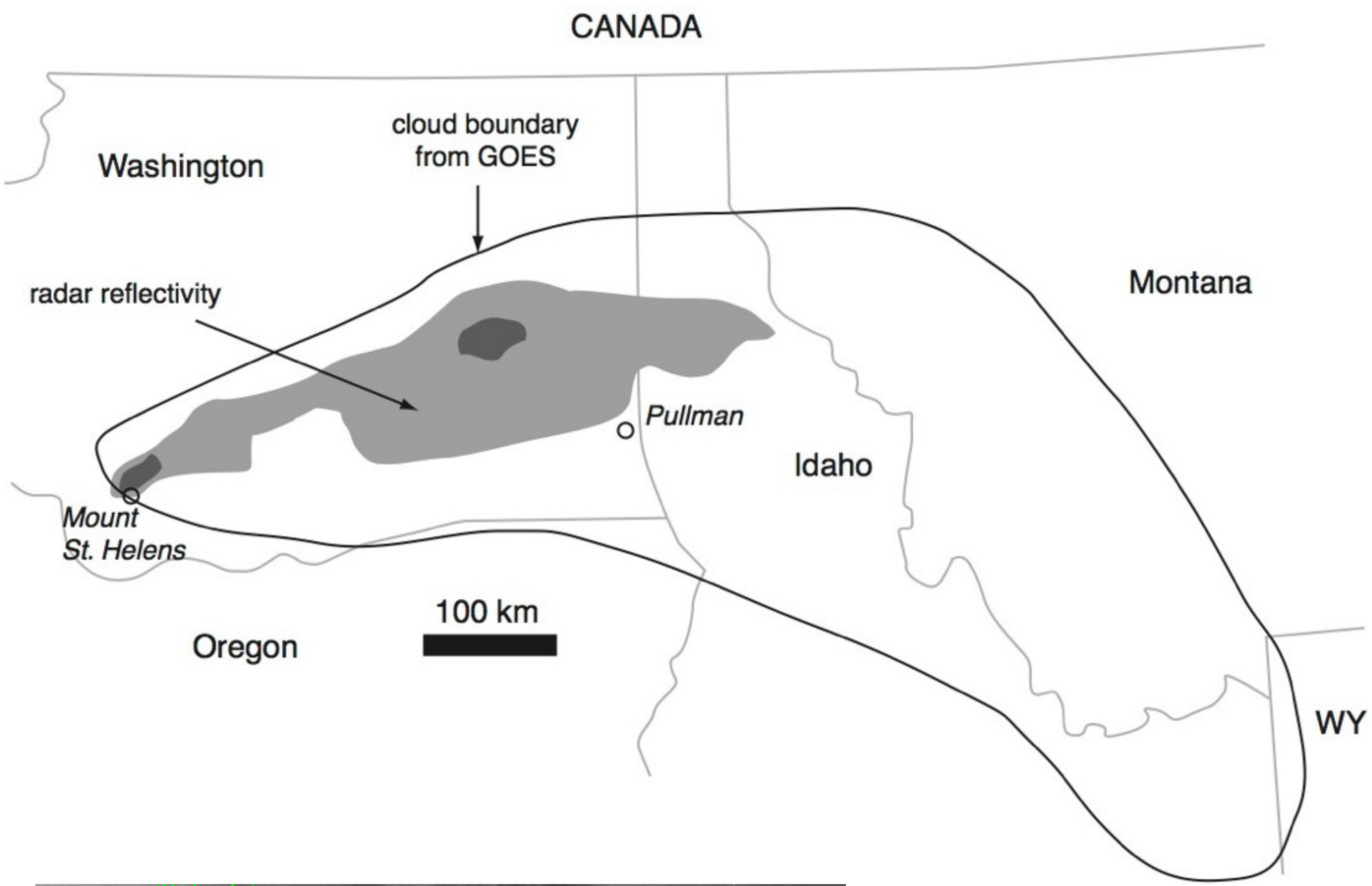

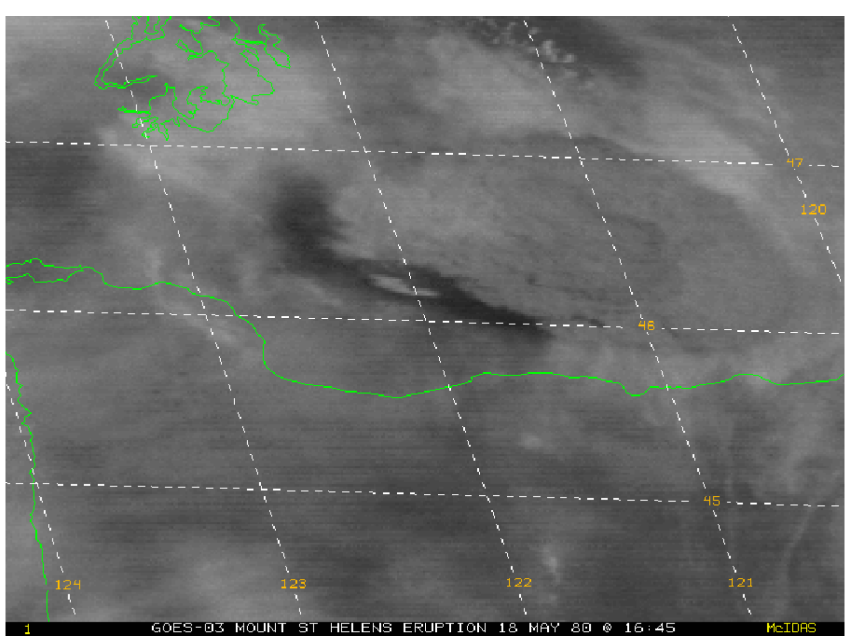

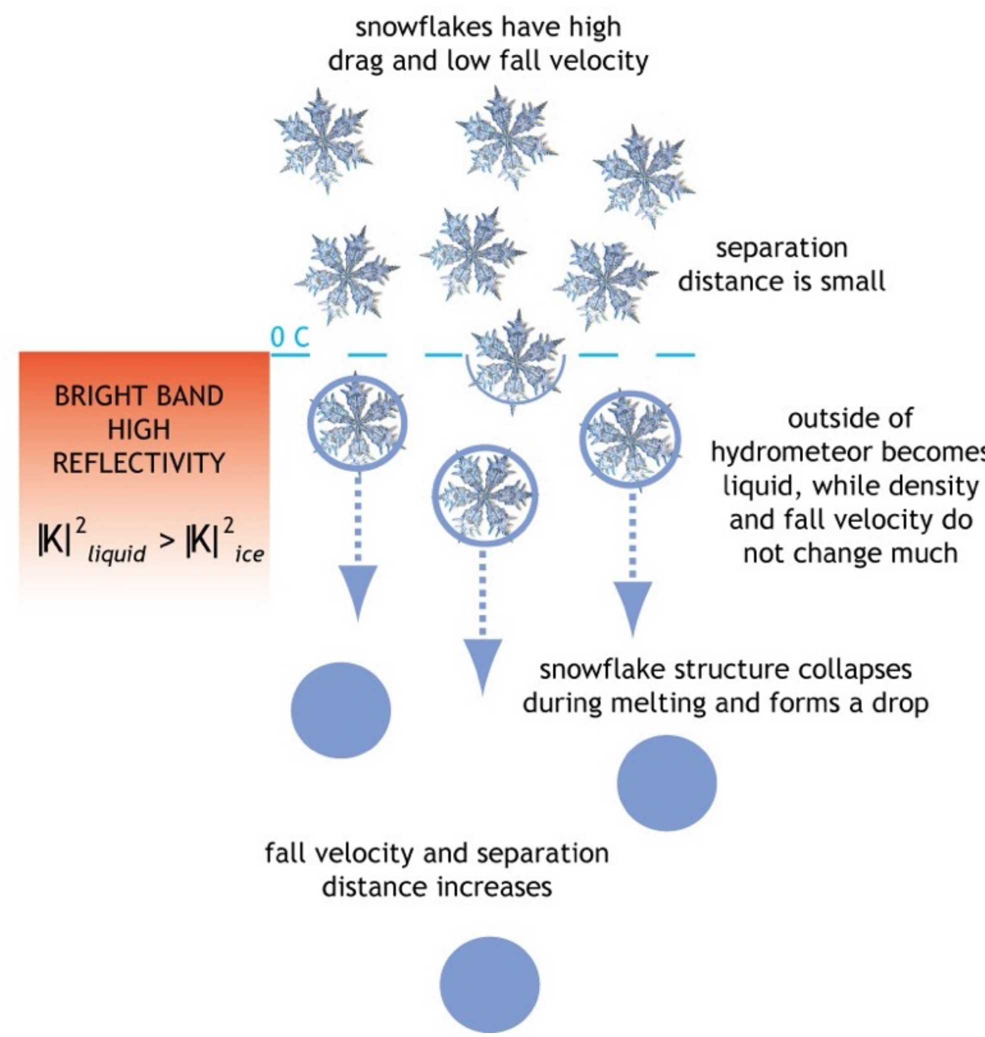

Enhanced reflectivity from either:
(1) increasing particle size
(2) “bright band”

Summary of observations

- **Sedimentology**
  - fine particle size
  - 20 μm subpopulation enhanced over secondary mass deposition maximum
- **Aggregation**
  - abundant aggregate observations in MSH80 cloud
  - loosely-bound aggregate fallout over secondary mass deposition maximum
- **Mammatus clouds**
  - cloud is turbulent, water-rich and rapidly subsiding
  - location corresponds to secondary mass deposition maximum

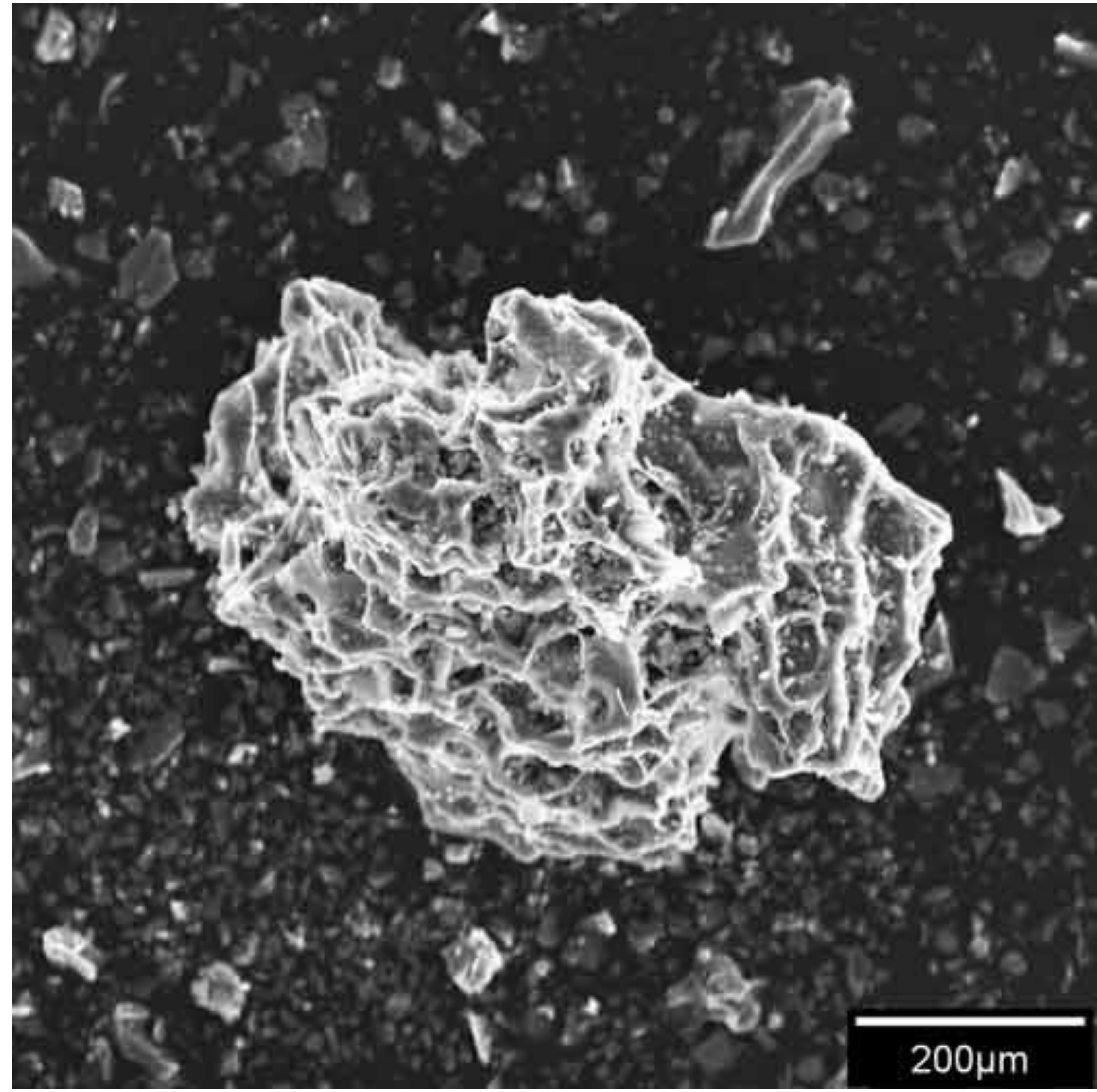

Distal aggregation: conceptual model

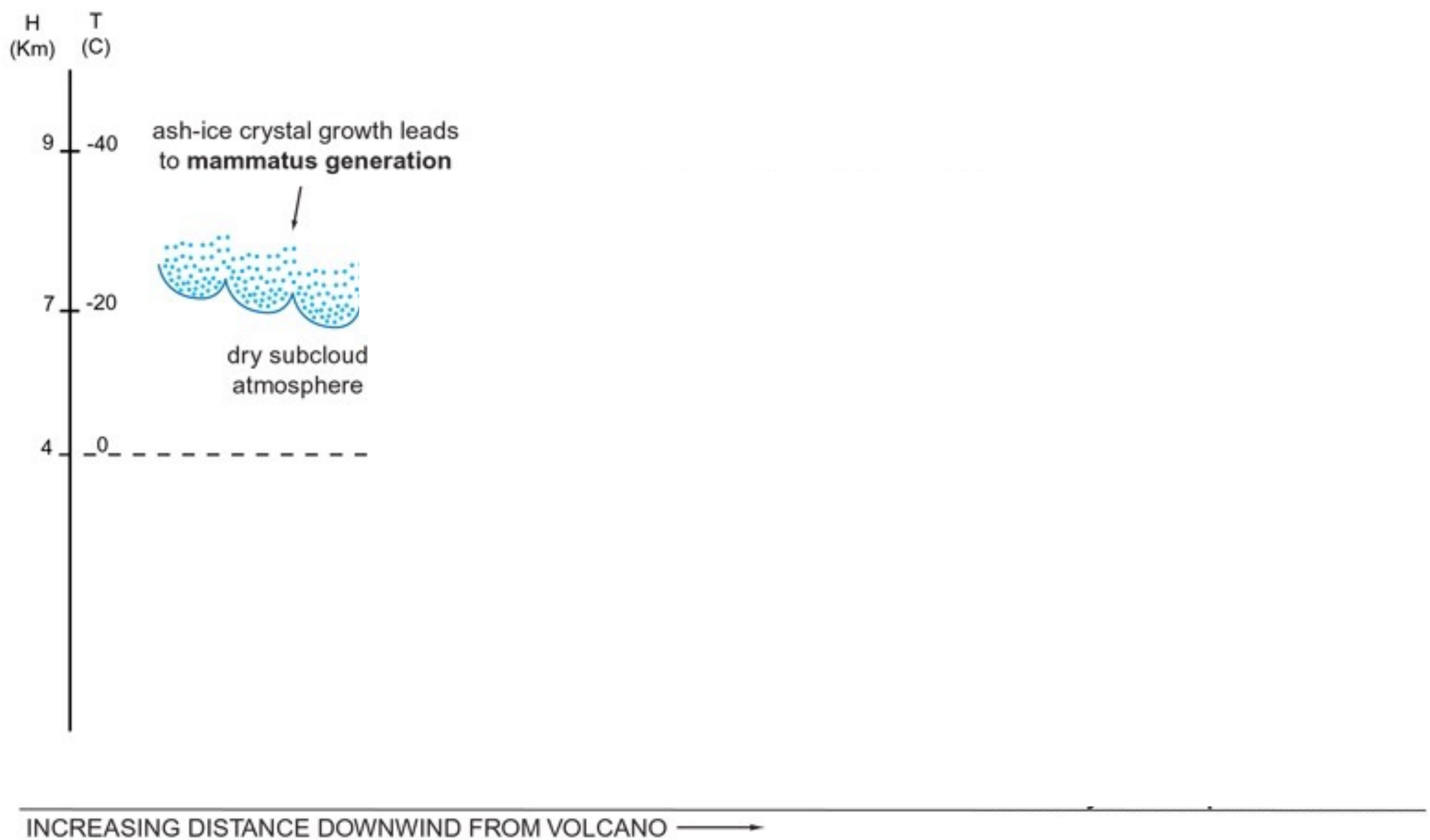

Durant AJ, Rose WI, Sarna-Wojcicki AM, Carey S, Volentik ACM (2009), **Hydrometeor-enhanced tephra sedimentation: Constraints from the 18 May 1980 eruption of Mount St. Helens**, J. Geophys. Res.,114, doi:10.1029/2008JB005756

AGGREGATION MODELLING

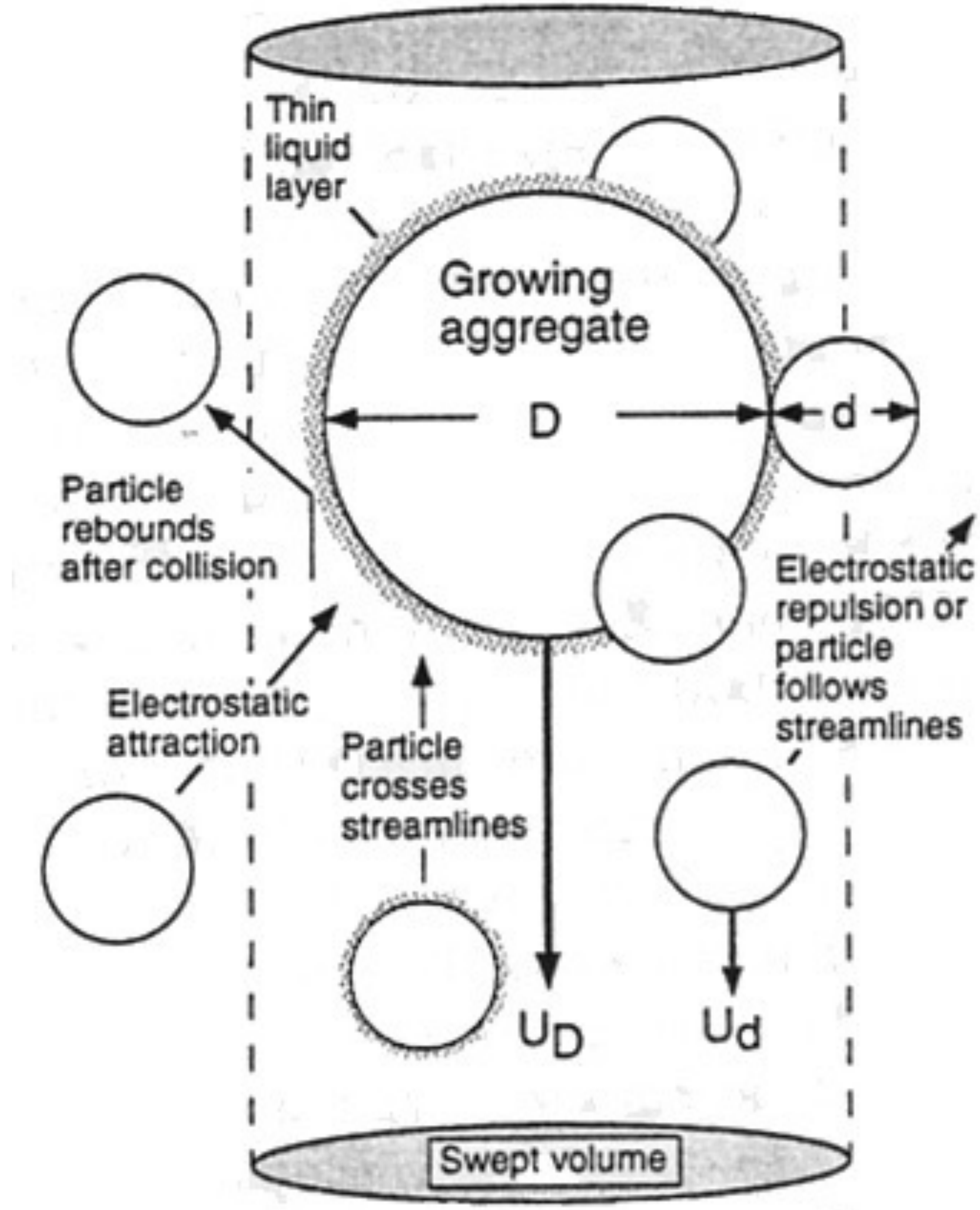

Gilbert and Lane, 1994

Modified Smoluchowski (1917) equation (Costa et al. 2010)

the rate of formation of aggregates with volume between v and v + dv

$$\frac{\partial n_v}{\partial t} = \frac{1}{2}\int_0^v \alpha(s, v-s)\beta(s, v-s)n_v(s)n_v(v-s)ds - \int_0^\infty \alpha(v, s)\beta(v, s)n_v(s)n_v(v)ds$$

rate of loss of aggregates of volume between v and v + dv to form larger aggregates

α = sticking efficiency

β = collision frequency

v = particle volume

n_v = number of particles in volume v

$K = \alpha\ \beta$ = coagulation or collection kernel

Aggregation model validation

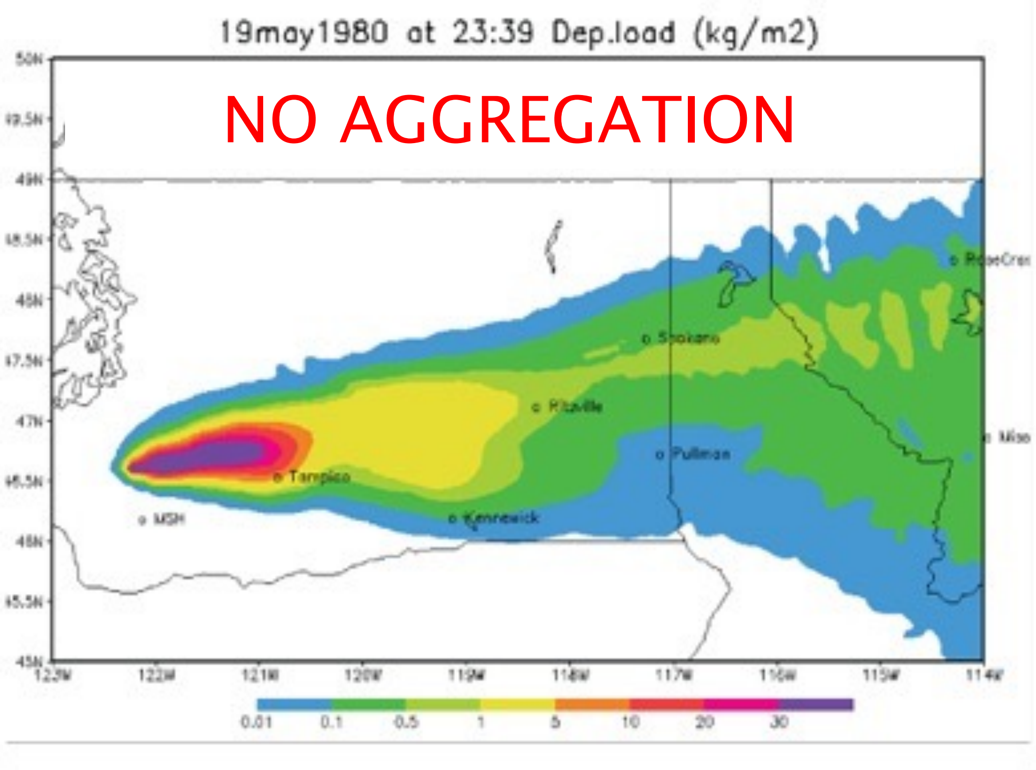

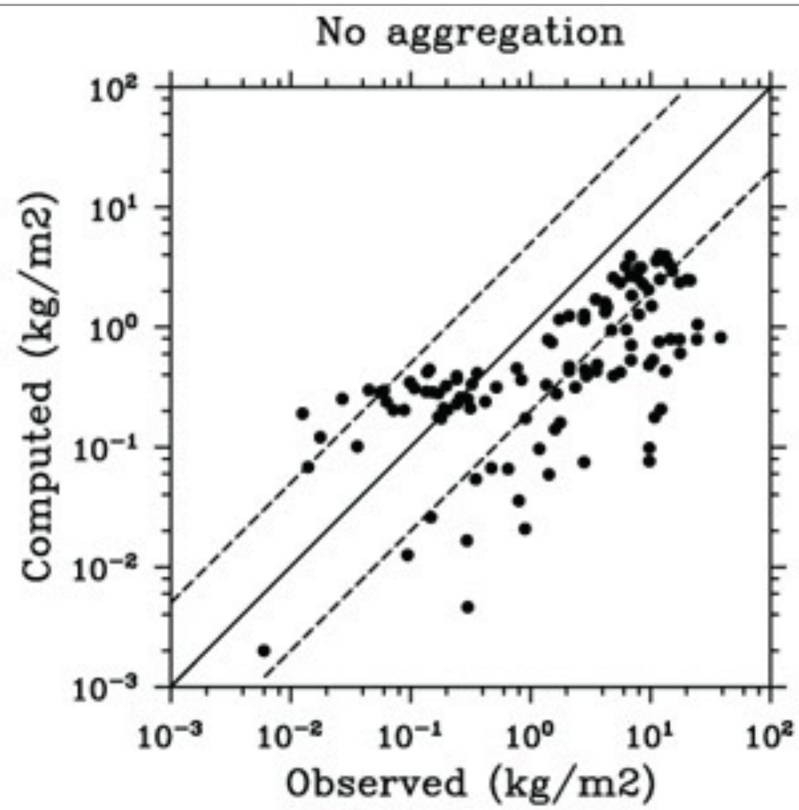

Costa A, Folch A, Macedonio G (2010), **A model for wet aggregation of ash particles in volcanic plumes and clouds: 1. Theoretical formulation**, J. Geophys. Res., 115(B9), B09201

Folch, Costa, Durant, Macedonio (2010), **A model for wet aggregation of ash particles in volcanic plumes and clouds: 2. Model application**, J. Geophys. Res, 115(B9), B09202

Conclusions

- Fine ash (<63 microns) particle aggregation occurs in all ash clouds and reduces atmospheric lifetime

- Amount and phase of water present has primary control on aggregation process

- Gravitational instabilities need to be included in models of ash sedimentation

How much fine ash?

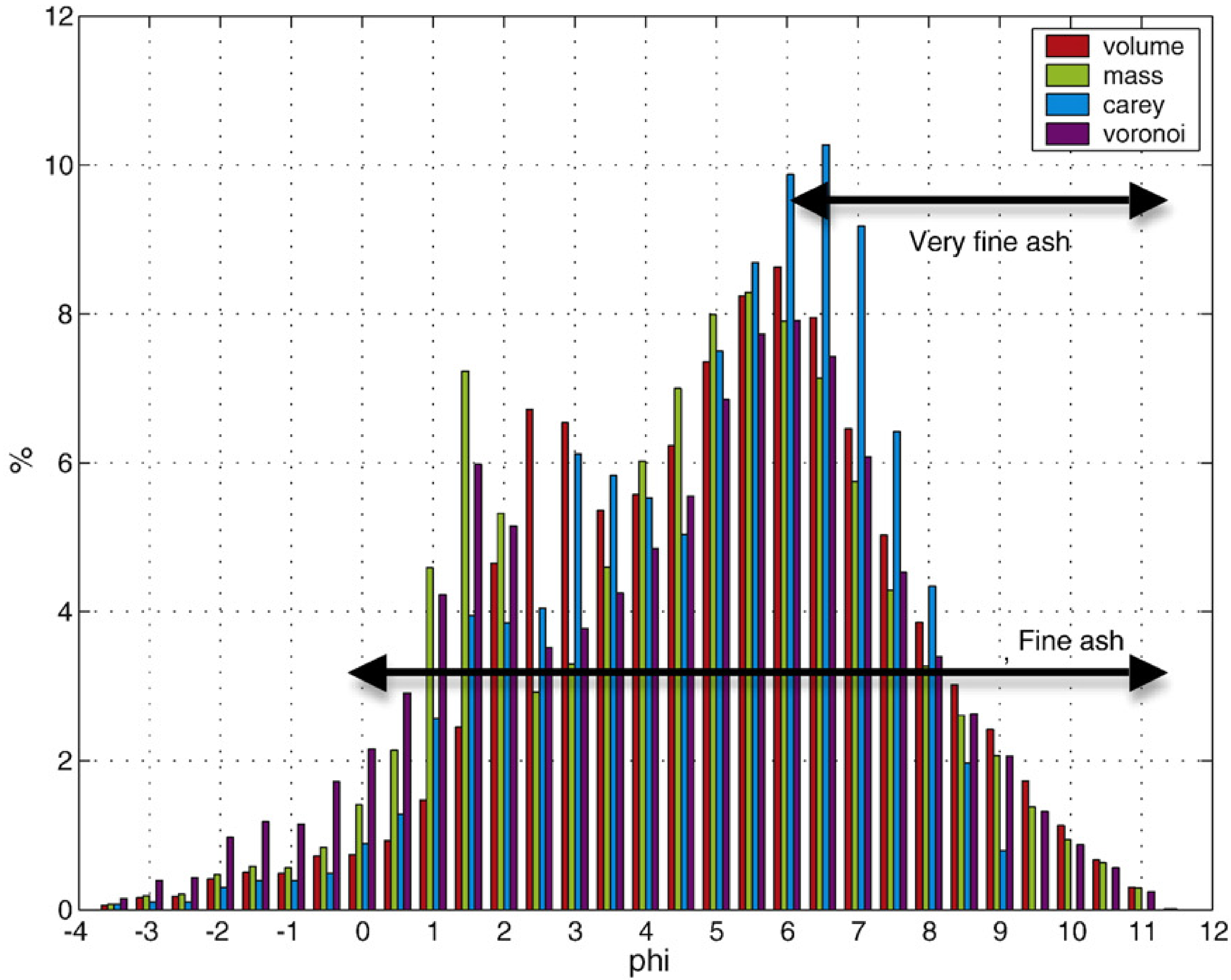

How much fine ash?

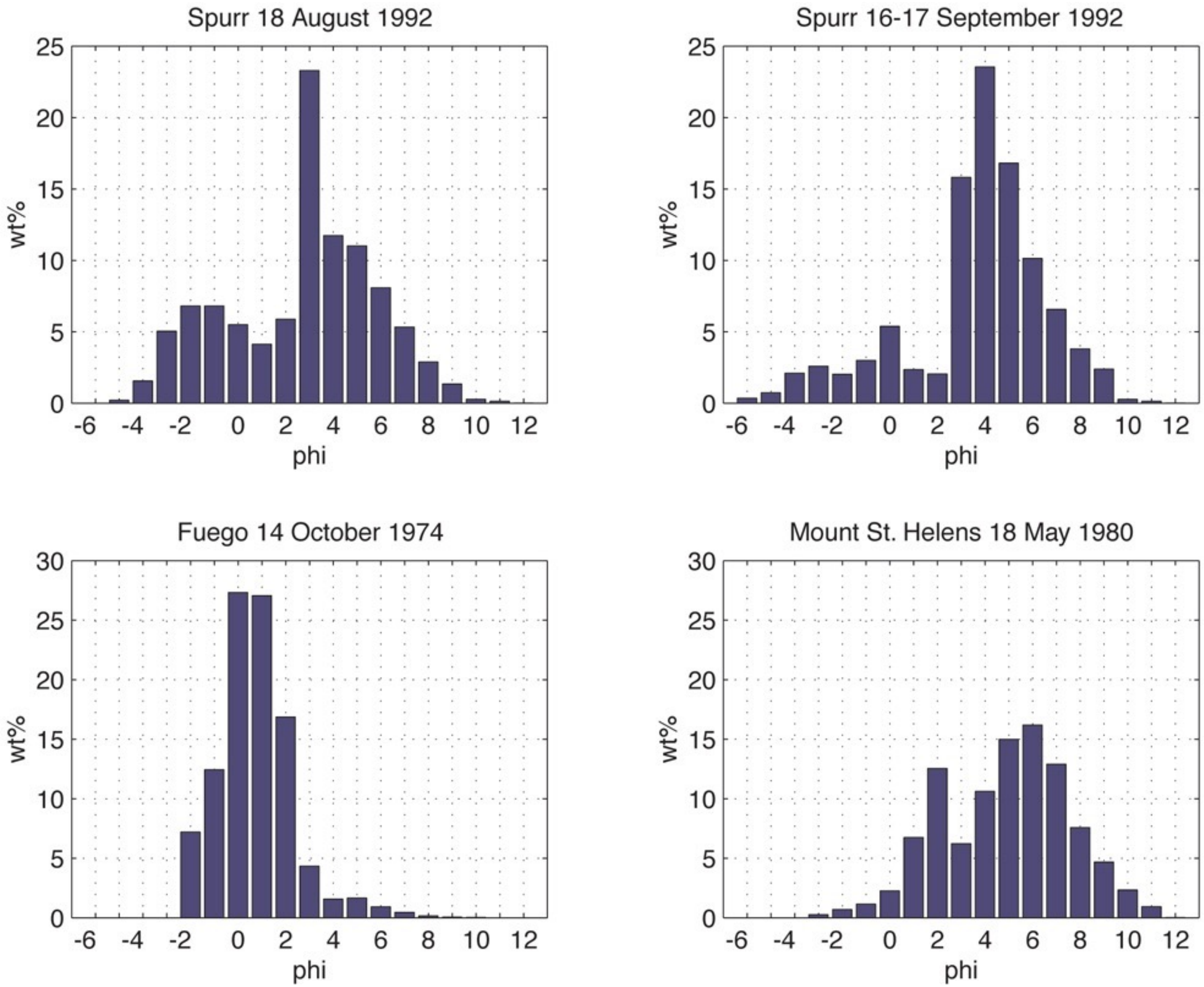

Rose WI, Durant AJ (2009) Fine ash content of explosive eruptions, JVGR.

Electrostatic aggregation (James et al. 2002)

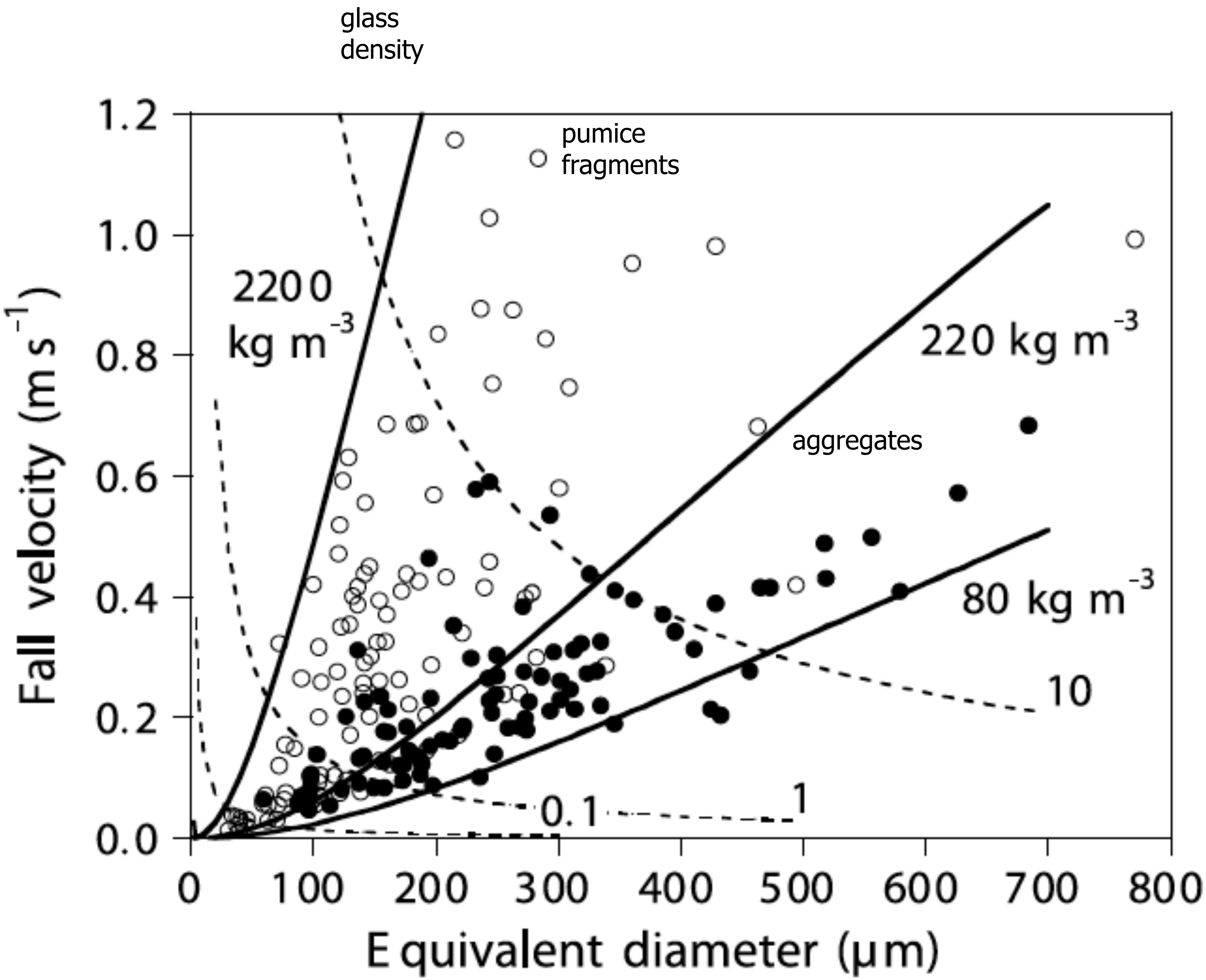

Ash sink term: particle settling

Particle Reynolds number, Re_p:

- ratio of inertial force to viscous force per unit mass

$Re_p = V_t d / v$

V_t = particle terminal fall velocity

d = particle diameter

v = fluid kinematic viscosity

***Re*$_p$ regimes:**

> 500 turbulent

1-500 transitional

<1 laminar